Space Sci Rev (2019) 215:34
https://doi.org/10.1007/s11214-019-0597-7

# Interplanetary Dust, Meteoroids, Meteors and Meteorites

**Detlef Koschny[1,2] · Rachel H. Soja[3] · Cecile Engrand[4] · George J. Flynn[5] · Jérémie Lasue[6] · Anny-Chantal Levasseur-Regourd[7] · David Malaspina[8] · Tomoki Nakamura[9] · Andrew R. Poppe[10] · Veerle J. Sterken[11,12] · Josep M. Trigo-Rodríguez[13]**

Received: 23 April 2018 / Accepted: 23 April 2019


**Abstract** Interplanetary dust particles and meteoroids mostly originate from comets and asteroids. Understanding their distribution in the Solar system, their dynamical behavior and their properties, sheds light on the current state and the dynamical behavior of the Solar system. Dust particles can endanger Earth-orbiting satellites and deep-space probes, and a good understanding of the spatial density and velocity distribution of dust and meteoroids in the Solar system is important for designing proper spacecraft shielding. The study of inter-

Cosmic Dust from the Laboratory to the Stars
Edited by Rafael Rodrigo, Jürgen Blum, Hsiang-Wen Hsu, Detlef Koschny, Anny-Chantal Levasseur-Regourd, Jesús Martín-Pintado, Veerle Sterken and Andrew Westphal

✉ D. Koschny
detlef.koschny@esa.int

1 SCI-S, European Space Agency, Keplerlaan 1, 2200 AZ Noordwijk ZH, The Netherlands

2 Lehrstuhl für Raumfahrttechnik, Technische Universität München, Boltzmannstr. 15, 85748 Garching, Germany

3 Institut für Raumfahrtsysteme, Universität Stuttgart, Pfaffenwaldring 29, 70049 Stuttgart, Germany

4 CSNSM CNRS/Univ. Paris Sud, Univ. Paris-Saclay, Batiment 104, 91405 Orsay Campus, France

5 Dept of Physics, State University of New York at Plattsburgh, 101 Broad St., Plattsburgh, NY 12901, USA

6 IRAP, Université de Toulouse, CNRS, UPS, 9 avenue du Colonel Roche, 31400, Toulouse, France

7 LATMOS, Sorbonne Univ., CNRS, UVSQ, Campus Pierre et Marie Curie, 4 place Jussieu, 75005 Paris, France

8 Laboratory for Atmospheric and Space Physics, University of Colorado, 1234 Innovation Dr., Boulder, CO 80303, USA

9 Tohoku University, Aoba, Sendai, Miyagi 980-8578, Japan

10 Space Sciences Laboratory, University of California at Berkeley, 7 Gauss Way, Berkeley, CA 94720, USA

11 Institute of Applied Physics, University of Bern, Hochschulstrasse 4, 3012 Bern, Switzerland

12 Astronomical Institutute, University of Bern, Hochschulstrasse 4, 3012 Bern, Switzerland

planetary dust and meteoroids provides clues to the formation of the Solar system. Particles having formed 4.5 billion years ago can survive planetary accretion and those that survived until now did not evolve significantly since then. Meteoroids and interplanetary dust can be observed by measuring the intensity and polarization of the zodiacal light, by observing meteors entering the Earth's atmosphere, by collecting them in the upper atmosphere, polar ices and snow, and by detecting them with in-situ detectors on space probes.

**Keywords** Interplanetary dust · Meteors · Meteorites · Zodiacal light · Dynamics · Formation · Evolution

## 1 Introduction

The interplanetary dust and meteoroid cloud is the ensemble of refractory and possibly icy particles in the Solar system in the size range from a few microns to about a meter. The main sources are asteroids, comets, and, in the outer Solar system, in-spiraling particles coming from objects in the Edgeworth-Kuiper Belt. The goal of this paper is to summarize our current knowledge in this field and refer to other relevant papers.

When an asteroid or a comet gets close to the Sun, sublimating gases carry solid particles away from the object at a certain ejection velocity. Solar radiation pressure quickly moves the less massive particles away from the parent, larger particles remain near to the source (see Sect. 2). Their ejection velocity causes their orbits to disperse away from the parent with time. When an object (usually a comet) produces a continuous release of particles over a period of time, these particles may form a visible trail that appears to follow the parent along its orbit (Kresak 1993), see Fig. 1. When they are slightly dispersed mainly by non-gravitational forces, they form meteoroid streams. Meteoroid streams entering the Earth's atmosphere generate so-called meteor showers.

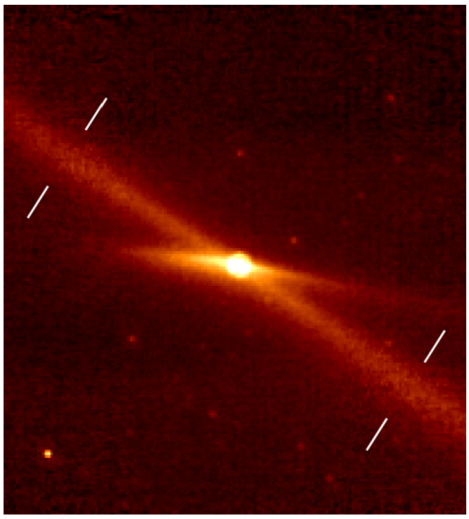

**Fig. 1** Spitzer space telescope image of the dust trail of comet Encke. The trail is marked with white lines. The more horizontally distributed material is from recent cometary activity. Image size is about $3' \times 3'$ (from Kelley et al. 2006)

[13] Institute of Space Sciences (CSIC-IEEC), Campus UAB, c/Can Magrans s/n, 08193 Cerdanyola del Vallès (Barcelona), Catalonia, Spain


**Fig. 2** A Perseid meteor, recorded with an image-intensified meteor camera. Image size is about 30° in diameter (image: D. Koschny)

Over long time periods, the orbits of the dust particles and meteoroids will change under the effect of both gravitational and non-gravitational forces. In particular the small dust will leave the vicinity of the meteoroid stream and form the almost, but not quite randomly distributed interplanetary background dust cloud. It can be observed from the Earth as the zodiacal light. Astronomical observations of the zodiacal light in visual and infrared from space-based instrumentation provide a comprehensive picture of the distribution of particles and their polarization. In-situ detectors on spacecraft, such as Galileo and Ulysses, probe the dust cloud at the smallest sizes up to a few microns. The larger meteoroids form the sporadic meteoroid complex, which can be observed as sporadic meteors when they enter the Earth's atmosphere. Interplanetary Dust Particles and micrometeorites—typically in the size range from micrometers to 1 mm—can be collected in the Earth's stratosphere, and by extracting them from ocean water or ice and snow in the polar caps. These collection techniques allow to directly obtain extraterrestrial samples without the need of a sample-return spacecraft mission.

Meteorites—rocky or metallic material that reaches the ground—provide examples of generally asteroidal material, in some cases also with a record of its flight through the atmosphere. The synthesis of the observations provides us with an overall picture of the interplanetary dust and meteoroid cloud—its mass flux distribution; chemical, material and structural properties; and the importance of different cometary and asteroidal sources in populating the inner Solar system with dust. This information has implications for the interpretation of the meteoroid deposition in planetary atmospheres (e.g Plane et al. 2014), on the Moon (e.g. Szalay and Horányi 2015), and on other planets and airless bodies (e.g. Christou et al. 2015). In this paper we describe the current state of knowledge of the interplanetary dust and meteoroid cloud. There is also an interstellar contribution, which is described in Sect. 4.4.

In this and the following chapters, we use the terminology as defined by the IAU Commission F1 on Meteors, Meteorites and Interplanetary Dust:

- 'Meteor' is the light and associated physical phenomena (heat, shock, ionization), which result from the high speed entry of a solid object from space into a gaseous atmosphere (see Fig. 2).
- 'Meteoroid' is a solid natural object of a size roughly between 30 μm and 1 meter, moving in, or coming from, interplanetary space.

- 'Interplanetary dust' is finely divided solid matter, with particle sizes in general smaller than meteoroids, moving in, or coming from, interplanetary space.
- 'Meteorite' is any natural solid object that survived the meteor phase in a gaseous atmosphere without being completely vaporized. Meteorites smaller than 1 mm in size are also called micrometeorite. These may be too small to experience ablation in an atmosphere.

For more explanations, see the IAU web site.[1] Note that in particular in the cometary science community, the term 'dust' is used in a wider context and can also be used for larger particles. In that case, the term 'particles' is used without any size qualifier like 'dust' or 'meteoroid'.

## 2 Formation and Evolution of the Interplanetary Dust Cloud

### 2.1 Overview

The main sources of interplanetary dust and meteoroids are asteroids and comets. These minor bodies are relatively fragile and generate dust particles due to collisions and the evaporation of volatiles. They accreted from primitive material in cold regions of the protoplanetary disk that included high-temperature components, around the Sun about 4.5 Gyr ago. They formed km-sized rocky planetesimals, that kept growing by mutual collisions. Early-formed asteroids, hundreds of km or larger in diameter, experienced melting and planetary differentiation, thus modifying their rock-forming materials into igneous counterparts. Later-formed smaller asteroids released their radiogenic heat at a rate quick enough to retain primitive features and to avoid differentiation.

Dust particles and meteoroids are refractory and possibly icy particles released by emission, impact or collision processes from these minor bodies. After release and escape from the environment of their parent body (Fig. 1), they are subject to the same set of dynamical forces as their parent. These forces are size-dependent, and they may change if the particle undergoes transformative processes such as collisional shattering or erosion, or sublimation near the Sun (Mukai et al. 2001). Here we examine the evolution of the emitted particles into the interplanetary dust and meteoroid cloud.

### 2.2 Dynamics

Gravitational, radiative, collisional, and electromagnetic forces alter the orbits of dust and meteoroid particles after their emission from the parent object. In terms of gravitational interaction with larger bodies, they act as massless objects. Radiative forces, on the other hand, are dependent on the particle size and mass. The composition determines the material density and thus the mass-to-surface area ratio of the particle, as well as absorption and scattering properties. The shape and structure of the particle will also play a role (Gustafson 1989; Kimura et al. 2002b). Here we provide an overview of the important effects and for what particle sizes they are relevant.

#### *2.2.1 Gravitational Forces*

Gravitational forces dominate the trajectories of larger particles ($> 100$ μm). Solar gravity dominates for heliocentric orbits, unless the particle passes within the Hill sphere of a

[1] https://www.iau.org/science/scientific_bodies/commissions/F1/.

planet, in which planetary gravity is the dominant effect. Close planetary encounters can shift their orbits to hyperbolic trajectories. This process is an important loss mechanism for in-spiraling particles in the outer Solar system (Liou et al. 1996a). Planetary encounters also disrupt and perturb meteoroid streams (e.g. Vaubaillon and Colas 2005; Vaubaillon et al. 2006). Particles with orbits within the scattering zones of Jupiter or Saturn suffer regular perturbations from these planets. Mean motion and secular resonances with respect to the giant planets are important factors influencing their long term dynamics (e.g. Liou and Zook 1997, 1999). Large particles trapped in resonances may remain there for significant time periods, protected from further close interactions with the planet and temporarily halting their evolution due to Poynting-Robertson drag (e.g. Sekhar and Asher 2014; Beauge and Ferraz-Mello 1994). Chaotic processes may in some cases remove particles from a resonant region. These processes create structures in the outer Solar system dust cloud (e.g. Poppe 2016). Particles trapped in resonant filaments in meteoroid streams may produce outbursts at Earth, due to their enhanced flux density relative to the rest of the stream.

### 2.2.2 *Radiative Forces*

Radiative forces generally are important for particles $< 100$ μm. Radiation pressure results from the momentum exchange of the incoming Solar radiation with the particle, producing a small force away from the Sun (Burns et al. 1979). Because Solar gravity and radiation pressure both decrease with the inverse of the heliocentric distance, the relative value of the radiation pressure is often quantified using the $\beta$ parameter, which is the ratio between the radiation and gravitational forces $F_r$ and $F_g$:

$$\beta = \frac{F_r}{F_g} = \frac{3 L_\odot Q_{pr}}{16 \pi G M_\odot c \rho s} = 5.7 \times 10^{-4} \frac{Q_{pr}}{\rho s}$$

where $L_\odot$ is the Solar luminosity in W, $G$ is the gravitational constant in $\mathrm{m^3\,kg^{-1}\,s^{-2}}$, $c$ is the speed of light in $\mathrm{m\,s^{-1}}$, $\rho$ is the particle bulk density in $\mathrm{kg\,m^{-3}}$, and $s$ the particle equivalent radius in m. $Q_{pr}$ is the efficiency factor for radiation pressure, defined by Mie scattering or measurements (Gustafson 1994; Kimura and Mann 1999). It has a maximum, along with $\beta$, at a particle equivalent radius of about 0.1 μm, although this depends on the particle's optical properties. For circular orbits, particles with $\beta = 1$ have a radiation force in excess of gravity and therefore escape the Solar system on hyperbolic trajectories. In the more general case, particles released from a parent body immediately assume an orbit different to that of the parent body, described by

$$a' = a \times \frac{1 - \beta}{1 - 2a\beta / r_h}$$

and

$$e' = \left| 1 - \frac{(1 - 2a\beta / r_h)(1 - e^2)}{(1 - \beta)^2} \right|$$

where $a$ the semi-major axis and $e$ the eccentricity of the particles' orbit. Because $\beta$ is size dependent, particles undergo a different evolution, depending on their size after release from their parent body. Larger meteoroids, which are not strongly affected by radiation pressure, stay near the orbit of their parent body. Smaller particles begin with orbits outside the parent body's orbit and form a tail (Fulle 2004). Very small micrometer-sized dust may be quickly blown out of the Solar system. Additionally, radiation pressure affects the trapping of particles into resonances. E.g., Weidenschilling and Jackson (1993) show that resonances under

Poynting-Robertson drag are "metastable" because trapped grains inevitably acquire eccentricities large enough to cause their orbits to cross that of the planet causing the resonance.

### 2.2.3 Poynting-Robertson Effect

The Poynting-Robertson effect results from the non-isotropic reemission of photons from a moving particle due to relativistic effects (Robertson 1937). Radiation in the direction of motion is blue-shifted, resulting in a higher momentum of the radiation in the direction of motion compared to the opposite direction. The result is a force similar to a drag force, causing the orbit to loose energy and spiral into the Sun. The eccentricity also drops and the orbit is circularized. This process is size and orbit dependent. The variations in the particle semi-major axis and eccentricity as a result of the Poynting-Robertson drag force are given by Wyatt and Whipple (1950):

$$\dot{a}_{PR} = -\frac{\alpha}{a} \frac{2+3e^2}{(1-e^2)^{3/2}}$$

$$\dot{e}_{PR} = -2.5\frac{\alpha}{a^2} \frac{e}{(1-e^2)^{1/2}}$$

where $\alpha = 3.55 \times 10^{-8}/(s\rho)$ au$^2$ yr$^{-1}$. Other orbital elements are not affected. For the case of circular orbits, these equations can be solved to provide an approximate analytic formula for the in-spiraling time in years from an initial semi-major axis $a_0$: $\tau_{PR,circ} \approx 400 a_0^2/\beta = 7.0 \times 10^5 a_0^2 \rho s / Q_{pr}$. This timescale defines the importance of the Poynting-Robertson effect for the dynamical evolution of particles of different sizes. For a bulk density of 1000 kg m$^{-3}$, the in-spiraling lifetimes ranges from $\sim$ 700 yr for particles of equivalent radius 1 µm and 70000 yr for 100 µm radii, to $\sim$ 0.7 Myr for radii of 1 mm. Scattering Solar wind particles creates a similar drag force. It is generally taken to have an effect of $\sim$ 30% of the Poynting-Robertson drag force (Dermott et al. 2001), varying with the 11-year Solar cycle.

### 2.2.4 Yarkovsky Effect

The Yarkovsky effect results from the small recoil force that results when photons are re-radiated anisotropically due to thermal effects. The diurnal Yarkovsky effect occurs due to anisotropic emission of radiation from a rotating body (Bottke et al. 2002). While it can be the dominant dispersive force for meter-sized asteroids, it is in general not significant for small particles that spin fast relative to their size. However, the seasonal Yarkovsky force, which occurs due to a tilt in the spin axis, can be important for meteoroids (Rubincam 1995). Both result in a force comparable to a drag force, which will shrink the semi-major axis and circularize the orbit.

### 2.2.5 Lorentz Forces

Lorentz forces—the result of the traverse of a particle through the Solar magnetosphere—are important for dust particles with sizes a few microns or lower. Particles in the electromagnetic field have a charge $q = \epsilon \eta U m^{1/3}$, where $\epsilon = 8.85 \times 10^{-12}$ CV$^{-1}$ m$^{-1}$ is the permittivity, $\eta$ is a constant describing physical parameters of the particle, and $m$ is the particle mass in kg. The surface potential $U$ is about 5 V for a spherical particle, largely as a result of the photoelectric effect. The Lorentz force is then described by $F_L = \frac{q}{c}|\mathbf{v}_{rel} \times \mathbf{B}|$ where $\mathbf{v}_{rel}$ is

the relative velocity between the particle and the Solar wind, and **B** are the components of the interplanetary magnetic field.

Hamilton et al. (1996) showed that the magnitude of the Lorentz force depends on the Solar cycle. They modeled the trajectory of dust starting on circular, un-inclined orbits. They would reach high ecliptic latitudes with the configuration of the magnetic field as in Solar cycle no. 22 or 24, and finally escaping the Solar system. Currently we are in cycle 25, where the orientation of the magnetic field is reversed. This would result in orbits confined closer to the ecliptic, with particles still leaving the Solar system, but less readily.

## 2.3 Transformative Processes

### *2.3.1 Collisional Disruption*

Larger interplanetary meteoroids are broken up by collisions with smaller, more abundant ones. These collisions result in momentum transfer, altering the orbits of the particles, and producing smaller fragments, which are more significantly influenced by Solar radiation. Steel and Elford (1986) modeled the orbital evolution of 1-mm meteoroids released into the orbits of 28 specific meteoroid streams and found catastrophic collision lifetimes varying from 20 kyr to 400 kyr, shorter than the Poynting-Robertson lifetimes for many of these streams. Leinert et al. (1983a) found that at 1 au the maximum catastrophic collision lifetimes of 100- μm particles, 1-mm particles, and 1-cm particles are 200 kyr, 40 kyr, and 800 kyr, respectively, as a result of collisions with other interplanetary dust particles. These collision lifetimes are shorter than or comparable to the time required for that size particle to spiral into the Sun under Poynting-Robertson drag for the 1-mm and 1-cm particles, indicating that a significant fraction of these particles are fragmented into smaller particles over their lifetimes. Thus consideration of collisional disruption is critical to the understanding of the evolution of the interplanetary dust and meteoroid complex.

Detailed modeling of the collisional lifetimes of interplanetary dust and meteoroids requires a knowledge not only of the size-frequency distribution of the particles, which has been measured at 1 au, but also of the distribution of orbital eccentricities and inclinations, which is not well established. As a result, models of the collisional lifetimes by different investigators differ by an order-of-magnitude or more, depending on the orbital parameters that are assumed in the modeling.

The interplanetary dust and meteoroid mass-frequency distribution, measured at 1 au by impacts onto the Long Duration Exposure Facility during its 5.7 years in low-Earth orbit, peaks at about 250 μm in diameter (Love and Brownlee 1993). Particles near the peak size are disrupted but there are few larger particles to resupply the distribution. Using these measurements, Dermott et al. (2001) conclude that the mean particle diameter $s$ is expected to decrease with decreasing heliocentric distance.

Interstellar grains passing through the Solar system, which are expected to be much smaller than most interplanetary dust, also contribute to the collisional fragmentation of the interplanetary dust. The interstellar grains are generally $< 1$ μm in diameter, so they only fragment the smallest interplanetary dust particles. Liou et al. (1996a) analyze the contribution of dust grains coming from Edgeworth-Kuiper belt objects towards the inner Solar system. They conclude that for particles up to about 25 μm in size and migrating inwards from the Edgeworth-Kuiper Belt, collisions with interstellar grains are more important than mutual collisions in determining the collisional lifetimes. They find collisional lifetimes of interplanetary dust particles 1, 2, 4, 9 and 23 microns in size due to impacts by $\sim 1$ μm diameter interstellar grains to be 104, 49, 19, 4.8 and 0.86 Myr, respectively.

Modeling by Wyatt (2005) of the dust disks in other planetary systems indicates that in some massive disks mutual collisions are so frequent that they effectively prevent dust from reaching the inner regions of these systems under Poynting-Robertson drag. Similar conditions could have occurred early in Solar system history if the dust flux density was significantly higher than in the current era.

### *2.3.2 Disaggregation*

Some interplanetary dust and meteoroid particles are composed of ices or are aggregates of mineral grains held together by ices or other relatively weak materials. These particles may easily disaggregate after release from their parent bodies, as a result of Solar heating, photoelectric charging, or other mechanisms. Active dust counters on fast flyby missions through dust clouds of 1P/Halley by the Giotto, VEGA1, and VEGA2 spacecraft; 26P/Grigg-Skjellerup by the Giotto spacecraft; 81P/Wild 2 by the Stardust spacecraft; and 9P/Tempel 1 by the Stardust NexT spacecraft were interpreted as indicating widespread grain disaggregation in the coma (Green et al. 2004; Clark et al. 2004; Tuzzolino et al. 2004; Economou et al. 2013), although the cause of this disaggregation could not be determined.

### *2.3.3 Sublimation*

Grains are lost from the interplanetary dust cloud when they are heated to their sublimation temperatures by Solar radiation. The temperature reached by a grain depends on its distance from the Sun, its composition, which determines its efficiency in absorbing the Solar spectrum, and its size, with very small particles being less efficient at re-radiating energy at any specific grain temperature. Although the most detailed modeling has been performed for water ice, all small grains, even silicates, can sublimate before reaching the Sun.

Ice grains are modeled to sublime between 1 and 4 au (Kobayashi et al. 2011). Even beyond the snow line, there is significant loss of water ice because of Solar wind and Solar ultraviolet-induced sputtering (Grigorieva et al. 2007a).

The two most common minerals in interplanetary dust are olivine and pyroxene. The pyroxene grains sublimate at 4 to 6 Solar radii; olivine grains at 10 to 13 Solar radii (Kimura et al. 2002a). For porous dust particles consisting of a mixture silicates and absorbing material, Mann et al. (1994) have shown that, depending on the amount of absorbing material versus silicate material, they can reach as close as 2 to 3 Solar radii.

## 2.4 Modeling the Interplanetary Dust Cloud

Various efforts have been made to model the structure and evolution of the interplanetary dust and meteoroid distribution under the above processes, both to understand its formation and major constituents, and to assist in the development of impact hazard models for spacecraft. It should be noted that some of the models are called dust models, other meteoroid models. Nevertheless they normally cover the complete size range from micron-sized particles up to mm- or cm-sized particles.

The early development of space flight technology by NASA was supported by meteoroid penetration experiments on the Explorer XV1 and XXIII and Pegasus satellites (Naumann 1966). These were used to develop initial models of the near-Earth meteoroid risk to early missions (Cour-Palais 1969; Kessler 1970). The mass flux distribution at Earth orbit by Grün et al. (1985) also utilized these data, along with lunar crater counts (Morrison and Clanton 1979), and spacecraft dust measurements: Pioneer 8 and 9 (Berg and Richardson

1969; Berg and Gerloff 1971), Helios (Grün et al. 1980), and HEOS-2 (Hoffmann et al. 1975a,b). Love and Brownlee (1993) derived a mass flux at Earth based on impact craters on the Long Duration Exposure Facility (LDEF) that is higher than the Pegasus-derived flux. It should be noted that different characteristic velocities and densities were assumed in the different studies, which may well be the cause for the higher flux resulting from the LDEF measurements.

The first comprehensive model of the interplanetary dust flux was the Divine model (Divine 1993). The Staubach model provided an extension to small particles (Staubach et al. 1997). These models used the mass flux from Grün et al. (1985) for the meteoroids at the Earth, and used in-situ and zodiacal light data to constrain the flux of particles at other heliocentric distances.

The current meteoroid engineering models for space applications in the inner Solar system are NASA's Meteoroid Engineering Model or MEM (McNamara et al. 2004; Jones 2004; Moorhead et al. 2015) and ESA's Interplanetary Meteoroid Environment Model or IMEM (Dikarev et al. 2005, 2004). The NASA MEM uses a simple dynamical model, along with data from the Canadian Meteor Orbit Radar (CMOR), and zodiacal light observations from Helios to define the radial distribution. It can therefore be used for predictions of the flux, speed, and direction of dust and meteoroids within 0.2–2 au. The ESA IMEM model starts from the distribution of asteroidal and short period comets as sources of meteoroids and propagates them in space and time. However, the model assumes that only particles with $m \leq 10^{-9}$ kg are transported by the Poynting-Robertson effect towards the Sun, while larger particles remain on their initial orbits, creating a sharp discontinuity in the flux profile of particle sizes around this cutoff mass. IMEM uses infrared brightness data and in-situ spacecraft data to calibrate the model (Dikarev et al. 2005). Drolshagen et al. (2008) and Grün et al. (2013) discuss the differences between these existing meteoroid engineering models.

## 3 Astronomical Observations

### 3.1 The Zodiacal Light and Thermal Emission

The zodiacal light is a faint glow visible along the ecliptic plane in the night sky. It appears to the naked eye mainly as bright Solar-colored cones above the horizon at dusk and dawn as shown in Fig. 3. While this geometry is the most readily visible, the zodiacal light can be detected in every direction and results from the Solar light scattered by the small solid dust particles in the Solar system. As shown in Fig. 3, it is enhanced by backscattering in the anti-Solar direction, a phenomenon known as the *gegenschein*.

The zodiacal light intensity, $I$, varies with the position of the observer, the epoch of observation, the wavelength and the viewing direction. This is related to the distribution of the dust in the lenticular interplanetary dust cloud. The dust distribution essentially follows a mirror symmetry with respect to a plane close to the ecliptic, therefore heliocentric ecliptic coordinates are introduced as shown in Fig. 4a. The measurements integrated over the line-of-sight are described with the heliocentric ecliptic latitude $\beta$ and longitude $(\lambda_e - \lambda_{eo})$, the phase angle being $\alpha$.

For an observer located on Earth's orbit, small amplitude variations of $I$ are observed over a year. Annual oscillations up to $\pm 10\%$ at high and medium latitudes originate from the slight inclination of the zodiacal cloud's symmetry plane in relation to the ecliptic and the eccentricity of the Earth's orbit (Dumont and Levasseur-Regourd 1978). After correcting

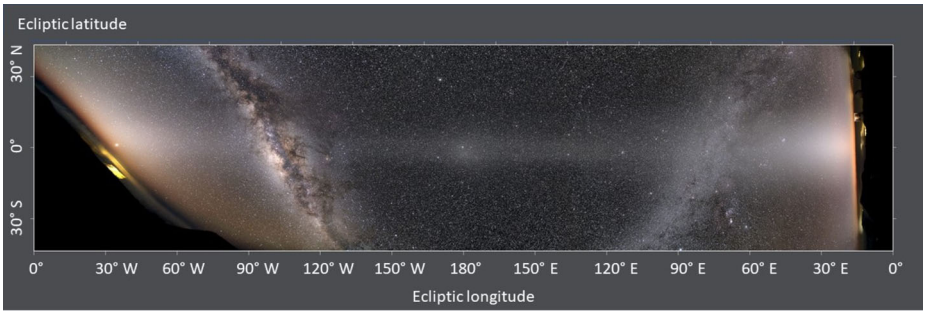


**Fig. 3** 360 degree panorama illustrating the zodiacal light along the Solar system's ecliptic plane. Mosaic of images taken during a single night at Mauna Kea. The zodiacal light cones are seen at dawn on the left and dusk on the right. The *gegenschein* enhanced backscattering is visible near 180° elongation. Venus and Saturn are marked. Image credit: Druckmüller and Habbal 2012, taken from Horálek et al. (2016)

for such geometrically induced variations, the zodiacal light intensity observed at 1 au remains consistently stable within 1.5% over a whole Solar cycle (Levasseur-Regourd 1996a). Taking into account the fact that the zodiacal light has a Solar spectrum, its intensity $I$ at 550 nm is then found to be close to $2.4 \times 10^{-5}$ W m$^{-2}$ sr$^{-1}$ μm$^{-1}$ at 30° Solar elongation in the ecliptic plane (which outshines the brightest part of the Milky Way). It reaches a minimum of $7.6 \times 10^{-7}$ W m$^{-2}$ sr$^{-1}$ μm$^{-1}$ in the vicinity of the ecliptic pole. In the ecliptic plane, a minimum of $1.8 \times 10^{-6}$ W m$^{-2}$ sr$^{-1}$ μm$^{-1}$ is reached at around 140°, which is still 2.3 times higher than the ecliptic pole value. In the *gegenschein* direction, the intensity increases again to reach a value about 1.3 times larger than the ecliptic minimum, because of a backscattering effect.

The survey from Tenerife by Dumont and Sanchez (1975a,b) remained the most reliable and complete reference until the end of the twentieth century. It was found to be in excellent agreement with spacecraft data obtained at 90° phase angle, without any atmospheric contamination (Levasseur-Regourd and Dumont 1980). Figure 4b presents a compilation of whole sky observations as published in the review by Leinert et al. (1998). The symmetries in the data are used to present just one fourth of the sky. The relative uncertainty in the intensity data remains below 5%, the resolution of the data is between 5° and 15°. The symmetry plane at 1 au has been determined to have an ascending node at $95° \pm 20°$ with an inclination of $1.5° \pm 0.4°$ (Dumont and Levasseur-Regourd 1978).

A re-analysis of Weinberg's observations from Hawaii has recently yielded a new intensity map with a 2° resolution from which the ascending node position gives around 80° while the inclination of the cloud's symmetry plane is around 2° (Kwon et al. 2004), see Fig. 4c. With the continuous photometric observations of the Solar Mass Ejection Imager onboard the Coriolis spacecraft over the whole sky, an updated map of the zodiacal light has been generated with the unprecedented precision of 0.5°, as shown in Fig. 4d (Buffington et al. 2016). Based on the 8.5 years of data collected by the spacecraft, an upper limit to zodiacal light intensity changes of 0.3% was obtained for this time period. Using the same satellite data, Buffington et al. (2009) determined that the *gegenschein* is located at the anti-Solar point, but varies by ≈ 10% of its intensity over time, with a portion of the variation repeating seasonally. Similarly, the latest high-resolution (5' per pixel) survey of the *gegenschein* using a wide-angle camera showed that the maximum scattered intensity is consistently located at the anti-Solar point. The models fitted to the *gegenschein* constrain a very low geometric albedo of 0.06 for those particles (Ishiguro et al. 2013).

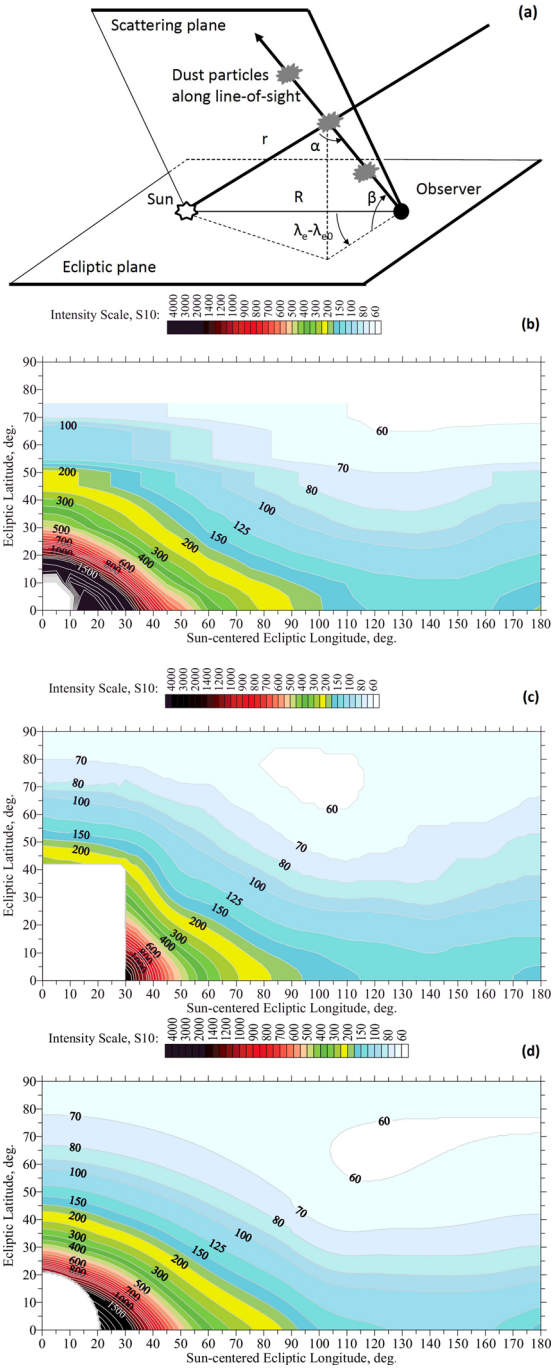


**Fig. 4** (**a**) Geometry of observation of the zodiacal light with representation of the different values described in the text (adapted from Levasseur-Regourd et al. 2007). (**b**) Map of the zodiacal light compiled by Leinert et al. (1998), 5° to 15° precision. (**c**) Reanalysis of the Weinberg's observations by Kwon et al. (2004), 2° precision. (**d**) Modeled results of intensity observations from the Solar Mass Ejection Imager averaged over a period of a year in $S_{10}$ units. Measurements limited to $> 20°$ from the Sun with angular bins of $1° \times 1°$, figure taken from Buffington et al. (2016). Brightnesses are given in the so-called intensity scale, where $1S_{10}$ unit corresponds to $1.18 \times 10^{-8}$ W m$^{-2}$ sr$^{-1}$ μm$^{-1}$ at 550 nm

Short-term enhancements of the zodiacal light had tentatively been ascribed to the optical detection of meteoroid streams (e.g. Levasseur and Blamont 1973), as later confirmed by the

discovery of faint cometary trails by the Spitzer telescope in the infrared (Reach et al. 2007), as well as of linear dust features in the optical domain (Ishiguro et al. 1999).

Extensive descriptions of the results and methods of zodiacal light surveys can be found in the reviews previously published (Leinert 1975; Weinberg and Sparrow 1978; Leinert and Grün 1990; Leinert et al. 1998; Levasseur-Regourd et al. 2001; Mann et al. 2004; Lasue et al. 2015).

### 3.2 Spectral Observations

In the visible part of the spectrum, due to scattering, the zodiacal light shows a Solar spectrum. At large elongations, it is possible to determine the spectral gradient of the zodiacal light from space probes. Leinert et al. (1998) compiled a set of data from 8 different missions that indicated a possible reddening of the zodiacal light from 200 nm to 2 µm. Such a spectral gradient for low albedo particles as inferred from their scattering properties would be most consistent for D-type primitive asteroids or comets as indicated in Fig. 5 (Yang and Ishiguro 2015).

Measurements of the thermal emission originating from the zodiacal cloud have been obtained from balloons, rockets and satellites. The zodiacal thermal emission, which gradually takes over the Solar spectrum at 2 µm, is actually the most prominent source in the light of the night sky from 5 to 100 µm, at least away from the galactic plane (Leinert et al. 1998). For wavelengths larger than 100 µm, the sky brightness gets dominated by the interstellar medium, the cosmic diffuse infrared background and finally the cosmic microwave background.

Based on those long-wavelengths measurements, Fixsen and Dwek (2002) have modeled the thermal emission of the interplanetary dust particles using a single blackbody curve with a temperature of 240 K. A change of slope in the spectrum at a wavelength of about 150 µm is interpreted to represent a change in the dust size distribution at a radius of about 30 µm. Furthermore, the fit is improved if one considers a mixture of amorphous carbon and silicate dust with respective temperatures of 280 and 274 K at 1 au. Under those conditions,

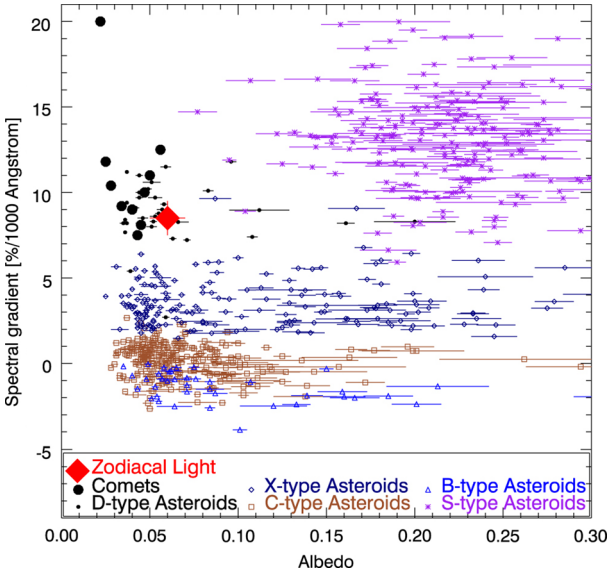


**Fig. 5** Comparison of the spectral gradient with the albedos of asteroids, comets, and zodiacal light. The measurements variance of spectral gradients is estimated to be $\approx 0.7\%/1000$ Angstrom (Yang and Ishiguro 2015)

the Pointing-Robertson drag of the particles towards the Sun limits their lifetime to about $10^5$ yrs, which requires a replenishment rate of $\approx 10^{11}$ kg yr$^{-1}$ from asteroids and comets.

Further analysis of the zodiacal light spectrum at a wavelength of around 10 μm from the camera on-board the ISO satellite indicate a dust distribution dominated by large (> 10 μm radius), low-albedo (less than 0.08), rapidly-rotating, gray particles at 1 au from the Sun. After continuum subtraction, a 6% excess in the 9 to 11 μm range remains that suggests the presence of small particles, with an equivalent radius of < 1 μm, of amorphous and crystalline silicates (Reach et al. 2003).

### 3.3 Polarimetric Observations

The zodiacal light is light scattered by an optically thin cloud of small dust particles and therefore shows a partial linear polarization, $P_Q$. It can reach values as high as 20% along the integrated line of sight as observed from the Earth, see Fig. 4a, Fig. 6 and Fig. 7a. $P_Q$, by definition within the $[-1, +1]$ interval, is positive if the direction of the electric field vector is perpendicular to the scattering plane, which is the case away from the backscattering region. In the ecliptic plane, $P_Q$ reaches a maximum of 19% at 60° heliocentric ecliptic longitude. The error in the measured polarization is estimated to be $\approx 2\%$. Around the *gegenschein*, at helio-ecliptic longitudes greater than 160°, the curve is smooth, with a slightly negative polarization in the backscattering region and an inversion at $15° \pm 5°$. The slope at inversion is $(0.2 \pm 0.1)$ percent per degree (Leinert et al. 1998). Such a polarimetric phase curve is commonly associated with scattering by irregular dust particles and/or fluffy aggregates of submicronic absorbing particles (Levasseur-Regourd et al. 1997; Lumme et al. 1997). This behavior is comparable to that of cometary dust or of C-type asteroids, which are the likely sources of interplanetary dust particles (e.g. Lasue et al. 2015; Lazarian et al. 2015; Kolokolova et al. 2015).

$P_Q$ remains practically constant as a function of the wavelength in the visible range (450 to 800 nm), but infrared observations suggest a weak decreasing trend with increasing wavelength (Berriman et al. 1994). As different spectral polarimetric trends are seen for different types of asteroids surfaces (Belskaya et al. 2017) and comets (Levasseur-Regourd et al.

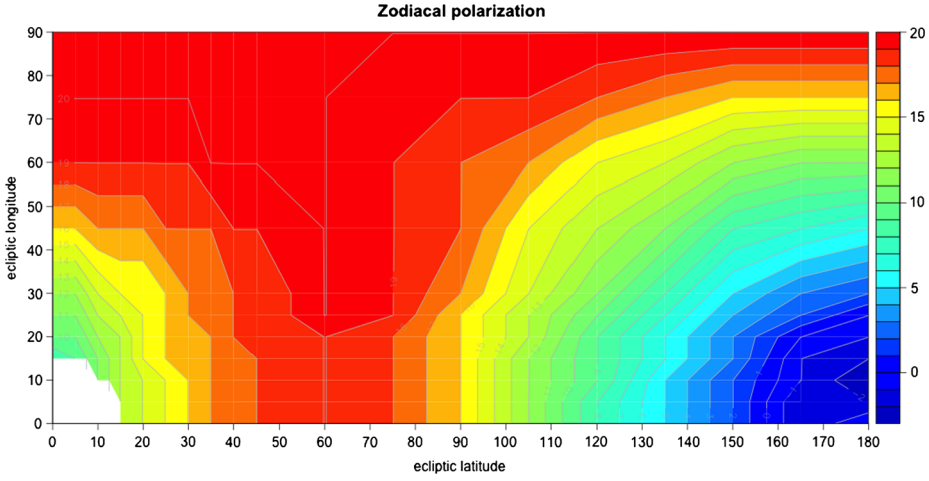


**Fig. 6** Polarization map of the zodiacal light (adapted from Dumont and Sanchez 1975a; Leinert et al. 1998)

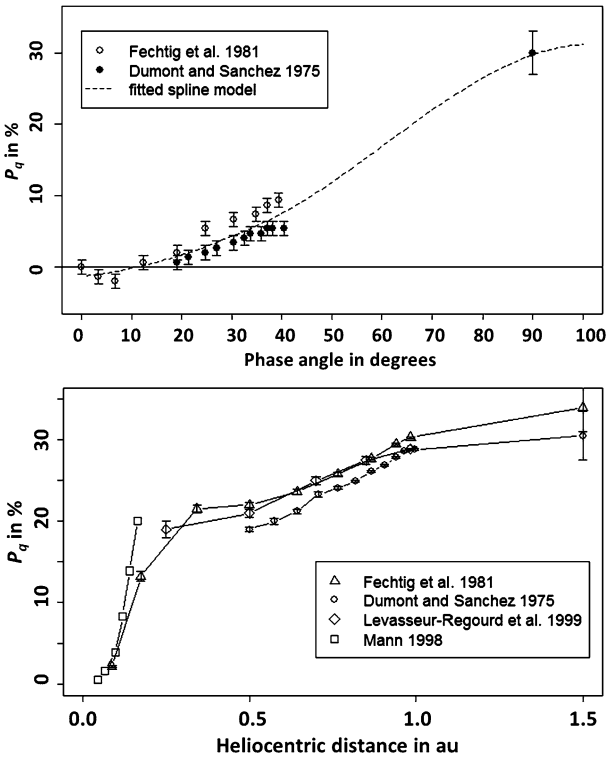


**Fig. 7** Top: Local polarization phase curve obtained at the 1.5 au node (adapted from Levasseur-Regourd et al. 2001). Bottom: local polarization as a function of the heliocentric distance between 0.1 and 1.5 au (adapted from Levasseur-Regourd et al. 2001)

1996; Hadamcik and Levasseur-Regourd 2003), further observations may indicate potential genetic links to sources.

Similarly, while the light scattered by the zodiacal dust is mostly linearly polarized, multiple scattering, partial alignment, or asymmetrical particles can introduce a circular polarization component (Mishchenko et al. 2002). Measurements of the circular polarization have been attempted but remain inconclusive as they are inconsistent or not reproducible (Staude and Schmidt 1972; Wolstencroft and Kemp 1972). Further observations may be of importance as a signal could indicate the origin of the particles (Lasue et al. 2015) and specific dynamic properties in the Solar magnetic field (Lazarian et al. 2015).

### 3.4 Inferred Local Properties of the Zodiacal Light

Because the observations integrated along the line-of-sight correspond to different Solar distances and phase angles and because the interplanetary dust cloud cannot be assumed to be homogeneous, it is necessary to invert the integrated intensity and polarization observations to obtain the local properties of the interplanetary dust particles. An inversion is feasible rigorously along the tangent to the observer's motion direction as a differential measurement (Dumont 1973; Levasseur-Regourd 1996b). The values at other locations can be derived by inversion with good accuracy based on the nodes of lesser uncertainty method as a function of the phase angle, $\alpha$. This is done at a given distance of 1.5 au, and for $\alpha = 90°$ between 0.1 and 1.5 au (Dumont and Levasseur-Regourd 1985; Renard et al. 1995). A summary of the local properties of the interplanetary dust (intensity, polarization, temperature, albedo, number density) in the symmetry plane as inverted from the data and at $\alpha = 90°$ is presented

**Table 1** Variation of the local properties of the dust in the symmetry plane. The properties are described as a function of Solar distance with a power law assumption. The optical properties (linear polarization, albedo, and intensity in $\mathrm{W\,m^{-2}\,sr^{-1}\,\mu m^{-1}\,rad^{-1}}$ at 550 nm) are retrieved at $\alpha = 90°$ (Levasseur-Regourd et al. 1996, 2001). The spatial density of the particles is inferred from the inverted values in intensity and polarization

| | Value at 1 au | Gradient | Domain in au |
|---|---|---|---|
| Intensity | $\approx 23 \times 10^{-7}$ | $-1.25 \pm 0.02$ | 0.5 to 1.4 |
| Linear polarization | $0.3 \pm 0.03$ | $+0.5 \pm 0.1$ | 0.5 to 1.4 |
| Temperature | $250\ \mathrm{K} \pm 10\ \mathrm{K}$ | $-0.36 \pm 0.03$ | 1.1 to 1.4 |
| Albedo | $0.07 \pm 0.03$ | $-0.34 \pm 0.05$ | 1.1 to 1.4 |
| Spatial density | $10^{-19}\ \mathrm{kg\,m^{-3}}$ | $-0.93 \pm 0.07$ | 1.1 to 1.4 |

in Table 1. The local values for the geometric albedo at a given phase angle are retrieved by combining the local values of the flux emission, the temperature and the intensity (Hanner et al. 1981).

The local polarization phase curve of the zodiacal light at 1.5 au near the ecliptic can readily be compared to numerical simulations to constrain the physical properties of the scatterers. Early models using Mie scattering and power-law size distributions indicated compositions consistent with pyroxenes (see e.g. Giese 1963, 1973). However, collections of interplanetary dust particles in the stratosphere (Brownlee 1979) have soon established that models relying on sphere and Mie theory are hardly relevant. More realistic light scattering behavior of irregular particles such as aggregates of spheres, were calculated by different groups and confirmed the results of previous studies with respect to the presence of silicates and carbonaceous compounds (Giese et al. 1978; Haudebourg et al. 1999; Nakamura and Okamoto 1999; Kimura 2001). The simulation results show that typical aggregate sizes are of the order of a micron, while constituting monomer sizes appear to be one order of magnitude lower at about 0.1 μm. Typical optical indices have a real part in the range of 1.5–2, and an imaginary part up to 0.6 for strongly absorbing material (see e.g. Kimura et al. 2003, 2006). A link between red polarimetric color variation of light scattered by fractal aggregates and a lower porosity of the aggregate has been demonstrated, indicating the likely presence of compact particles in the interplanetary dust cloud (Kolokolova and Kimura 2010; Lasue et al. 2007).

As shown in Table 1, important variations in local scattered intensity and polarization are measured as a function of the heliocentric distance. Such a variation is probably linked with a change in the local properties of the dust particles, either their composition or their size distribution. The variation in spatial density with heliocentric distance is consistent with dust particles spiraling under Poynting-Robertson drag inside the production region, which ranges from 0.1 to 10 or 20 au (Leinert et al. 1983b; Levasseur-Regourd et al. 1991). However, observations of the Solar F-corona indicates a sharp decrease in polarization below 0.3 au, suggesting a drastic change closer to the Sun (Mann 1996). The radial polarimetric variations may be interpreted as a change in particle composition with more absorbent carbonaceous particles dominant far from the Sun and less absorbing silicates particles more heat-resistant closer to the Sun (Lasue et al. 2007).

Other effects, such as the size distribution of the particles, their morphology and structure, and their optical index variations, may also contribute to changes in polarization with Solar distance.

Assuming a stable interplanetary dust cloud, interplanetary dust and meteoroid particles vanish while spiraling into the Sun and require sources to replenish them. Particle ejection

from comets as well as asteroidal collisions could easily replenish the inner zodiacal cloud (Whipple 1955; Dermott et al. 1984). Other minor contributions come from the environment of the giant planets, from the Kuiper belt, and from intruding interstellar dust particles (see e.g. Grün et al. 1993b). We have seen above that models of the light scattering properties of interplanetary dust particles are consistent with a population of dark, absorbent dust particles and/or fluffy aggregates of cometary and asteroidal origin (somehow comparable in volumetric contributions, see Lasue et al. 2007). A dynamical model of dust in the inner Solar system (Nesvorný et al. 2010, 2011a) and an improved model of the zodiacal dust cloud infrared emission (Rowan-Robinson and May 2013) both indicate a large contribution ($> 70\%$) of cometary dust particles to the interplanetary dust cloud (Levasseur-Regourd et al. 2018). These characteristics also appear consistent with the properties of dust particle collections described in Sect. 8.

## 4 Meteor Observations

### 4.1 Overview

Meteor phenomena are produced when meteoroids, typically larger than a few tens of microns in size, impact a planetary atmosphere (e.g. Ceplecha et al. 1998; Plane et al. 2018, and references therein). The ablation of the meteoroid body in the Earth's atmosphere produces light and heat that is observable on the Earth visually, as well as being detectable by photographic and video cameras, radar systems, and infrasonic and seismic detectors. Different methods and equipment probe different particle sizes.

Meteor studies utilize the Earth's atmosphere as a large detector of the meteoroid cloud and its structure at 1 au. Various types of information are derived from meteor observations. Optical and radar systems can determine fluxes of meteors, along with their directionality and speeds. Masses can be estimated from the optical brightness or radar electron line density, but the accuracy is limited due to uncertainty in the ionization and luminous efficiencies (Campbell-Brown et al. 2012). They can also be estimated by combining light curve data with deceleration measurements, when available (e.g. Gritsevich and Koschny 2011). Spectra can provide compositional information (Vojáček et al. 2015).

Meteor showers are caused by meteoroid streams, appearing to come from the same direction in the sky, called 'radiant'. Associated particles will have similar incoming velocities. These meteoroids were recently ejected from a comet or asteroid, their 'parent body'. Particles that are not associated with any meteor shower are termed 'sporadic meteors'; they dominate the meteoroid flux at Earth. Here we discuss what meteor observations can tell us about the distribution of interplanetary meteoroids at 1 au, and how the structure of meteor showers and outbursts can provide information on the early history of these particles.

### 4.2 Meteor Sporadic Background

Sporadic particles dominate the environment at Earth. They represent particles from the interplanetary meteoroid cloud, with its origin in asteroid and comet dust production processes (Levasseur-Regourd et al. 2018, and as described earlier in this paper), along with a small proportion of interstellar particles. Their orbits have been altered by gravitational and radiation forces as well as collisional processes (see Sect. 2) such that it is difficult to link the parent object to the particle orbit. The largest datasets of these particles are detected using optical and radar meteor detection techniques. These methods allow the study of the flux and

directional characteristics of interplanetary meteoroids of sizes from a few tens of microns to a few cm.

The proportion of sporadic meteors increases with the limiting magnitude of the meteor detection method. This is a result of different ejection velocities and radiation forces on the small particles, and of collisions affecting the larger particles emitted by comets. Jenniskens et al. (2016c) found that about 36% of all meteors detected by the CAMS system of video cameras (generally between $-1$ and $+4$ visual magnitude) are in meteor showers. Koschny et al. (2017) find a comparable value of 31% down to $+5$ visual magnitude with their CILBO video camera system on the Canary Islands. The meteor database of the AMOR radar in New Zealand (limiting magnitude $\approx +14$) only contains about 1% shower meteors (Galligan and Baggaley 2005).

The appearance of the interplanetary meteoroid population in the meteor record is affected by the movement of the Earth around the Sun. This results in six sporadic 'sources' at the Earth. While the term 'sources' is widely used, they describe concentrations in radiant space that do not necessarily correspond to physical sources of meteoroids. The helion and anti-helion sources, found in the ecliptic plane at 70° from the apex direction, are usually the strongest sources, although the helion source is only detectable by radar. The north and south apex sources are centered towards the direction of the Earth's motion, with ecliptic latitude $\approx \pm 20°$ (Hawkins 1956; Weiss and Smith 1960; Jones and Brown 1993). The highly-inclined north and south toroidal sources are found 60° north and south of the apex direction (Hawkins 1962, 1963; Jones and Brown 1993). The high-resolution radiant distribution maps in Campbell-Brown (2008), produced from five years of CMOR data, show also a ring at 55° that is likely the result of Kozai oscillations (Kozai 1962) on high-inclination trajectories that are in-spiraling due to the Poynting-Robertson effect (Wiegert et al. 2009). Such a ring is also observed in SonotaCo video meteor data (Jakšová et al. 2015). An asymmetry between the strengths of the anti-helion and helion sources is suspected to be caused by the influence of comet 2P/Encke on the inner interplanetary dust cloud (Wiegert et al. 2009). New results from the SAAMER radar in Argentina provide data on the south toroidal source (Janches et al. 2015), which is not observable by systems in the northern hemisphere.

Different types of orbits are required to populate each source. Meteoroids observed in the helion and anti-helion sources have orbits that suggest an origin in short-period Jupiter-family comets (Jones et al. 2001; Wiegert et al. 2009; Nesvorný et al. 2010). Apex meteoroids have high speed or retrograde orbits that likely stem from Halley-type or Oort cloud comets (Wiegert et al. 2009; Nesvorný et al. 2011b; Pokorný et al. 2014). Recent work demonstrated the ability of evolved Halley-type comets to populate the toroidal sources (Pokorný et al. 2014).

The velocity distribution of meteoroids at the Earth, once corrected for observational biases, shows that most particles impact the Earth at relatively low velocities of typically $\approx 15\ \mathrm{km\,s^{-1}}$ (e.g. McBride et al. 1999; Huang et al. 2015; Moorhead et al. 2017, and references therein). The semi-major axis distribution at sizes below $\approx 1$ mm predominantly peaks at 1 au: these particles are therefore likely to be the result of significantly evolved cometary dust populations (Nesvorný et al. 2011b). Even larger cm-sized meteoroids, such as those detected by the CAMS video meteor system, show a only fraction of such evolved orbits (Jenniskens et al. 2016c). This likely demonstrates, as described also by Campbell-Brown (2008), that even mm- to cm-sized meteoroids survive in interplanetary space for long durations and do not suffer collisions with other dust particles in lifetimes of tens of thousands of years, as originally suggested by Grün et al. (1985) or Jenniskens (2015).

Of particular interest is the mass-dependent flux of particles at the Earth. The distribution given by Grün et al. (1985) is somewhat of a standard model for the mass flux, derived from

lunar crater counts (Hörz et al. 1975) and meteor data (Hawkins and Upton 1958; Whipple 1967). It gives a size distribution index $s = 2.34$ for sporadic meteors (where the number of meteor $N$ is a function of mass $M$ such that $dN \propto M^{-s} dM$). Newer radar studies of the sporadic meteor population have suggested this mass index may be lower, around $s \sim 2.0$–2.1 (Galligan and Baggaley 2004; Blaauw et al. 2011b; Pokorný and Brown 2016). Meteor showers have generally lower mass indices due to their young age (Blaauw et al. 2011a). The brightness of meteors provides direct information on their mass, in theory allowing similar information to be determined from meteor flux counts. However, large uncertainties in the efficiency in generating photons or electrons—the luminous efficiency for photographic or video meteors and the ionization efficiency for radar meteors—restricts the accuracy of such measurements. In particular, the behavior for higher velocities is not well understood. Weryk and Brown (2013) use simultaneous video and radar measurements to derive the ratio of the luminous and ionization efficiencies. Koschny et al. (2017) use these results to determine the flux of optical double-station meteors, and find a distribution comparable to that given by Grün et al. (1985). Recent laboratory experiments improve our understanding of the ionization efficiency and provide new constraints for it (Thomas et al. 2016).

Information on the physical and chemical properties of the meteoroids is obtained by studying their atmospheric ablation. Both for dynamically cometary and asteroidal meteors, a high proportion of small objects is seen, demonstrating evidence of fragmentation. Furthermore, the types of fragmentation are similar, although this could be indicative of a misunderstanding in the classification of the source population of these objects (Subasinghe et al. 2016). The beginning and end heights of the meteor are related to the impact speed (slower meteors start to ablate lower in the atmosphere), and also to the fragility of the material. Jenniskens et al. (2016c) demonstrated that meteoroids from asteroidal-type showers (Geminids, Quandrantids) have lower beginning heights, which could be consistent with their current or past low perihelion orbits. Kikwaya et al. (2011) used the dustball model of Campbell-Brown and Koschny (2004) and simultaneous optical meteor observations to derive statistics on the bulk density of meteoroids: on average 4200 $\mathrm{kg\,m^{-3}}$ for asteroidal meteoroids and $3100 \pm 300$ $\mathrm{kg\,m^{-3}}$ for meteoroids with Jupiter-family cometary orbits, and 360 to 1500 $\mathrm{kg\,m^{-3}}$ for Halley-type cometary (HTC) orbits. Moorhead et al. (2017a) developed a two-population spatial density distribution model, describing densities for HTC-like ($T_j < 2$) and non-HTC-like ($T_j > 2$) orbits. More complex models that describe the composition and structure of meteoroids in order to correctly describe their fragmentation and ablation processes are needed (Campbell-Brown et al. 2013; Stokan and Campbell-Brown 2015).

Meteor spectra, with lines from both the ablated meteor atoms and atmospheric constituents, can provide important information about the meteoroid composition and parent body (Trigo-Rodriguez et al. 2003; Jenniskens 2007). Borovička et al. (2005) and Vojáček et al. (2015) use a classification system based on the strength of the Na, Fe and Mg lines given in a ternary diagram, which can be used to study the differences between Jupiter-family, HTC-like, and asteroidal meteoroids. Sodium depletion is found to occur in cometary meteoroids on orbits with low perihelia or potentially due to longer exposure times in the Oort cloud, or asteroidal meteoroids with high iron content. Jupiter-family comet meteoroids tend to have a higher Na content. Variations in the Na content of Geminid meteors might indicate variations in their emission times from their parent. Large-scale video spectra campaigns provide spectra for meteors and fireballs, in order to improve our understanding of the chemical composition and origin of sporadic and shower objects (Jenniskens et al. 2014; Rudawska et al. 2016).

### 4.3 Meteor Showers, Outbursts and Storms

If a cluster of meteors is observed to appear from a similar radiant in the sky and with a similar velocity, it is presumed that their orbits are related and that they have a common parent object. The directional and velocity information can be propagated backwards to the Hill sphere of the Earth in order to determine heliocentric trajectories, which can then be compared to known parent bodies - comets or near-Earth asteroids. Note that in older work, often an analytical correction called zenithal attraction was used instead of a backward orbit propagation (for a more detailed discussion, see e.g. Gural 2001). In some cases there are clear associations between meteor showers and parent objects, such as for the Perseid meteor shower and the Halley-type comet 109P/Swift-Tuttle. In other cases no apparent source object has been observed. Such a link might be established by a simple comparison of orbital elements, with the aid of a dissimilarity criterion, e.g. the D-criterion. It describes the dissimilarity between two orbits by using either a combination of orbital elements (e.g. Southworth and Hawkins 1963; Drummond 1981) or geometric parameters such as velocity or radiant (Valsecchi et al. 1999; Jopek et al. 2008). The D-criterion has to be used with a cutoff value, which has been tested recently by Moorhead (2016) and Neslušan and Hajduková (2017). They attempted to characterize the false-positive rate for D-parameter-based shower association. Various other authors have defined dissimilarity criteria (Southworth and Hawkins 1963; Drummond 1981; Jopek et al. 2008). Rudawska et al. (2015) use a combination of a dissimilarity criterion and other techniques to improve meteor shower searches in the EDMOND database. Wavelet transform techniques have been used to extract shower structure within large radar datasets (Galligan and Baggaley 2002; Brown et al. 2008; Pokorný et al. 2017).

The result of such searches is a database of meteor showers at the Earth, and of the structure in the interplanetary meteoroid cloud, as observed at the Earth. In the last $\approx 15$ years large datasets of video and meteor data from systems such as CMOR, SonataCo, CAMS, and SAAMER have expanded the existing database of known stream structure, with meteor radars such as CMOR and SAAMER probing the 100- μm to mm-size range (Brown et al. 2008; Pokorný et al. 2017), while video camera systems such as SonataCo, EDMOND and CAMS detect streams at cm sizes (Jenniskens et al. 2016a,b,c; Koschny et al. 2017). In particular, the southern hemisphere location of SAAMER and some CAMS stations have facilitated detection of a larger number of showers in a previously poorly surveyed region of the sky. The Meteor Data Center, administered by commission F1 of the IAU, maintains an online database of 'established', 'working' and 'pro tempore' showers (Jopek and Jenniskens 2011; Jopek and Kaňuchová 2014). As of 1 Jan 2017, 701 showers are listed: 112 established, 507 working, and 35 pro tempore (with 23 to be removed). There are also 24 (4 established, 1 pro tempore) shower groups. Less than half of these established showers have a known parent body, demonstrating the limits of knowledge on the origin of the structure in the interplanetary meteoroid cloud. Resolution of this issue requires a comprehensive study of the dynamical and physical (dust emission) history of potential parent bodies.

Modeling of the meteor showers has improved significantly over the last years (e.g., Vaubaillon et al. 2005) and benefits from enhanced computer resources, which now allow integration of the individual orbits of millions of meteoroids. However, our ability to fully model their dynamics and evolution is hampered by the lack of knowledge about the parent comets and their emission processes. Necessary parameters such as the ejection velocity are still poorly constrained (Ryabova 2013). Nonetheless, studies of specific meteor showers, coupled with modeling, provides important information on the parent bodies (comets and asteroids) and their dust emission processes, and on the dynamical and collisional processes that govern the behavior of these dust particles after emission. Observations of the

Camelopardalids in 2015 demonstrated that the mass distribution of particles in the stream leans toward untypically small particles, that are more easily observable by radar (Campbell-Brown et al. 2016). Ye et al. (2016) use the combination of meteor observations of the Camelopardalids, comet observations of the parent 209P/LINEAR, and dynamical studies of the dust emission to demonstrate that the comet may be near the end of its active lifetime. Studies of meteor shower groups such as the Taurid complex can illuminate the dynamical history of these streams, which may result from the dispersion of a parent body into a cascade of smaller objects and particles (Asher and Steel 1995; Dubietis and Arlt 2007; Jenniskens et al. 2016a). A full review of meteor shower studies beyond these individual examples is found in Jenniskens (2017).

### 4.4 Interstellar Meteors and Meteoroids

The presence of interstellar dust in the Solar system was confirmed by in-situ spacecraft measurements from Ulysses in 1992 (Grün et al. 1993a), and later Galileo (Baguhl et al. 1996; Altobelli et al. 2005), Helios (Altobelli et al. 2006) and Cassini (Altobelli et al. 2003, 2016).

Also, three likely contemporary interstellar dust particles of micron-size were brought back to the Earth by the Stardust sample return mission in 2006 (Westphal et al. 2014) and infrared space telescope observations indicated the presence of interstellar dust in the Solar system (Rowan-Robinson and May 2013). The measured and captured interstellar dust particles in the Solar system are typically smaller than a few microns. Their apparent speed relative to the Solar system is about 26 km $s^{-1}$ (Grün et al. 1994) and they generally come from a direction of 259° ecliptic longitude and −8° ecliptic latitude (Landgraf 1998; Frisch et al. 1999; Strub et al. 2015), due to the motion of the Solar system relative to the local interstellar cloud.

For the past two decades, a debate has existed about the presence of interstellar meteoroids in the meteor data from various radar, video and optical systems. This debate is important, because the detection of interstellar dust larger than a couple of microns may have large implications for the mass distribution and thus for the dust-to-gas mass ratio in the diffuse nearby interstellar medium. Reliable detection of big interstellar dust would provide more insight in the mixing of dust populations and about processes in the interstellar medium. Grün and Landgraf (2000) elaborate on the implications of big interstellar meteoroids in the interstellar medium.

Sub-micron-sized interstellar dust particles are coupled to the interplanetary magnetic field on scales of a few tens to a few hundreds of au when they travel through the Solar system. The dynamics of interstellar meteoroids in the Solar system differs from sub-micron particles in that they are influenced by mainly the Solar gravity and to a smaller extent Solar radiation pressure force, instead of by the Lorentz forces. Particles larger than a few tens of microns are thus considered uncoupled from the (local) interstellar and interplanetary magnetic fields because of their low charge-to-mass ratio (Grün and Landgraf 2000; Landgraf 2000). As a consequence, these could come from different directions than the stream of interstellar dust currently known from the in-situ data (depending on their ejection velocity) and these may directly represent their source direction. Meteoroids with velocities above about 73 km $s^{-1}$ are on unbound orbits from the Sun. This is the sum of the escape speed from the Solar system (42.1 km $s^{-1}$), the Earth orbital velocity in a head-on collision (30.3 km $s^{-1}$), and the effect of the terrestrial gravitational field (Taylor et al. 1996). Meteoroids with smaller velocities but above about 11 km $s^{-1}$ may still be interstellar, but cannot be classified as such by examining their velocity alone.

### 4.4.1 Radar Observations of Interstellar Particles

When cosmic dust particles larger than a couple of microns enter the atmosphere at high velocities, they ablate and leave a streak of ionized air that reflects the radar signals. Even though the radar limit of a minimum particle size of about 5 μm (Baggaley et al. 2007) is a disadvantage to detect interstellar dust because it typically is micron or sub-micron in size, the large detection surface of the Earth and the ability to detect large particles of several tens of microns and bigger, is an advantage and complementary to in-situ instruments and astronomical observations. A major challenge is the reliable estimation of the meteoroid velocity which determines whether a meteoroid is hyperbolic and hence, whether it is interstellar.

Taylor et al. (1996) announced the discovery of the first interstellar dust detections by radar in the Advanced Meteor Orbit Radar (AMOR) meteor data. These were coming from two distinct directions other than the known radiant of the (smaller) interstellar dust from the local interstellar cloud determined by in-situ measurements. Baggaley (2000) reported on the existence of a flux of particles coming from southern ecliptic latitudes, and on a discrete stream of interstellar dust particles coming from the direction of $\beta$-Pictoris: a main-sequence star with a debris disk. These particles are much bigger (tens of microns, about 40 μm) than the particles detected by in-situ instruments. However, the results—like from other radar-based studies—are highly debated (Hajduková 2016; Hajduková et al. 2018).

The Canadian Meteor Orbit Radar (CMOR) data have a larger minimum detectable radius of 100 μm (assuming particle bulk densities of 3000 kg m$^{-3}$ for masses of $1 \cdot 10^{-8}$ kg) (Weryk and Brown 2004). Two and a half years of data have been analyzed and a small fraction of 0.0008% was determined to be hyperbolic and thus not bound to the Solar system. The total statistics from this dataset were too low to distinguish a collimated stream of particles (Weryk and Brown 2004). The flux of particles derived from the observations is in line with the extrapolation of the size distribution of the data from Ulysses and Galileo (Weryk and Brown 2004), although they are likely from different populations. For all of these radar-based studies, meteoroids were only selected as "interstellar dust" when their heliocentric speed was larger than $3\sigma$ above the hyperbolic threshold, thus the numbers presented in these studies are lower boundaries. However, Moorhead et al. (2017a) re-analyzed data from CMOR with updated ionization efficiencies. Especially high-velocity meteoroids have lower speeds as a result. This was confirmed by Moorhead (2018), who shows that after applying a sharpening algorithm to the velocity distribution, no meteoroids with velocities larger than escape velocity are left.

Meisel et al. (2002) reports on interstellar meteoroids detected by the Arecibo radar, and uses different techniques for orbit and velocity determination especially as these particles are generally smaller than with the AMOR or CMOR radars.

### 4.4.2 Video and Optical Observations of Interstellar Particles

Video and optical methods have a higher accuracy for the velocity and radiant determination than radar (Baggaley 1999) and thus these are valuable complementary datasets for verification. Hajduková (1994) and Hajduková (2008) analyzed photographic and radar measurements from the IAU Meteor Data Center catalog and concluded that the majority of interstellar meteors were from velocity determination errors. Hawkes and Woodworth (1997) report on the detection of two interstellar meteoroids with video detectors. The meteoroids have estimated velocities of $4\sigma$ and $8\sigma$ above the hyperbolic escape speed of the Solar system. Hill et al. (2005) discusses meteor ablation for high velocities and concludes that these, with mass larger than about $10^{-8}$ kg, should be observable with optical methods. Musci et al.

(2012) reports on the search for interstellar particles in one year of data from a two station automated electro-optical system (the *Canadian Automated Meteor Observatory*), but found no convincing evidence for a collinear stream of interstellar dust, perhaps because of low statistics. Hajduková (2011) and Hajduková et al. (2014a,b) analyzed the SonotaCo and EDMOND video meteor data and also concluded from this study that the majority of the hyperbolic meteoroids were due to velocity measurement errors. For instance, about 50% of the identified hyperbolic meteors belonged to meteor showers. For SonotaCo and EDMOND, the limiting magnitudes are +2 and +4 respectively, corresponding to limiting masses of roughly $10^5$ kg, but this largely depends on meteor velocity (Hajdukova 2018, pers. comm.). If at all, then planetary perturbations have little influence on the hyperbolicity of the dust, hence most hyperbolic meteors were due to velocity determination errors. Wiegert (2014) confirmed that hyperbolic meteoroids can be generated by planetary perturbations of Solar system dust, but that the velocity of such locally generated hyperbolic meteoroids in the Solar system is only marginally larger than the heliocentric escape velocity at the Earth, and that the rate of locally generated hyperbolic meteors is relatively low (about one in every $10^4$ optical meteors).

Musci et al. (2012) summarize a few of the observations discussed above, together with in-situ data from spacecraft, in one plot. Although in many observations, a percentage of hyperbolic meteors are found, it seems from many studies, that the majority of these observations resulted from measurement errors. A comprehensive review of the radar observations of hyperbolic meteoroids is given in Hajduková (2016) and Hajduková et al. (2018), who show in their Fig. 2 the estimated interstellar dust flux from various observation methods.

## 5 In-Situ Measurements

The previous sections have described remote methods of studying the interplanetary meteoroid cloud. Here we discuss recent developments in the measurement of the meteoroid distribution in-situ. A history of in-situ detection up until the year 2000 is given in Grün et al. (2001).

### 5.1 Antenna Detections Using the STEREO and Wind Spacecraft

Cosmic dust striking a spacecraft surface at high velocity (more than a few km $s^{-1}$) vaporizes and ionizes upon impact, creating a transient plasma cloud near the spacecraft. The generation of this cloud perturbs the spacecraft floating potential and can be detected by instruments designed to measure electric fields in space.

Detections of cosmic dust using electric field antennas have been reported in a variety of dusty environments, including near the gas giant planets: Jupiter, (Tsintikidis et al. 1996), Saturn (Gurnett et al. 1983, 2004; Kurth et al. 2006; Meyer-Vernet et al. 2009a), Uranus (Meyer-Vernet et al. 1986; Gurnett et al. 1987), Neptune (Gurnett et al. 1991; Pedersen et al. 1991), and near comets (Giacobini-Zinner (Gurnett et al. 1986), Halley (Laakso et al. 1989; Neubauer et al. 1990), and P/Borrelly (Tsurutani et al. 2003).

More recently, dust has been observed using electric field instruments in the open Solar wind at 1 au, far from any known dust sources, both on the STEREO and Wind spacecraft (Meyer-Vernet et al. 2009b; St Cyr et al. 2009; Zaslavsky et al. 2012; Malaspina et al. 2014; Kellogg et al. 2016).

STEREO observes two populations of interplanetary meteoroids: beta-meteoroids, micron-sized dust coming from the direction of the Sun due to Solar radiation pressure (Zaslavsky et al. 2012; Malaspina et al. 2015), and nanometer dust (Meyer-Vernet et al. 2009b;

Zaslavsky et al. 2012). The Wind spacecraft observed micron-sized interplanetary dust, primarily grains one to two orders larger than the beta-meteoroids detected on STEREO (Malaspina et al. 2015; Kellogg et al. 2016). Wind does not observe nanometer dust (Kellogg et al. 2016).

The nanometer dust detected by STEREO has important implications for the dynamics of heliospheric dust and Solar wind plasma. Nanometer dust has a charge to mass ratio large enough that it can act as a massive pickup ion, getting accelerated to Solar wind velocities (about 400 km $s^{-1}$) away from the Sun through electromagnetic interactions with the interplanetary magnetic field (Czechowski and Mann 2010; Juhász and Horányi 2013). Because nano-dust can efficiently exchange momentum with the Solar wind, it can slow the Solar wind near its injection point. This effect has been observed in relation to destructive collisions between large bodies in the Solar wind (Lai et al. 2014), and could potentially play an important role in the evolution of the near-Sun Solar wind. Variations in the flux of nanometer dust observed at 1 au may also contain information about the rate of collisional grinding occurring in the near-Sun environment.

Finally, it is important to mention that a publicly accessible database of all dust impacts recorded by the Wind spacecraft over its 22-year mission (> 107 000 impacts as of 2015) was recently created (Malaspina and Wilson 2016). This database provides an unprecedented opportunity to study the flux and variation of interplanetary dust near 1 au over two full Solar cycles. The Wind dust database was recently made available (early 2017) through NASA's Space Science Data Facility Coordinated Data Analysis Web.[2]

### 5.2 Impact Dust Detector on New Horizons

The New Horizons mission was launched in January 2006 on an initial reconnaissance of the Pluto-Charon system (Stern 2008). After launch, New Horizons underwent a gravitational assist from Jupiter in February 2007 followed by nearly eight-and-a-half years of interplanetary cruise from Jupiter to Pluto. The Pluto-Charon fly-by was successfully executed in July 2015 and the spacecraft re-entered a period of interplanetary cruise through the Edgeworth-Kuiper Belt. An additional fly-by of Kuiper Belt object 2014 $MU_{69}$ is now scheduled for 01 January 2019.

While not part of the original payload, the Venetia Burney Student Dust Counter (SDC) was added to the manifest as a student-led project (Horányi et al. 2008). SDC is a polyvinylidene fluoride (PVDF) based impact dust detector, with heritage from laboratory designs (e.g. Simpson and Tuzzolino 1985; Simpson et al. 1989; Simpson and Tuzzolino 1989; Tuzzolino 1991, 1992; James et al. 2010) and previous instruments such as Space Dust (SPADUS, Tuzzolino et al. 2001a,b), the Dust Flux Monitor Instrument on Stardust (DFMI, Tuzzolino et al. 2003, 2004), the Cassini High Rate Detector (HRD, Srama et al. 2004), and the Cosmic Dust Experiment on-board the Aeronomy of Ice in the Mesosphere mission (Poppe et al. 2011). SDC operates by detecting individual dust impact events on twelve PVDF detectors mounted on the ram side of the New Horizons spacecraft. Two additional, identical detectors operate under the main deck of SDC, protected from any dust impacts in order to serve as references for the background noise rate from spacecraft vibrations (which can register as hits on PVDF detectors) and/or cosmic ray hits in the instrument electronics. When dust grains impact one of the twelve exposed PVDF films, they create micron-sized craters in the material inducing a change in electrostatic surface charge density on the PVDF detectors (Poppe et al. 2010a; Shu et al. 2013). This change in surface charge density is recorded by

[2] https://cdaweb.sci.gsfc.nasa.gov/index.html/.

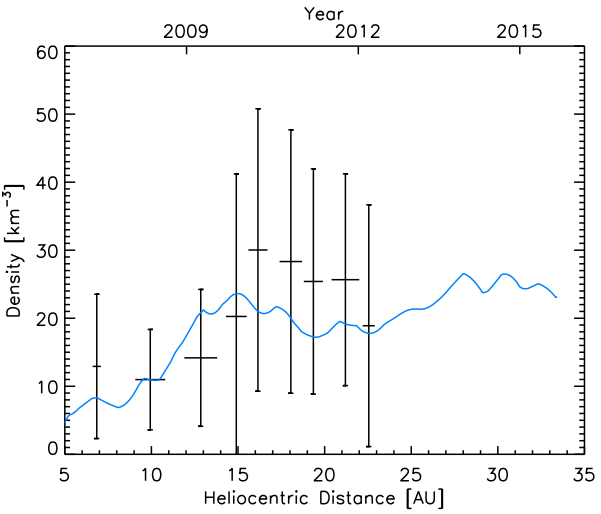


**Fig. 8** The spatial density of interplanetary dust grains with radii greater than 0.5 μm as measured by the New Horizons Venetia Burney Student Dust Counter as of 2013. The blue continuous line is a model prediction; the black bars indicate the measurements including their errors (reproduced from Szalay et al. 2013)

associated electronics and empirically calibrated to the dust grain mass assuming an impact speed. Impact speeds are calculated from the assumption that most grains can be approximated as being on circular, keplerian orbits. The keplerian velocity is then vector added to the New Horizons velocity to determine the impact speed. Based on ground calibrations, SDC is sensitive to dust grains with radii larger than approximately 0.5 μm. Between 0.5 and 5 μm, SDC can resolve the mass of the impacting dust grain, while for grains larger than $\sim 5$ μm, a hit is registered, however, internal electronics saturate and the size is only constrained to be greater than 5 μm.

SDC has operated successfully throughout the New Horizons mission, including through interplanetary cruise before the Jupiter encounter, through interplanetary cruise before and after the Pluto-Charon encounter, and for limited periods of time during the main Pluto encounter itself. First results from SDC were reported in 2010, approximately half-way through the interplanetary cruise to Pluto at 15 au (Poppe et al. 2010b) with later interplanetary results presented before the Pluto encounter at 23 au (Szalay et al. 2013). SDC measured fluxes of interplanetary dust grains greater than 0.5 μm between (2–5) $\times 10^{-4}$ m$^{-2}$ s$^{-1}$. Assuming heliocentric Kepler velocities for the dust grains and appropriately computing the relative impact velocity of these grains onto SDC, this equates to cumulative IDP densities $> 0.5$ μm of $\approx 10$ km$^{-3}$ between 5 and 15 au with an increase to $\approx$ 20–30 km$^{-3}$ between 15 and 23 au. Figure 8 shows the interplanetary dust spatial density measured by SDC as a function of heliocentric distance (Szalay et al. 2013). These invaluable data have been used to constrain models of interplanetary dust grain production in the outer Solar system (Han et al. 2011; Vitense et al. 2014; Poppe 2016), see Sect. 6 for further discussion. Within the Pluto-Charon system, SDC detected a single valid dust grain impact greater than $\approx 1.4$ μm in radius. Note that the instrument minimum detection threshold was raised for the Pluto encounter in order to filter out anticipated background noise (Bagenal et al. 2016). This is consistent with densities for grains $> 1.4$ μm in radius measured between 20 and 30 au before the Pluto encounter. SDC will continue to make measurements of the interplanetary dust flux through the Edgeworth-Kuiper Belt and beyond.

### 5.3 Impact Ionization Detectors—Recent Reanalyses

Impact ionization detectors have been flown on Ulysses, Galileo and Cassini. These detectors are able to provide orbital and mass information for detected grains, and in the case of the Cassini instrument, also compositional information. Those on Galileo and Cassini were designed to study the circumplanetary environments of Jupiter and Saturn. All three instruments, however, also sampled the interplanetary dust cloud, providing information on very small particle sizes up to a few microns. In addition, all three instruments also observed nano-dust particle streams originating from Io's volcanoes in interplanetary space near Jupiter (Grün et al. 1993c, 1996; Graps et al. 2000).

Ulysses flew a highly inclined orbit in order to explore the Solar polar regions. This allowed it to sample meteoroids outside the ecliptic plane, and in particular to observe interstellar dust (see Sect. 4.4). Outside of the ecliptic plane, accelerated beta-meteoroids were a dominant source (Wehry and Mann 1999; Wehry et al. 2004). The Staubach model of the interplanetary dust cloud (Grün et al. 1997; Staubach et al. 1997) is partially based on five years of Ulysses data, and is supported by further Ulysses dust data (Krüger et al. 2006, 2010).

Galileo and Cassini remained in the ecliptic plane during their cruise phases. Galileo's Dust Detection System (DDS) detected interplanetary particles during the cruise phase (Krüger et al. 1998). Cassini's Cosmic Dust Analyzer (CDA) detected both interplanetary particles in the inner planet region and between Jupiter and Saturn (Altobelli et al. 2007). The Chemical Analyzer of the CDA detected two iron-rich interplanetary dust particles, which have most probable orbits similar to Aten and Apollo asteroids, but the orbit uncertainty means they could also have Jupiter-family comet-like orbits (Hillier et al. 2007).

Normally particles are detected when they hit the back wall of the detector, then the direction of the particle can be constrained by the relative opening angle as seen from the back wall through the detector aperture. However, impacts may also generate a charge—and thus be detected—when hitting the side walls of the detector. This has only recently been taken into account (Altobelli et al. 2004). Neglect of this effect could lead to an overestimation of the rates of interplanetary particles (Willis et al. 2005).

## 6 Outer Interplanetary Dust and Meteoroid Cloud

In the outer Solar system, typically defined as outside Jupiter's orbit at 5.2 au, meteoroids originate from several sources, including Edgeworth-Kuiper Belt objects, Halley-type comets, Jupiter-family comets, and Oort Cloud comets (e.g. Liou et al. 1996a; Landgraf et al. 2002). Cometary bodies are known to release significant amounts of dust and gas through heating, sublimation, and disruption. Such activity is typically strongest in the inner Solar system, although cometary outgassing and disruption has been observed in the outer Solar system as well (e.g. Fulle 1992; Sekanina 1996; Kelley et al. 2013; Epifani et al. 2016). Dust production from Edgeworth-Kuiper Belt objects has also been long hypothesized, with mutual collisions (Stern 1995, 1996), bombardment by interstellar dust grains (Yamamoto and Mukai 1998), and bombardment by interplanetary dust grains (Poppe 2015) all theorized as possible production mechanisms. The relative balance between these hypothesized production mechanisms at EKBs is currently unclear and it is possible that all three contribute substantially. Dust grains can also be produced in the outer Solar system through grain-grain collisions, discussed in further detail below. Thus, the equilibrium distribution of dust in the

outer Solar system is comprised of contributions from various sources, each with their own individual spatial and velocity distributions.

As dust grains are shed from their parent bodies, several forces and processes affect both their dynamical and compositional evolution. Just as in the inner Solar system, meteoroids in the outer Solar system are subject to Solar and planetary gravity, Solar radiation pressure, Poynting-Robertson and Solar wind drag, and the electromagnetic Lorentz force as a result of grains becoming electro-statically charged (see review by Gustafson 1994). In the outer Solar system, gravitational forces from the Sun and the giant planets dominate. In the absence of planetary gravity, meteoroids will slowly spiral in towards the Sun due to Poynting-Robertson and Solar wind drag on the particle, with lifetimes in years as described in Sect. 2. For typical grains from the Kuiper Belt, the Poynting-Robertson drag lifetime assuming no planetary perturbations is about one million years per micron of radius (i.e., a 1-μm Kuiper Belt dust grain would spiral into the Sun in about 1 million years).

The role of the giant planets in sculpting the equilibrium spatial density distribution of interplanetary dust grains in the outer Solar system has long been recognized (Liou et al. 1996a; Liou and Zook 1997, 1999). As dust grains spiral inwards from their birth due to Poynting-Robertson and Solar wind drag, they encounter mean motion resonances (MMR) with planets. For Kuiper Belt grains, typically born outside the orbit of Neptune, trapping occurs mainly in neptunian MMRs. Such trapping can extend the lifetime of the dust grains by temporarily halting their inward progression due to Poynting-Robertson drag (e.g., Liou and Zook 1997, 1999; Moro-Martín and Malhotra 2002, 2003), potentially forming a circumstellar ring of dust grains just outside the orbit of Neptune.

In addition to dynamical perturbations, dust grains are subject to various mass loss processes that, over time, can significantly reduce the size of the grain relative to its size at birth. These mechanisms primarily include charged particle sputtering (e.g., Mukai and Schwehm 1981), photo-sputtering (Westley et al. 1995; Grigorieva et al. 2007b; Öberg et al. 2009), and grain-grain collisions (e.g., Borkowski and Dwek 1995; Stark and Kuchner 2009). Sputtering is the process of energetic particles or photons hitting the surface of a grain, releasing individual atoms, ions, or molecules from this grain.

Sublimation, a mass loss process that is highly effective in the inner Solar system, does not operate efficiently in the outer Solar system due to the far colder equilibrium grain temperatures (e.g., see Mukai and Schwehm 1981). It has been hypothesized by Kobayashi et al. (2010), however, that sublimation of icy grains from Edgeworth-Kuiper Belt objects may be responsible for the fairly flat distribution of interplanetary dust measurements by Pioneer 10 (Humes 1980) and Voyager (Gurnett et al. 1997). Such calculations would appear to be at odds with simulations by Grigorieva et al. (2007b), which showed that photodesorption (atomic or molecular species leaving a surface) is a highly efficient process even in the outer Solar system. Thus, icy grains would rapidly become $\beta$-meteoroids before being able to migrate inwards from their birth place in the Edgeworth-Kuiper Belt. The ultimate fate of icy grains generated from the Edgeworth-Kuiper Belt is still unclear and warrants further study.

Grain-grain collisions are also a critical process for the evolution of interplanetary dust grains, yet have only recently been successfully included in dynamical models (e.g., Stark and Kuchner 2009; Vitense et al. 2012). Stark and Kuchner (2009) have described a novel algorithm for incorporating the effects of grain-grain collisions on the calculation of equilibrium dust grain distributions in $N$-body simulations. This so-called "collisional grooming" technique operates by first producing a non-collisional spatial density distribution and then repeatedly recalculating the collisional degradation of the dust disk by computing the collisional history of each individual dust grain through the previous equilibrium spatial density distribution. Kuchner and Stark (2010) used this technique to model the Kuiper Belt, finding

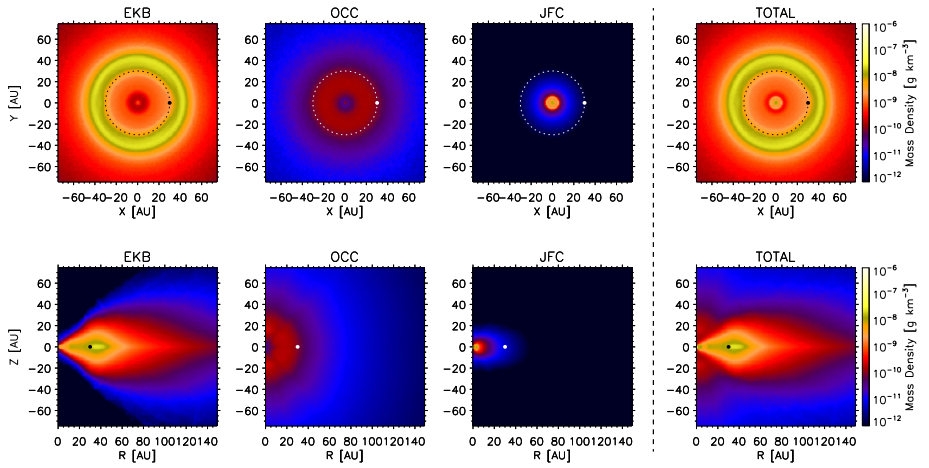


**Fig. 9** (top row) The modeled mass density of interplanetary dust grains from Edgeworth-Kuiper Belt objects (EKB), Oort Cloud comets (OCC), Jupiter-family comets (JFC), and total in the ecliptic plane. The dot and dotted line denotes the position and orbit of Neptune, respectively. (bottom row) Same as top row but in the meridional plane. From the model of Poppe (2016)

that collisions are an important process even in today's EKB dust disk. Later models of the Kuiper Belt debris disks have incorporated various forms of this technique for collisions, yielding similar results (e.g., Poppe 2016).

Several dynamical models have explored various aspects of the spatial density and velocity distributions of interplanetary dust in the outer Solar system including those by Liou and Zook (1999), Landgraf et al. (2002), Moro-Martín and Malhotra (2002, 2003), Kuchner and Stark (2010), Vitense et al. (2012, 2014), Han et al. (2011), and Poppe (2015, 2016). These models have progressively increased in both theoretical and computational sophistication over time. As an example, Fig. 9 shows the ecliptic and meridional mass density distributions of 0.5–100 μm dust grains for three separate families (Edgeworth-Kuiper Belt objects, or EKBs, Oort Cloud comets, or OCCs, and Jupiter-family comets, or JFCs) and the total, respectively, from the Poppe (2016) dynamical model.

EKB grains form a broad, $\approx 10$ au thick ring centered at 40 au, just outside the orbit of Neptune, while extending both into the inner Solar system and out past 150 au. The peak in mass density of $\approx 10^{-6}$ g km$^{-3}$ near 40 au indicates the primary birth location centered on the main Edgeworth-Kuiper Belt.

Reflecting the nearly isotropic inclination distribution of parent body comets (e.g., Dones et al. 2004), the OCC dust grains form a three-dimensional halo (or shell) in the outer Solar system centered between the orbits of Jupiter and Neptune ($\approx$ 5–30 au). Mass densities of OCC grains are estimated to be lower than that of Kuiper Belt grains, based on fits to Pioneer 10 and New Horizons SDC measurements (Poppe 2016).

JFC dust grains are highly concentrated within the orbit of Jupiter and do not extend beyond the orbit of Neptune in appreciable numbers. Nevertheless, JFC grains form the dominant dust species in the inner Solar system as shown by Nesvorný et al. (2010, 2011a).

Finally, the right-most column of Fig. 9 displays the total mass density in the outer Solar system. Kuiper Belt grains dominate the mass density in the ecliptic plane in the outer Solar system and beyond, with OCC grains dominating over Kuiper Belt grains only at high ecliptic latitudes.

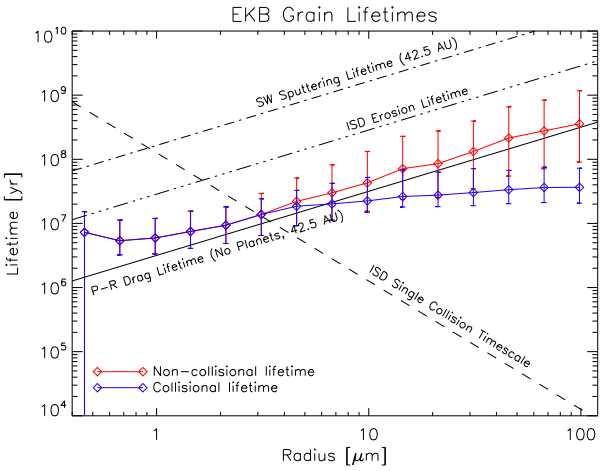


**Fig. 10** A comparison of relevant time scales for Edgeworth-Kuiper Belt grains, more explanations in the text. The red and blue lifetime curves are taken from the model of Poppe (2016), combining all the different processes

Figure 10 shows a comparison of various theoretical and dynamically modeled lifetimes for EKB grains as a function of grain radius in the outer Solar system from the model of Poppe (2016). Theoretically derived lifetimes include the Poynting-Robertson drag lifetime (solid black line) assuming zero initial eccentricity and an initial semi-major axis of 42.5 au (Wyatt and Whipple 1950; Burns et al. 1979), the lifetime due to erosion by interstellar dust grain impacts (dash-triple dot line), and the lifetime due to charged particle sputtering from the Solar wind assuming values at 42.5 au (dash-dot line). The time-scale for a single stochastic collision with an interstellar dust grain is shown as the dashed line. The ISD erosion lifetime is calculated from a characteristic ISD flux of $\Gamma_{ISD} \approx 10^{-4}$ m$^{-2}$ s$^{-1}$ and grain size of 0.5 μm (Grün et al. 1997), and an impact cratering yield from Borkowski and Dwek (1995). The Solar wind sputtering lifetime is calculated assuming a Solar wind composition of 97% protons, 3% alphas ($He^{++}$), a flux at 1 au of $\Gamma_{sw} = 10^8$ cm$^{-2}$ s$^{-1}$ with radial dependence as $r^{-2}$, and proton and alpha sputtering yields of $10^{-2}$ and $10^{-1}$, respectively (Biersack and Eckstein 1984; Behrisch and Eckstein 2007). The dynamical lifetimes of dust grains subjected to the full panoply of forces as described in Poppe (2016) is shown in color for both non-collisional (red) and collisional (blue) cases. For all sizes, the non-collisional lifetimes are slightly higher than the theoretical P-R drag lifetime. The relatively broad error bars (representing the 10% and 90% levels) are due to the broad range of initial semi-major axes and eccentricities in the dynamical model. As the grain size increases, the non-collisional lifetime scales as the radius, in agreement with theory. In the collisional case, dust grain lifetimes are identical to those in the non-collisional case for radii of ≈ 3 μm or less. Grains with radii larger than ≈ 3 μm have lifetimes that asymptote to a maximum of approximately $3 \times 10^7$ years, significantly shorter than either the dynamical or theoretical lifetimes. While subject to some uncertainty given model assumptions, the transition between transport-dominated dust grains and collisionally-dominated dust grains in the Kuiper Belt occurs near 3 μm. Note also that Solar wind sputtering and ISD collisional erosion are much longer processes than Poynting-Robertson drag transport and interplanetary grain-grain collisions. The grain radius at which the collisional lifetime (blue) is equal to the approximate Poynting-Robertson drag lifetime in the absence of planets (solid line), termed the "critical radius", occurs near ≈ 7 μm, similar to that found by Kuchner and Stark (2010) in their dynamical, collisionally groomed model of the EKB dust disk. Strictly speaking, Kuchner and Stark (2010) found a critical radius for the EKB near 15 μm. However, given various

model assumptions, the agreement between Kuchner and Stark (2010) and Poppe (2016) is good.

## 7 Meteorites

### 7.1 Overview

Meteorites are the surviving pieces of a meteoroid or asteroid passing through the atmosphere. Most of them come from chondritic bodies, primitive asteroids formed in the early Solar system which never reached the melting limit temperature in their interiors. Because of this, they have preserved chemical clues of the early Solar system (see e.g. Trieloff et al. 2003; Scott and Krot 2003) which can be directly measured in ground-based laboratories. Figure 11 shows a graphical representation of the classification of these objects, whose relevant properties will be addressed in detail in this section. Besides chondrites, stony achondrites, stony-iron, and iron meteorites exist. However, these comprise only about 7% of our meteorite collection, and are therefore not discussed here.

When linking meteorite properties to those of meteoroids, selection effects need to be taken into account. Only meteoroids larger than typically tens of centimeters in size will survive the passage through the atmosphere; smaller objects will completely disintegrate and not reach the ground. The material properties will also play a role - very fragile material will break apart more easily in the atmosphere than compact material. Only under rare circumstances, e.g. very shallow entry angles, can fragile material be recovered on the ground, as has happened for the Tagish Lake meteorite fall (Brown et al. 2000).

'Chondritic' means that they contain chondrules, about 1 mm-sized objects of glass and crystalline silicates formed by melting followed by rapid cooling. They also contain Ca- and Al-rich inclusions (CAIs) formed by condensation of high-temperature nebular gas. CAIs are composed mainly by refractory oxides and silicates. Other components in chondrites

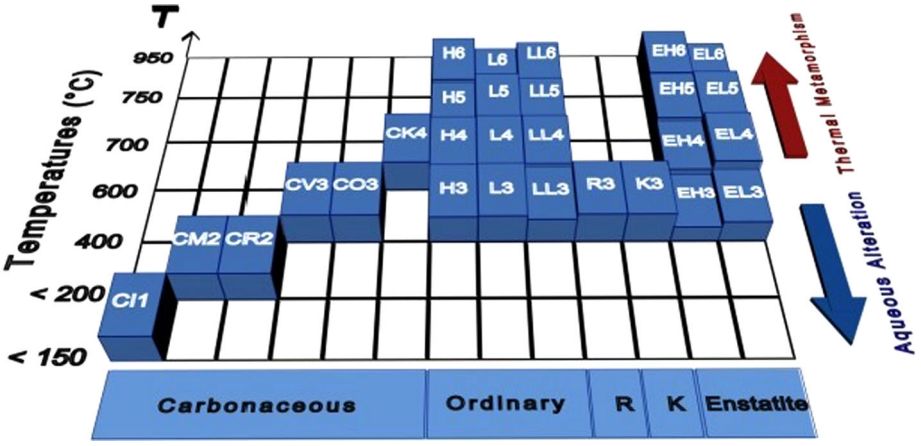


**Fig. 11** Classification of chondritic meteorites. This basic diagram is useful for a general understanding of the key processes modifying asteroidal compositions over time. They are grouped in classes (carbonaceus, ordinary, R, K, and enstatite). The letters indicate so-called groups. The number indicates the thermal metamorphic grade (image E. Dotto)

are fine-grained matrix material (Brearley and Jones 1998) and a very small amount of tiny particles formed in other stars (Huss 1997; Messenger et al. 2003; Zinner 2003).

The classification is done based on mineralogical and petrologic characteristics, as well as chemical and isotopic compositions, see Fig. 11. The first letter in the figure denotes the class, the second a subclass. For carbonaceous meteorites, the second letter is based on the name of the first meteorite found in that subclass. L, H, and LL stand for low iron, medium iron, and low iron and low metal, respectively. 15 subclasses are known (Weisberg et al. 2006), 13 of which are shown in the figure.

### 7.2 Petrologic Types

Within the chondritic group, six different so-called thermal metamorphic grades or petrologic types have been defined, depending on their thermal or aqueous processing. These are marked by numbers in Fig. 11. Types 1 and 2 denote meteorites affected by aqueous alteration at low temperatures (Trigo-Rodríguez 2015). These groups come from water-bearing early-formed small asteroids, or larger asteroids formed later that never suffered significant radioactive heating since most of the nuclides responsible for heating were already gone. Type 3 is represented by chondrites that experienced little aqueous alteration and metamorphism, so they can be considered the most pristine chondrites. Thermal metamorphism increasingly affected petrologic types 3 to 6, type 6 being the most affected by in-situ parent body heating and shock-induced melting. A comprehensive review on the thermal metamorphism experienced by all chondrite groups has been published by Huss et al. (2006). In summary, the degree of thermal metamorphism and aqueous alteration is highly variable among the different chondrite groups as a consequence of different degrees of processing on the parent body.

### 7.3 Evolution of Meteorites

After formation of the chondritic bodies through accretion of planetesimals in the early Solar system, most of them soon became exposed to impacts with other bodies (Beitz et al. 2016). After being bombarded over 4.5 Gyr, these bodies exhibit impact-excavated structures, and have suffered significant erosion of their surfaces.

Progressive collisional gardening excavates craters and produces dust and meteoroids with enough energy to escape the gravitational field of their parent bodies. These erosive processes deliver chondritic material to Earth and other terrestrial planets. The observed chemical differences in the 15 known subclasses support the idea that each of them was formed in a different reservoir, probably from the separate rings observed in disks found around young stars (Zhang et al. 2015). This idea has been reinforced by the fact that relatively few chondrite breccias exist that contain clasts belonging to different chondrite groups (Bischoff et al. 2006). Primitive asteroids are covered by pebbles produced by continuous impacts that have excavated and fragmented their surfaces, called regolith. Consequently, chondrite breccias are mainly formed by the compaction of this asteroidal regolith under the action of impacts, whereas at the typical encounter velocities the original projectile material would be preferentially vaporized.

Meteorite breccias have complex and diverse constituents, often containing different lithologies, as measured e.g. in the Almahatta Sitta meteorite (Bischoff et al. 2010). This provides evidence for the substantial mixing of material in the early Solar system, as predicted by dynamical models as a consequence of the migration of the giant planets (see e.g. DeMeo and Carry 2014).

### 7.4 Ordinary Chondrites

It is estimated that about 500 meteorites reach the surface of our planet every year, most as small rocks with a mass of few grams (Halliday et al. 1996). Nowadays, meter-sized ordinary chondritic meteoroids (hereafter OCs) dominate the current terrestrial flux, but their parent asteroids (S spectral type, Gaffey and McCord 1978) represent only about the 17% of the asteroids in the main belt. The reason for OCs being the most common meteorites reaching our planet is because the composition is dominant for asteroids located between the inner belt and the near-Earth region (Gradie and Tedesco 1982). In addition, most asteroids are covered by regolith grains that have been exposed to space weathering over the eons, significantly modifying their reflectance properties and mineralogy. This was first measured by the Hayabusa sample return mission from asteroid 25143 Itokawa, (e.g. Nakamura et al. 2011b).

From the study of almost fifty thousand OCs available in meteorite collections,[3] we know that they have experienced different degrees of thermal metamorphism. The reason is that they come from moderately large chondritic asteroids that were fractured by large impacts, ejecting chondritic materials that were buried at different depths in their interiors. It is thus not easy to find pristine chondrites among the different subclasses of ordinary chondrites (H, L, and LL). Only a few examples exist, e.g. LL3.0 Semarkona, and LL3.1 Bishunpur (Mostefaoui et al. 2004). These few well-preserved rocks contain highly unequilibrated material, whose study reveals that most chemically homogenized OCs have suffered significant mineralogical and chemical modifications. This is associated with heating induced by radiogenic decay, and shock-induced annealing from impacts. The heat associated with these processes was cementing OCs together, i.e. they chemically reacted to produce asteroids with higher strength, less bulk porosity and higher bulk density (Trigo-Rodriguez and Blum 2009; Moyano-Cambero et al. 2017). The collisional products of such asteroids have been proved to be different of those coming from fragile aggregates (Blum et al. 2006).

Chondrite materials that have experienced thermal processing over the eons become progressively "cooked" and compacted (Huss et al. 2003; Trigo-Rodríguez and Blum 2008). These properties are important because the collisional products of these bodies depend on the processes having occurred on asteroids (Flynn and Durda 2004). In fact, laboratory experiments to produce aggregates as proxies of chondrites have demonstrated that the parent bodies of chondrites accreted as highly porous bodies (Blum et al. 2006). Subsequent large impacts collapsed pore spaces and produced shock heating, resulting in fragmented and compacted objects (Beitz et al. 2016). This thermal processing homogenized the chemical composition of the chondritic components, resulting in different levels of asteroid compaction depending on the amount of volatiles which acted as a buffer for the impact-delivered heat (Trigo-Rodriguez and Blum 2009; Beitz et al. 2016).

### 7.5 Carbonaceous Chondrites

Carbonaceous chondrites (CCs) are associated with bodies formed around or outwards the protoplanetary disk snow line (Brearley and Jones 1998). Their main parent asteroids are called C-type, constituting about 80% of the main belt asteroids. Their spectra indicate a relatively high amount of carbon compounds, that make them extremely dark objects (Fornasier et al. 1999). These asteroids are located in the outer half of the asteroid belt, and their surfaces have very low visible albedos of 0.03–0.09 (Jewitt et al. 2007; Trigo-Rodríguez

[3] Meteoritical Bull. Database: https://www.lpi.usra.edu/meteor/metbull.php.

et al. 2014). The asteroids have low densities, similar to the CCs they produce, ranging from about 2 $g\,cm^{-3}$ for the ones with a significant content of water and porosity, to 3.5 $g\,cm^{-3}$ for the driest and Fe-rich ones (Britt and Consolmagno 2000). Among these CCs, the CI and CM groups are associated with transitional objects with significant abundance of water, mostly as hydrated minerals that could have exhibited cometary activity at some point of their evolution (Trigo-Rodríguez 2015). They experienced extensive aqueous alteration, and many of them escaped thermal metamorphism.

They contain phyllosilicates as major phases, serpentine in CM and sponite-serpentine mixed layers for CI chondrites. Some CM and CI chondrites were heated and dehydrates after aqueous alteration, as summarized in Nakamura et al. (2005). This indicates that a dehydration process is common in the hydrated C-type asteroids, as also suggested by reflectance spectra (Hiroi et al. 1993).

CO, CV, and CR chondrites suffered much less severe aqueous alteration, but some CVs and CRs are certainly moderately aqueously altered as well. Thermal metamorphic grades for these groups are ranging from low (3.0) to nearly type 4 (Scott and Jones 1990; Russell et al. 1998), except for the CV and CK groups that can have members with higher values. In general, carbonaceous chondrites can be considered "pristine" as they retain a bulk chemistry close to Solar abundance. But only a few meteorites retain highly unequilibrated mineral assemblages relatively unaffected by thermal and aqueous modifications. The most primitive CCs identified so far are the CO chondrite ALHA77307, the CM2 chondrite Yamato791198, and the CM-like un-grouped chondrite Acfer094 (Rubin et al. 2007).

The degree of metamorphism in chondrites reflects thermal effects associated with burial due to self-gravity, or with the propagation of heat in shock waves generated in collisions (Scott and Krot 2003). Chondritic materials have then experienced such thermal processing over the eons, and become progressively "cooked" and compacted (Huss et al. 2003; Trigo-Rodriguez and Blum 2009). These properties are important as the meteorites are the collisional products of asteroids on which these processes have occurred (Flynn and Durda 2004), thus letting us constrain the asteroid's evolution. Laboratory experiments to produce aggregates as proxies of chondrites have demonstrated that the parent bodies of chondrites accreted as highly porous bodies, see Blum et al. (2006). Large impacts contributed to collapse pore spaces and produced shock heating, so most asteroids are fragmented and compacted objects (Beitz et al. 2016). This thermal processing homogenized the chemical composition of the chondritic components forming asteroids. They were compacted to different extents, depending on the amount of volatile material acting as a buffer of the impact-delivered heat (Trigo-Rodriguez and Blum 2009; Beitz et al. 2016).

### 7.6 Other Classes

Other classes are less relevant here, but mentioned briefly for completeness: Rumuruti (R) chondrites are a new chondrite group formed mostly by brecciated meteorites with chemical patterns that differ from carbonaceous, ordinary, and enstatite chondrites. The Kakangari (K) chondrite group have a similar set of petrologic and oxygen-isotopic characteristics that distinguishes them from other chondrite groups. Enstatite chondrites are chemically reduced meteorites, with most of their iron taking the form of metal or sulfide rather than an oxide, and being mostly formed by the mineral enstatite (MgSiO3), from which they derive their name.

### 7.7 Summary

Summarizing, as a direct result of the collisional processing of chondritic bodies which dominates the population of asteroids and possibly comets, most of the interplanetary space

contains rocks and particles of chondritic nature. Fragile, water-bearing bodies such as C- and D-type asteroids and comets are the main contributors to the interplanetary dust and meteoroid cloud, see e.g. Engrand and Maurette (1998). As a direct consequence, most meteoroids ablate in the terrestrial atmosphere producing a luminous phase that usually exhibits chondritic bulk elemental chemistry (Trieloff et al. 2003; Trigo-Rodríguez et al. 2004). Only recently, researchers started to directly study the ablation of chondrites in the laboratory. This allows obtaining new clues about the delivery of chondritic materials to Earth by simulating the factors regulating the ablation of meteoroids in the Earth's atmosphere (see e.g. Gómez Martín JC et al. 2017). Chondritic material is also important from an astrobiological perspective. Its rock-forming minerals, under aqueous alteration and in presence of Nitrogen-bearing species, are able to catalyze extremely diverse organic species (Rotelli et al. 2016). These findings are relevant as they show a natural way of increasing the chemical complexity as needed to explain the ubiquity of life in planetary bodies (Trigo-Rodríguez et al. 2017).

## 8 Dust Particle Collection

### 8.1 Introduction

The interplanetary dust environment in Earth orbit was investigated by the deployment of dust collectors on the Gemini 10 mission, the Long Duration Exposure Facility (LDEF), the MIR Space Station, and the Space Shuttle, as well as by the examination of space-exposed surfaces retrieved during the repair of the Solar Maximum satellite and the Hubble Space Telescope. Elemental analyses of the residue left in impact craters from the LDEF experiment identified three major classes of extraterrestrial materials, particles with roughly chondritic abundances of Fe, Mg, and Si suggestive of fine-grained aggregates, mono-mineralic silicates, and Ni-Fe-sulfides (Horz and Bernhard 1992), as well as a population of man-made particles.

The LDEF experiment yielded a measure of the meteoroid mass flux at the top of the Earth's atmosphere. This flux is dominated by particles around 250 μm diameter, and accounts for $30\,000 \pm 20\,000$ tons/year (from Love and Brownlee 1993). This is $\sim 1000$ times the contemporary flux of meteorites (Bland et al. 1996).

As discussed previously, interplanetary dust particles can enter the terrestrial atmosphere with velocities varying between $\sim 11$ km s$^{-1}$ to $\sim 73$ km s$^{-1}$, depending on the origin of the particles. As early as 1937, Opik recognized that small particles entering the Earth's atmosphere could radiate away heat as rapidly as it was being regenerated by friction in the atmosphere, allowing them to survive entry. Detailed modeling by Whipple (1950) indicated that particles around 10 μm in size could survive atmospheric entry without severe heating, particularly those particles having the lowest bulk densities and entry speeds. Although small particles at the surface of the Earth are dominated by local dust, the anticipated survival of interplanetary dust motivated high-altitude collection efforts by rockets, balloons, and eventually aircraft. For larger particles ($> 25$ μm), the high speed impact with the atmosphere causes the evaporation of a large fraction of the incoming dust, but $\sim 20\%$ of them reach the terrestrial surface (Taylor et al. 1998; Duprat et al. 2006; Plane 2012) and can be collected on Earth, either in the stratosphere (Brownlee 1985), in the polar caps from ice/snow (Maurette et al. 1987, 1991; Yada and Kojima 2000; Nakamura et al. 2001; Duprat et al. 2007) or by being trapped in ice in the transantarctic mountains (Rochette et al. 2008). Dust particles reaching the Earth from space deposit on the surface to form sediments, at a rate as slow

as 1 particle $m^{-2}$ $day^{-1}$ (Brownlee et al. 2006). The effects of the vaporized material on the atmosphere are discussed in Plane et al. (2018).

For historical reasons, particles collected in the stratosphere are called "Interplanetary Dust Particles" (IDPs). Their sizes range typically from a few µm to ∼ 50 µm. Particles collected in polar caps are named "micrometeorites" (MMs), and have larger sizes, from ∼ 25 µm to ∼ 1 mm. The difference in the size ranges between IDPs and MMs is due to the collection mode, and these two collection techniques are complementary.

The stratospheric collection of IDPs is inherently biased. Particles smaller than a micron or so in diameter are generally trapped in the air stream, and flow past the collector, while the abundance of particles > 50 µm in diameter is so low that few are ever collected. After flight, particles are removed individually from the collectors and examined optically and by electron beam instruments, allowing them to be characterized as "cosmic", "possibly cosmic", "natural terrestrial", or "man-made terrestrial" material. Even at the collection altitude, a majority of the particles are terrestrial material, either naturally occurring dust or man-made particles such as rocket exhaust. Due to their very low bulk densities, the more porous particles settle more slowly, so they are preferentially collected at these altitudes. Further, all Earth collections are biased by gravitational focusing, which significantly enhances the flux of particles with the lowest geocentric velocities.

IDPs and MMs collected on Earth originates both from asteroids and comets. Recognizing their origin requires comparing their characteristics to those of meteorites and comets. So far two families of cosmic dust of probable cometary origin have been proposed both in the IDP and micrometeorite collections. The abundance of icy and carbon-rich asteroids in the asteroid belt has recently been revisited (DeMeo and Carry 2014) and they are underrepresented in the meteorite collections, possibly due to preferential destruction of carbonaceous chondrites on Earth, during atmospheric entry or by weathering on Earth. The cosmic dust collected on Earth could be more representative of the interplanetary matter than meteorites.

### 8.2 Interplanetary Dust Particles (IDPs) Collected in the stratosphere

NASA has been collecting IDPs from the Earth's stratosphere since 1981. U2, ER2 and WB-57 aircrafts collect IDPs at altitudes between 17–20 km, with flight durations from a few hours to 65 hours (Brownlee 1985). Collector plates covered with a layer of high viscosity silicon oil, which needs later to be rinsed from the particles, are deployed to collect particles from the stratosphere by impact.

Due to their small sizes, IDPs, like the ones shown in Fig. 12, usually do not suffer from extreme atmospheric entry heating effects. Ceplecha et al. (1998) give a size limit of roughly 10 µm; the precise values depend on the velocity. IDPs are classified according to their composition into two main categories: chondritic IDPs, with a bulk chemical composition compatible with the average chondrite composition; and non-chondritic IDPs, e.g. large single crystals of silicates, Fe-sulphide minerals, or refractory minerals (e.g. McKeegan 1987a; Zolensky 1987). Chondritic IDPs are in turn classified according to their mineralogy, i.e. olivine-, pyroxene-, or layer-lattice-silicate-dominated, or by their textures: (i) chondritic porous, abbreviated CP; (ii) chondritic filled, less porous than CP IDPs; and (iii) chondritic smooth IDPs, abbreviated CS (e.g. Bradley 2005; Flynn et al. 2016).

CP IDPs are unequilibrated aggregates of mostly sub-micron grains of diverse compositions, sampling a wide variety of formation conditions. Most CP IDPs have never experienced any significant hydrous or thermal parent body processing, gravitational compaction, or impact shock, which have affected most meteorites, and many were minimally heated during atmospheric deceleration. They have a chondritic composition for the major rock-forming elements (Fig. 13). These CP IDPs consist mainly of anhydrous crystalline phases,

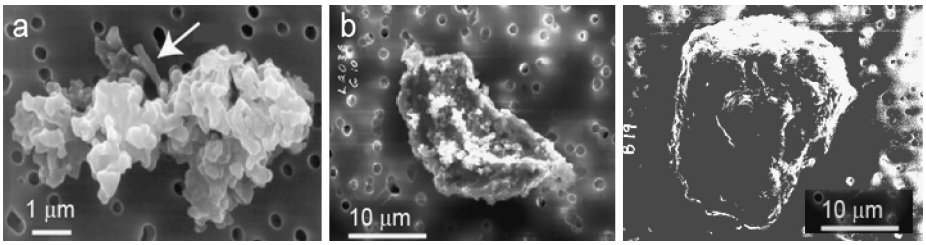


**Fig. 12** Typical IDPs include: (left) anhydrous aggregate CP-IDPs, (center) single mineral IDPs, and (right) compact, hydrous IDPs. The arrow in the frame points to a pyroxene whisker

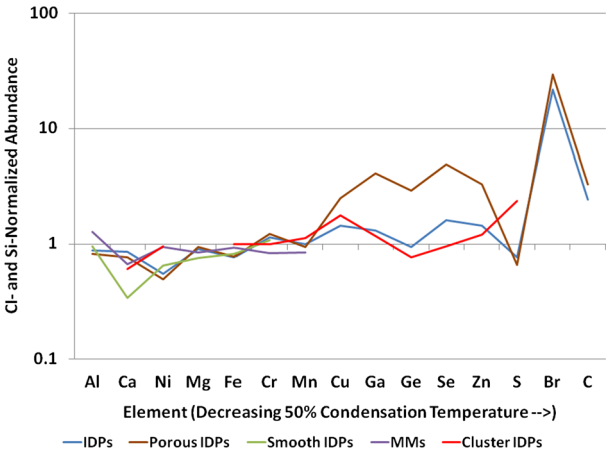


**Fig. 13** Si- and CI-normalized elemental abundance patterns in representative samples of IDPs, porous (CP) IDPs, smooth IDPs, micrometeorites, and Larger Cluster IDPs. The IDPs are collected in silicone oil, which is never completely removed by hexane washing, so the IDP data is typically Fe-normalized. The Si-normalized values shown were generated assuming a Si/Fe ratio as in CI meteorites (adapted from Flynn et al. 2016)

mostly Mg-rich olivines, pyroxenes and low-Ni Fe sulphides (Bradley 2005), as well as primitive glassy components called Glass Embedded with Metals and Sulphides (GEMS) that may be of pre-Solar interstellar origin (Bradley 1994; Klöck and Stadermann 1994; Bradley et al. 1999). These highly unequilibrated IDPs, containing individual olivine and pyroxene grains, span a wide range of Fe contents, with Mg/(Mg + Fe) varying from nearly 100 to ∼ 50 mol%. The mineralogy of CP IDPs is compatible with that of comets Halley and Hale-Bopp (e.g. Hanner and Zolensky 2010, and references therein).

Detailed studies of the CP IDPs indicate that they are the most primitive materials of the Solar system currently available for laboratory study (Ishii et al. 2008), providing the best available samples of the materials present in the Solar protoplanetary disk. Low-Fe, Mn-enriched olivines, commonly observed in CP IDPs and sometimes found in unequilibrated ordinary chondrite meteorites, as well as exotic whisker (Fig. 12) and platelet morphologies of the crystalline silicate enstatite found in CP IDPs have been proposed to form directly as a high temperature condensates from the disk (Ishii et al. 2008, and references therein). A comparative study of the sizes of the crystalline Mg-rich silicate and the Fe-sulfides, the two most abundant phases in CP IDPs, shows that the mean constituent grain size varies from one CP IDP to another. They have a size-density relationship that can be explained with an aerodynamic-type sorting mechanism operating in the disk prior to grain aggregation (Wozniakiewicz 2012). In many CP IDPs the individual mineral grains are coated with a thin (∼ 100 nm) layer of organic carbon (Flynn et al. 2013), consistent with modeling by Ciesla and Sandford (2012) showing that ultraviolet and thermal processing of ice coated grains

in the cold, outer Solar nebula can produce complex organic molecules. These organic rims likely aided in the grain aggregation in the Solar nebula (Flynn et al. 2013), since bare crystalline grains can stick together only in very slow collisions.

The composition of hydrated IDPs is broadly chondritic, with a depletion in Ca (Fig. 12), likely related to an aqueous alteration event on their parent body (Schramm et al. 1989). The mineralogy of hydrated IDPs is dominated by phyllosilicates and carbonates, and also contains Ni-rich Fe sulphides like pentlandite. The phyllosilicates are usually smectite, possibly linking some of them to CI chondrites (Keller et al. 1992), although most hydrated IDPs still contain anhydrous parts, with is not the case for CI chondrites that have been fully aqueously altered.

Both the CP IDPs and the CS IDPs are significantly enriched in C over the most carbon-rich meteorites, with C contents ranging from $\sim 5$ to $\sim 45$ wt% (Keller et al. 1994).

Large isotopic anomalies interpreted as pre-Solar interstellar signatures have been found in IDPs, both in the organic matter and in the mineral components, including GEMS and silicates (Messenger 2000; Messenger et al. 2003; Floss and Stadermann 2004). Oxygen, which is the most abundant element in chondritic materials, varies with heliocentric distance within the Solar system. Isotopic imaging of IDPs demonstrates that some sub-micron grains have O isotopic ratios outside the range seen in Solar system materials, suggesting these grains formed in outflows or explosions of previous generations of stars and survived the incorporation into the Solar system without equilibration (Messenger et al. 2003). Some of these IDPs also exhibit elevated D/H ratios (Zinner et al. 1983; McKeegan et al. 1985; McKeegan 1987b; Messenger 2000).

It has been proposed that a large proportion (if not all) of CP IDPs could be of cometary origin (e.g. Bradley and Brownlee 1986; Ishii et al. 2008, and references therein). Vernazza et al. (2015) proposed that anhydrous IDPs could originate from icy asteroids.

### 8.3 Micrometeorites Collected in the Polar Caps

Micrometeorites ranging from $\sim 25$ μm to $\sim 500$ μm have been most efficiently collected from ice or snow in the polar caps: in Greenland (Maurette et al. 1986, 1987) and in Antarctica (Maurette et al. 1991; Taylor et al. 1998, 2000; Yada and Kojima 2000; Nakamura et al. 2001; Duprat et al. 2007). Larger micrometeorites up to $\sim 1$ mm with older terrestrial ages in the order of Myr have been collected at the surface of the transantarctic mountains (Rochette et al. 2008).

Since MMs are larger than IDPs, they suffer more extensively from atmospheric entry effects. They are first classified according to the textures resulting from atmospheric entry heating (Genge et al. 2008):

- unmelted particles comprising fine-grained particles (Noguchi et al. 2017);
- partially melted scoriaceous particles;
- and fully melted cosmic spherules (CS), see Fig. 15 and Duprat et al. (2007).

In terms of composition, two main families are found in the MM collections: the chondritic particles ($\sim 99\%$ of the particles, both anhydrous and hydrated), and the ultra-carbonaceous particles that have been identified in the last decade (Nakamura et al. 2005; Duprat et al. 2010), see Fig. 14.

Chondritic micrometeorites $< \sim 500$ μm are mostly related to the carbonaceous chondrites (Kurat et al. 1994; Engrand and Maurette 1998; Herzog et al. 1999; Engrand et al. 2005; Genge 2008; Genge et al. 2008; Dobrică et al. 2009), whereas larger micrometeorites show more affinity with ordinary chondrites, which dominate the meteorite collections (van

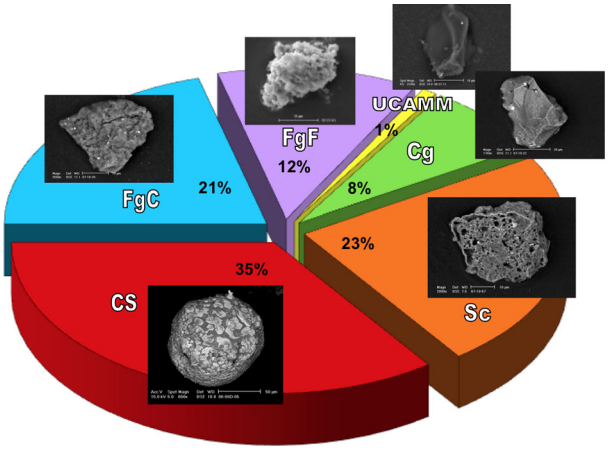


**Fig. 14** Proportion and types of MMs from the Concordia collection (updated from Dobrică et al. 2010)

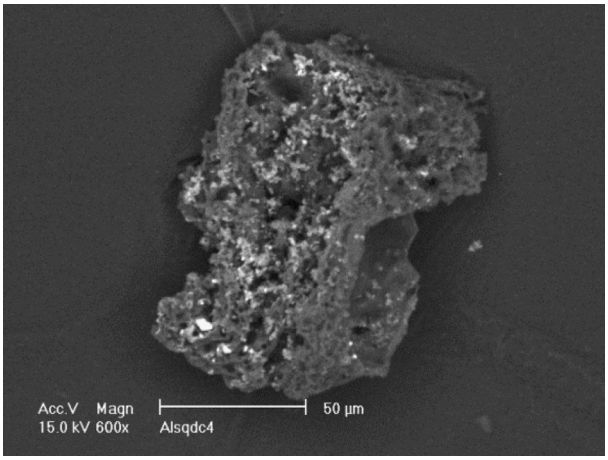


**Fig. 15** Backscattered electron micrograph of Concordia Ultracarbonaceous Antarctic Micrometeorite (UCAMM) DC02-11-19. All dark gray patches are constituted of organic matter. Brighter flakes are silicates or Fe-Ni sulphides

Ginneken et al. 2017). The chondritic MMs exhibit a composition for major and minor elements that is comparable within a factor of 2 to the bulk CI composition (Dobrică et al. 2009). The mineralogy of anhydrous MMs is dominated by crystalline silicates, mainly olivine and low-Ca pyroxene, followed by Fe–Ni sulfides in abundance. The olivine compositions range from almost pure forsterite (Mg-olivine) to relatively high Fe-olivine, up to Fe/Mg about 1. The low-Ca pyroxenes show a similar range of Fe contents (van Ginneken et al. 2017). The mineralogical compositions, in particular the composition of the olivines, show that the constituents of cosmic dust have sampled a wide range of conditions in the protoplanetary disk.

The number ratio of pyroxene versus olivine in micrometeorites is about 1, while it is on the order of 0.2 in CM chondrites, which are the closest relatives to MMs in the meteorite collections (Kurat et al. 1994; Engrand and Maurette 1998). The CR chondrites are the only carbonaceous chondrites with a high abundance of pyroxenes relative to olivines. Since Fe-Ni sulfides are ubiquitous, they can be used for comparison between families of extraterrestrial objects. In MMs, most Fe-Ni sulfides show a composition close to that of troilite, containing less than 3 wt% of Ni. Pentlandite is only rarely detected, mainly in scoriaceous MMs (Engrand et al. 2007). Refractory minerals (spinel, anorthite, melilite, hibonite, Ca-Al-

rich pyroxene, and perovskite) or refractory inclusions have been reported in a few dozen of micrometeorites (e.g. Hoppe et al. 1995; Engrand et al. 1999c; Genge et al. 2008). The relative abundance of MMs containing refractory minerals or inclusions is less than 1%. Chondrules are also rare in MMs, but present in the coarse-grained population of micrometeorites (Walter et al. 1995; Kurat et al. 1996; Genge et al. 2005; Genge 2008). Hydrated MMs contain saponite or serpentine in association with organic matter, that show similarities but also differences with phyllosilicates in carbonaceous chondrites (Genge et al. 1997; Nakamura et al. 2001; Noguchi et al. 2002; Battandier et al. 2016; Noguchi et al. 2017).

The hydrogen isotopic composition of hydrous phases in micrometeorites is centered on the terrestrial value (Engrand et al. 1999a), suggesting that MMs could have played a role in the delivery of water to Earth (Maurette et al. 2000). Fossil micrometeorites trapped as clasts in HED meteorites (HED = howardite, eucrite, diogenite, thought to come from asteroid (4) Vesta) also bear the same H isotopes (Gounelle et al. 2005a). The oxygen isotopic composition of anhydrous minerals in MMs $< 500$ μm show similarities with that of carbonaceous chondrites (Engrand et al. 1999b). For larger micrometeorites—melted into cosmic spherules—a larger proportion of ordinary chondrite-related particles is found (van Ginneken et al. 2017).

The carbon content of MMs (except for UCAMMs) has a range between 0.2 to 2.8 wt% (Maurette et al. 2000; Matrajt et al. 2003). The MMs exhibit Raman signatures of the first-order carbon bands G and D, suggesting the presence of polyaromatic carbonaceous matter. The width and position of these bands, as well as high-resolution Transmission Electron Microscope imaging, show a very disordered organic matter that did not experience thermal metamorphism (Dobrică et al. 2011). MMs also contain nanoglobules comparable to those observed in primitive meteorites and Wild 2 samples (Maurette et al. 1995; Nakamura-Messenger et al. 2006; de Gregorio BT et al. 2011). MMs also contain complex organics in the form of PAHs (Clemett et al. 1998) and amino acids (Brinton et al. 1998; Matrajt et al. 2004).

The origin of chondritic micrometeorites—asteroidal or cometary—is still debated (e.g. Maurette 2006; Genge 2008; Genge et al. 2008; Dobrică et al. 2009, and references therein). Models predict that a large fraction of dust on Earth could originate from Jupiter-family comets (e.g. Nesvorný et al. 2010; Poppe 2016).

UCAMMs are most probably of cometary origin. They contain up to 85% of organic matter in volume, thus showing carbon contents up to 10 times that of the most C-rich carbonaceous chondrites (Kerridge 1985; Grady and Pillinger 1986; Pizzarello et al. 2001). Such concentrations of carbonaceous matter are comparable with that of the most C-rich IDPs (Thomas et al. 1993; Keller et al. 2004), and bear similarities with CHON grains detected in comet Halley by the Giotto and Vega spatial missions in 1986 showing the association of dominant organic matter with a minor rocky component (Kissel and Krueger 1987; Lawler and Brownlee 1992), and with cometary grains from 67P/Churyumov-Gerasimenko (Fray et al. 2016; Bardyn et al. 2017; Fray et al. 2017).

The hydrogen isotopic composition of the UCAMM organic matter shows extreme deuterium enrichments (up to 30 times the terrestrial value—i.e. 300 times the proto-Solar value, Duprat et al. 2010). Their organic matter is a disordered polyaromatic carbonaceous phase, and contains at least two organic phases with different nitrogen contents. The bulk N concentration of their organic matter reaches 20 wt%, that is about 5 times that of insoluble organic matter (IOM) extracted from meteorites and the O/C ratio of UCAMM organic matter is lower than that of meteoritic IOM (Dartois et al. 2013; Engrand et al. 2015; Charon et al. 2017; Dartois et al. 2018). UCAMMs contain both low and high temperature components, and their micro-structure is intriguing: unequilibrated mineral assemblages with

individual submicrometer sizes are enclosed in the organic matter (Dobrică et al. 2012). The formation of the UCAMMs nitrogen-rich organic matter may result from galactic cosmic ray irradiation of N2- and CH4-rich surfaces of icy bodies in the outer regions of the Solar system (Dartois et al. 2013; Augé et al. 2016).

The minerals in UCAMMs cover a size range between 50 nm and several hundreds of nanometers (Dobrică et al. 2012). The minerals are usually associated to the organic matter that does not show very high N contents (Engrand et al. 2015; Charon et al. 2017). Their mineralogy mainly consist of Mg-rich olivines and pyroxenes, Fe-Ni sulphides, and GEMS. The pyroxene to olivine abundance ratio in UCAMMs is on average larger than 1. In addition, UCAMMs contain a significant abundance of silica-rich glass. Accessory mineral phases such as Mg-Al spinel, sphalerite, niningerite, perryite and Cr-rich pyroxenes are also observed (Dobrică et al. 2012). So far, no carbonate nor phyllosilicate minerals have been found in UCAMMs. The analysis of the hydrogen and nitrogen isotopic composition of organic matter in UCAMMs from the Concordia collection does not show clear spatial correlation between the D-rich and 15N-rich phases (Duprat et al. 2014; Bardin et al. 2015).

The unusually large concentration of organics in UCAMMs is of utmost interest for the early Earth prebiotic matter input.

### 8.4 Interplanetary Dust Versus Meteorites as Representatives of Interplanetary Matter

One of the most striking results of micrometeorite research consists in their relationship to carbonaceous chondrites that represent only 4% of the meteorites (e.g. Kurat et al. 1994; Engrand and Maurette 1998; Engrand et al. 1999c). In other words, 96% of all meteorite types are not represented in the incoming cosmic dust flux. Based on the following two points, it is suggested that collected dust particles are better representatives of cosmic dust and meteoroids than meteorites:

- The dynamical evolution of grains resulting in IDPs and MMs is less biased than that of meteorites. It is dominated by non-gravitational forces like Poynting-Robertson drag (Burns et al. 1979), whereas meteorites are delivered to Earth as a result of interactions with resonances, into which they are brought by the Yarkowsky effect (Vokrouhlický and Farinella 2000).
- The high proportion of carbonaceous chondrite-like objects (CC) in the collected IDPs better agrees with the proportions of C-type versus S-type asteroids than those of meteorite collections: More than 80% of the IDPs are carbonaceous chondrites (e.g. Kurat et al. 1994; Engrand and Maurette 1998; Engrand et al. 1999c), but only 5% of the meteorite collection is of this type, whereas $> 55\%$ of the asteroids are C-type, $< 20\%$ are S-type. The meteorite collections could in fact under-represent the CCs with regard to ordinary chondrites linked to S-type asteroids (Fujiwara et al. 2006; Buczkowski et al. 2008; Lim and Nittler 2009; Nakamura et al. 2011a), as these fragile CC meteorites may be preferentially destroyed during atmospheric entry and by weathering at the Earth's surface before recovery (e.g. Meibom and Clark 1999).

Analyzing the composition of micrometeorites in old ("fossile") rocks gives evidence that the composition did not change significantly over time (Gounelle et al. 2003; Engrand et al. 2005; Gounelle et al. 2005b) or toward smaller sizes (Gounelle et al. 2005b; Aléon et al. 2009).

This view was recently challenged by new dynamical models that favor a preferential formation of large amounts of dust from Jupiter-family comets that could explain the high

abundance of carbonaceous chondrite-like objects in the micrometeorite collections (Bottke et al. 2008; Nesvorný et al. 2010). This work would thus imply that most—if not all—micrometeorites with sizes $< 500$ µm are of cometary origin, and thus that the mineral components of cometary material are close to that of carbonaceous chondrites (Dobrică et al. 2009). This is a result also suggested by analyses of Stardust samples (e.g. Brownlee et al. 2006).

Larger micrometeorites ($> 500$ µm) collected in the transantarctic mountains (Rochette et al. 2008) seem to form a population that is intermediary between micrometeorites with sizes $< 500$ µm and meteorites, as large amounts of ordinary chondritic material ($\sim 30\%$, Suavet et al. 2010) and objects from differentiated bodies (Cordier et al. 2011) are present in this collection. In the following we present the limits of the classical distinction between inner and outer regions of the protoplanetary disk.

Comets contain Mg-rich silicates, olivines and pyroxenes, identified by infrared spectroscopy (e.g. Wooden et al. 2000). Stardust samples showed that Wild 2 cometary dust also contain very high-temperature phases like CAIs and chondrules (Brownlee et al. 2006). More than 50% of Wild 2 material recovered by Stardust was processed in the inner regions of the Solar system (Ogliore et al. 2009; Westphal et al. 2009). This corresponds mainly to the fraction $> 2$ µm, as the finer matrix was mostly destroyed during the impact with the collection device. The presence of high-temperature phases (formed or severely processed close to the protosun) in the comet-forming regions requires large-scale radial mixing mechanism(s) in the early Solar system.

Since both CAIs and chondrules have been found in Stardust samples, this mechanism(s) had to operate for at least a few million years, as chondrules formed a few million years after CAIs (Brownlee et al. 2006; Zolensky et al. 2006; Nakamura et al. 2008). Several models have been proposed to explain this radial transport, by viscous diffusion by turbulence (Bockelée-Morvan et al. 2002; Ciesla 2007), by jets (Shu et al. 1997), or radiation pressure processes (Vinković 2009). Other evidences for transport in the protoplanetary disk are given by the oxygen isotopic composition of high temperature phases (e.g. Simon et al. 2011), as well as by the hydrogen isotopic composition of low temperature phases (Remusat et al. 2010). Comet Wild 2 present similarities with primitive meteorite matter (carbonaceous chondrites), strongly supporting the hypothesis of a continuum between primitive asteroids and cometary matter. In fact, the outer asteroid belt contains objects that show cometary activity (Bertini 2011), reinforcing the concept of this continuum. Cosmic dust particles, in the form of micrometeorites (Duprat et al. 2010) and primitive IDPs (Ishii et al. 2008) are the preferred objects to study the primitive interplanetary matter, and this continuum between primitive asteroids and comets.

## 9 Summary and Outlook

This paper summarizes our knowledge of the interplanetary meteoroid and dust cloud. It describes how their properties are constrained by ground- and space-based observations of the zodiacal light, by observing meteors entering the Earth's atmosphere, by in-situ collection in space, in the upper atmosphere, and on the ground by analyzing meteorites.

Interplanetary meteoroids (larger than $\sim 30$ µm) and dust particles (smaller than $\sim 30$ µm) are continuously produced by the outgassing of comets and asteroids, and by collisional processes. Depending on the particle size, different things happen: smaller objects decouple from their parent object quickly and are dispersed by Solar radiation pressure.

Larger meteoroids stay close to the orbit of their parent body, forming so-called meteoroid streams. When entering the Earth's atmosphere, they can be observed as meteor showers.

In particular non-gravitational forces (radiation pressure, Poynting-Robertson drag, Lorentz forces) move the orbits of the particles away from their parent, until they form a background interplanetary cloud. The size distribution of the initially escaped particles is modified by collisions, disaggregation, and sublimation.

Detailed observations of the zodiacal light, including polarimetric and spectroscopic measurements, show that most dust particles in the zodiacal cloud present similarities with cometary dust and asteroid regoliths. Particles consist of a mix of amorphous carbon and silicate dust. Polarization measurements indicate that a significant fraction of the particles are irregular and fluffy aggregates.

A few critical open points remain: (a) the exact origin and physical properties of the dust particles contributing to the zodiacal cloud; the possible time evolution of the zodiacal cloud over decades; (b) the circular polarization that can probe the interplanetary magnetic fields structure; the dust evolution in the circum-Solar region; (c) how can we link our knowledge of the interplanetary dust, observed via zodiacal light, to that of exo-zodiacal dust clouds? Their structure could be quite different, taking into account the possible presence of "hot Jupiters" and variety in the orbital planes of exoplanets.

When meteoroids enter the Earth's atmosphere, they generate a streak of light, called a meteor. The emitted light intensity can be used to estimate the mass of the object; spectral observations constrain the chemical composition. The percentage of the kinetic energy converted to light as a function of wavelength is not yet well known, resulting in large uncertainties in these mass estimates. Still, the determined mass flux densities confirm the distributions obtained via other means, such as in-situ measurements or lunar secondary crater counts on returned lunar samples.

The directional distribution of meteors constrains the dynamical behavior of the meteoroid population. It can be seen that the sporadic background is not isotropic, even when taking observational biases into account. Some of these inhomogeneities can be attributed to comet 2P/Encke as a source, others to the Kozai effect. Many meteor showers, re-occurring on a yearly basis, are a result of meteoroids close to the orbit of their parent body. However, for about half of the meteor showers the identification of the related parent bodies has not yet been successful. Attempts to predict meteor showers have become better over the last few decades. While predicting the times of peak activity is possible with good accuracy, predicting the flux density is not. This would need better quantitative models of the ejection of meteoroids from their parent object.

While the observation of meteors with optical means and radar systems is a cost-effective way of studying meteoroids, a big open point is the percentage of kinetic energy converted into light, or radar reflection capability (luminous efficiency and ionization efficiency, respectively). These could be better constrained by combining light curve data with deceleration data, and by combining optical with radar observations. Also, laboratory experiments, properly simulating the typical velocities of meteoroids, have to be performed.

When larger objects penetrate our atmosphere, they can reach the ground as meteorites. However, they may be processed by their interaction with the atmosphere. Small dust can stay fairly unmodified, as it can re-radiate the imparted energy fully. Interplanetary dust can be collected via airplanes, balloons, or sounding rockets in the upper atmosphere. It can also be found in ice at the polar caps and in dust traps in the transantarctic mountains.

Most meteorites contain chondrules, mm-sized spheres of glass and crystalline silicates, formed by melting in the early Solar system. They also contain Ca-Al-rich inclusions, called CAIs, all held together by a fine-grained silicate matrix. 15 chondritic types have been identified, which presumably are linked to different source regions in the early Solar system.

Meteorite types can be linked to spectral classes of asteroids. The collected dust samples can also be classified into chondritic and non-chondritic groups. It is interesting to note that most collected dust grains are related to carbonaceous chondrites - which constitute only $\sim 5\%$ of all meteorites. This indicates that the collected dust in the upper atmosphere or arctic ice and snow could be more representative of interplanetary meteoroids than meteorites.

The flux density of the dust and meteoroid cloud can be described by dynamical models, like NASA's Meteoroid Environment Model (MEM) or ESA's Interplanetary Meteoroid Model (IMEM). However it is still difficult to explain all observational data consistently with one model. More work is needed in this area; possibly adding the meanwhile abundant optical data can help.

Space-based sensors could be used to both increase our observational data of the zodiacal light, or to look back to the Earth's atmosphere and allow continuous meteor and fireball observations without any constraints by clouds or by the Earth's atmosphere that absorbs certain wavelength ranges. So-called 'US government sensors' are providing data in particular on larger (> tens of cm) objects entering the Earth's atmosphere (https://cneos.jpl.nasa.gov/fireballs/). However, no public information is available on the properties of these sensors, making the data difficult to interpret. A dedicated sensor for scientific work could greatly enhance our dataset.

A recently emerging research field to better constrain the flux of meteoroids, in particular in the size range larger than a few cm, is the observation of Lunar impact flashes. NASA has been operating an observing system since many years (e.g. Suggs et al. 2014), and recently new systems went on-line in other countries (e.g. Xilouris et al. 2018). These observations would particularly benefit from space-based observations. A system close to the Moon would increase the sensitivity, and avoid being constrained by observing geometry or clouds (Topputo et al. 2018).

Meteorites could be a good proxy of the properties of interplanetary meteoroids. However, during their passage through the Earth's atmosphere they are modified. To better understand these modifications, ablation experiments in the laboratory—e.g. in wind tunnels or shock tubes, are necessary. Sample return missions from asteroids like OSIRIS-REx (Lauretta 2012), or Hayabusa-2 (Tsuda et al. 2013), or from comets, would allow to return unaltered material into ground-based laboratories.

Interplanetary dust may even be detectable by spacecraft not designed to detect them, and it may be possible to detect and characterize them by analyzing spacecraft attitude or guidance data, e.g. as proposed for the Lisa Pathfinder mission (Thorpe et al. 2016). The authors show that changes in the attitude of the spacecraft can be linked to micro-meteoroid impacts, thus allowing us to study the population in-situ without dedicated dust detectors.

While we already know a lot about interplanetary dust and meteoroids, we still need to know more details to obtain a better understanding of our Solar system and to improve our capabilities of shielding our spacecraft around the Earth or going to another planet.

**Acknowledgements** This paper was made possible by the International Space Science Institute, Bern, who brought the authors together for a whole week in 2016 and supported the meeting location and stay of the participants. All of the authors acknowledge their respective institutes and funding agencies for their support. In particular, JMTR thanks Spanish Ministry of Science and Innovation under research project AYA2015-67175-P. We acknowledge the hard work done by two referees whose comments were extremely valuable to improve this review.

## References


J. Aléon, C. Engrand, L.A. Leshin, K.D. McKeegan, Oxygen isotopic composition of chondritic interplanetary dust particles: a genetic link between carbonaceous chondrites and comets. Geochim. Cosmochim. Acta **73**, 4558–4575 (2009). https://doi.org/10.1016/j.gca.2009.04.034

N. Altobelli, S. Kempf, M. Landgraf, R. Srama, V. Dikarev, H. Krüger, G. Moragas-Klostermeyer, E. Grün, Cassini between Venus and Earth: detection of interstellar dust. J. Geophys. Res. Space Phys. **108**, 8032 (2003). https://doi.org/10.1029/2003JA009874

N. Altobelli, H. Krüger, R. Moissl, M. Landgraf, E. Grün, Influence of wall impacts on the Ulysses dust detector on understanding the interstellar dust flux. Planet. Space Sci. **52**, 1287–1295 (2004). https://doi.org/10.1016/j.pss.2004.07.022

N. Altobelli, S. Kempf, H. Krüger, M. Landgraf, M. Roy, E. Grün, Interstellar dust flux measurements by the Galileo dust instrument between the orbits of Venus and Mars. J. Geophys. Res. Space Phys. **110**(A9), 7102 (2005). https://doi.org/10.1029/2004JA010772

N. Altobelli, E. Grün, M. Landgraf, A new look into the Helios dust experiment data: presence of interstellar dust inside the Earth's orbit. Astron. Astrophys. **448**, 243–252 (2006). https://doi.org/10.1051/0004-6361:20053909

N. Altobelli, V. Dikarev, S. Kempf, R. Srama, S. Helfert, G. Moragas-Klostermeyer, M. Roy, E. Grün, Cassini/Cosmic Dust Analyzer in situ dust measurements between Jupiter and Saturn. J. Geophys. Res. Space Phys. **112**, A07105 (2007). https://doi.org/10.1029/2006JA011978

N. Altobelli, F. Postberg, K. Fiege, M. Trieloff, H. Kimura, V.J. Sterken, H.W. Hsu, J. Hillier, N. Khawaja, G. Moragas-Klostermeyer, J. Blum, M. Burton, R. Srama, S. Kempf, E. Grün, Flux and composition of interstellar dust at Saturn from Cassini's Cosmic Dust Analyzer. Science **352**, 312–318 (2016). https://doi.org/10.1126/science.aac6397

D.J. Asher, D.I. Steel, Theoretical meteor radiants for macroscopic Taurid complex objects. Earth Moon Planets **68**, 155–164 (1995). https://doi.org/10.1007/BF00671504

B. Augé, E. Dartois, C. Engrand, J. Duprat, M. Godard, L. Delauche, N. Bardin, C. Mejía, R. Martinez, G. Muniz, A. Domaracka, P. Boduch, H. Rothard, Irradiation of nitrogen-rich ices by swift heavy ions. Clues for the formation of ultracarbonaceous micrometeorites. Astron. Astrophys. **592**, A99 (2016). https://doi.org/10.1051/0004-6361/201527650

F. Bagenal, M. Horányi, D.J. McComas, R.L. McNutt, H.A. Elliot, M.E. Hill, L.E. Brown, P.A. Delamere, P. Kollman, S.M. Krimigis, M. Kusterer, C.M. Lisse, D.G. Mitchell, M. Piquette, A.R. Poppe, D.F. Strobel, J.R. Szalay, P. Valek, J. Vandegriff, S. Weidner, E.J. Zirnstein, S.A. Stern, K. Ennico, C.B. Olkin, H.A. Weaver, L.A. Young (NHS Team), Pluto's interaction with its space environment: solar wind, energetic particles, and dust. Science **351**, 6279 (2016)

W.J. Baggaley, The interstellar particle component measured by AMOR, in *Meteroids 1998*, ed. by W.J. Baggaley, V. Porubcan (1999), p. 265

W.J. Baggaley, Advanced Meteor Orbit Radar observations of interstellar meteoroids. J. Geophys. Res. **105**, 10353–10362 (2000). https://doi.org/10.1029/1999JA900383

W.J. Baggaley, S.H. Marsh, S. Close, Interstellar meteors. Dust Planet. Syst. **643**, 27–32 (2007)

M. Baguhl, E. Grün, M. Landgraf, In situ measurements of interstellar dust with the ULYSSES and Galileo spaceprobes. Space Sci. Rev. **78**(1/2), 165–172 78:165–172 (1996)

N. Bardin, J. Duprat, C. Engrand, G. Slodzian, D. Baklouti, E. Dartois, R. Brunetto, L. Delauche, M. Godard, T.D. Wu, J.L. Guerquin-Kern, D/H and 15N/14N isotopic ratios in organic matter of ultracarbonaceous Antarctic micrometeorites, in *78th Annual Meeting of the Meteoritical Society*. LPI Contributions, vol. 1856 (2015), p. 5275

A. Bardyn, D. Baklouti, H. Cottin, N. Fray, C. Briois, J. Paquette, O. Stenzel, C. Engrand, H. Fischer, K. Hornung, R. Isnard, Y. Langevin, H. Lehto, L. Le Roy, N. Ligier, S. Merouane, P. Modica, F.R. Orthous-Daunay, J. Rynö, R. Schulz, J. Silén, L. Thirkell, K. Varmuza, B. Zaprudin, J. Kissel, M. Hilchenbach, Carbon-rich dust in comet 67P/Churyumov-Gerasimenko measured by COSIMA/Rosetta. Mon. Not. R. Astron. Soc. **469**, S712–S722 (2017). https://doi.org/10.1093/mnras/stx2640

M. Battandier, L. Bonal, E. Quirico, P. Beck, C. Engrand, J. Duprat, Characterization of the organic matter and hydration state of a series of Antarctic micrometeorites, in *Lunar and Planetary Science Conference*, vol. 47 (2016), p. 1475

C. Beauge, S. Ferraz-Mello, Capture in exterior mean-motion resonances due to Poynting-Robertson drag. Icarus **110**, 239–260 (1994). https://doi.org/10.1006/icar.1994.1119

R. Behrisch, W. Eckstein, *Sputtering by particle bombardment: experiments and computer calculations from threshold to MeV energies*. Topics in Applied Physics, vol. 110 (Springer, Berlin, 2007)

E. Beitz, J. Blum, M.G. Parisi, J. Trigo-Rodriguez, The collisional evolution of undifferentiated asteroids and the formation of chondritic meteoroids. Astrophys. J. **824**, 12 (2016). https://doi.org/10.3847/0004-637X/824/1/12. arXiv:1604.02340

I. Belskaya, S. Fornasier, G. Tozzi, R. Gil-Hutton, A. Cellino, K. Antonyuk, Y.N. Krugly, A. Dovgopol, S. Faggi, Refining the asteroid taxonomy by polarimetric observations. Icarus **284**, 30–42 (2017)

O.E. Berg, U. Gerloff, More than two years of micrometeorite data from two Pioneer satellites, in *Space Research XI*, ed. by K.Y. Kondratyev, M.J. Rycroft, C. Sagan (1971), pp. 225–235

O.E. Berg, F.F. Richardson, The Pioneer 8 cosmic dust experiment. Rev. Sci. Instrum. **40**, 1333–1337 (1969). https://doi.org/10.1063/1.1683778

G. Berriman, N. Boggess, M. Hauser, T. Kelsall, C. Lisse, S. Moseley, W. Reach, R. Silverberg, Cobe dirbe near-infrared polarimetry of the zodiacal light: initial results. Astrophys. J. **431**, L63–L66 (1994)

I. Bertini, Main Belt comets: a new class of small bodies in the solar system. Planet. Space Sci. **59**, 365–377 (2011). https://doi.org/10.1016/j.pss.2011.01.014

J.P. Biersack, W. Eckstein, Sputtering studies with the Monte Carlo program TRIM.SP. Appl. Phys. A **34**, 73–94 (1984)

A. Bischoff, E.R.D. Scott, K. Metzler, C.A. Goodrich, *Nature and Origins of Meteoritic Breccias* (2006), pp. 679–712

A. Bischoff, M. Horstmann, M. Laubenstein, S. Haberer, Asteroid 2008 TC3—Almahata Sitta: not only a ureilitic meteorite, but a breccia containing many different achondritic and chondritic lithologies, in *Lunar and Planetary Science Conference*, vol. 41 (2010), p. 1763

R.C. Blaauw, M.D. Campbell-Brown, R.J. Weryk, A meteoroid stream survey using the Canadian Meteor Orbit Radar, III: mass distribution indices of six major meteor showers. Mon. Not. R. Astron. Soc. **414**, 3322–3329 (2011a). https://doi.org/10.1111/j.1365-2966.2011.18633.x

R.C. Blaauw, M.D. Campbell-Brown, R.J. Weryk, Mass distribution indices of sporadic meteors using radar data. Mon. Not. R. Astron. Soc. **412**, 2033–2039 (2011b). https://doi.org/10.1111/j.1365-2966.2010.18038.x

P.A. Bland, T.B. Smith, A.J.T. Jull, F.J. Berry, A.W.R. Bevan, S. Cloudt, C.T. Pillinger, The flux of meteorites to the Earth over the last 50,000 years. Mon. Not. R. Astron. Soc. **283**, 551 (1996). https://doi.org/10.1093/mnras/283.2.551

J. Blum, R. Schräpler, B.J.R. Davidsson, J.M. Trigo-Rodríguez, The physics of protoplanetesimal dust agglomerates, I: mechanical properties and relations to primitive bodies in the solar system. Astrophys. J. **652**, 1768–1781 (2006). https://doi.org/10.1086/508017

D. Bockelée-Morvan, D. Gautier, F. Hersant, J.M. Huré, F. Robert, Turbulent radial mixing in the solar nebula as the source of crystalline silicates in comets. Astron. Astrophys. **384**, 1107–1118 (2002). https://doi.org/10.1051/0004-6361:20020086

K.J. Borkowski, E. Dwek, The fragmentation and vaporization of dust in grain-grain collisions. Astrophys. J. **454**, 254–276 (1995)

J. Borovička, P. Koten, P. Spurný, J. Boček, R. Štork, A survey of meteor spectra and orbits: evidence for three populations of Na-free meteoroids. Icarus **174**, 15–30 (2005). https://doi.org/10.1016/j.icarus.2004.09.011

W.F. Bottke, H.F. Levison, A. Morbidelli, K. Tsiganis, The collisional evolution of objects captured in the Outer Asteroid Belt during the late heavy bombardment, in *Lunar and Planetary Science Conference*, vol. 39 (2008), p. 1447

W.F. Bottke Jr, D. Vokrouhlický, D.P. Rubincam, M. Broz, *The Effect of Yarkovsky Thermal Forces on the Dynamical Evolution of Asteroids and Meteoroids* (2002), pp. 395–408

J.P. Bradley, Chemically anomalous, preaccretionally irradiated grains in interplanetary dust from comets. Science **265**, 925–929 (1994). https://doi.org/10.1126/science.265.5174.925

J.P. Bradley, *Interplanetary Dust Particles* (Elsevier, Amsterdam, 2005), p. 689

J.P. Bradley, D.E. Brownlee, Cometary particles—thin sectioning and electron beam analysis. Science **231**, 1542–1544 (1986). https://doi.org/10.1126/science.231.4745.1542

J.P. Bradley, L.P. Keller, T.P. Snow, M.S. Hanner, G.J. Flynn, J.C. Gezo, S.J. Clemett, D.E. Brownlee, J.E. Bowey, An infrared spectral match between GEMS and interstellar grains. Science **285**, 1716–1718 (1999). https://doi.org/10.1126/science.285.5434.1716

A.J. Brearley, R.H. Jones, Chondritic meteorites, in *Planetary Materials*, ed. by J.J. Papike (Mineralogical Society of America, Washington, 1998), pp. 1–398

K.L.F. Brinton, C. Engrand, D.P. Glavin, J.L. Bada, M. Maurette, A search for extraterrestrial amino acids in carbonaceous Antarctic micrometeorites. Orig. Life Evol. Biosph. **28**, 413–424 (1998)

D.T. Britt, G.J. Consolmagno, The porosity of dark meteorites and the structure of low-albedo asteroids. Icarus **146**, 213–219 (2000). https://doi.org/10.1006/icar.2000.6374

P. Brown, R.J. Weryk, D.K. Wong, J. Jones, A meteoroid stream survey using the Canadian Meteor Orbit Radar, I: methodology and radiant catalogue. Icarus **195**, 317–339 (2008). https://doi.org/10.1016/j.icarus.2007.12.002

P.G. Brown, A.R. Hildebrand, M.E. Zolensky, M. Grady, R.N. Clayton, T.K. Mayeda, E. Tagliaferri, R. Spalding, N.D. MacRae, E.L. Hoffman, D.W. Mittlefehldt, J.F. Wacker, J.A. Bird, M.D. Campbell, R.

Carpenter, H. Gingerich, M. Glatiotis, E. Greiner, M.J. Mazur, P.J. McCausland, H. Plotkin, T. Rubak Mazur, The fall, recovery, orbit, and composition of the Tagish lake meteorite: a new type of carbonaceous chondrite. Science **290**, 320–325 (2000). https://doi.org/10.1126/science.290.5490.320

D. Brownlee, Interplanetary dust. Rev. Geophys. **17**(7), 1735–1743 (1979)

D. Brownlee, P. Tsou, J. Aléon, C.M.O. Alexander, T. Araki, S. Bajt, G.A. Baratta, R. Bastien, P. Bland, P. Bleuet, J. Borg, J.P. Bradley, A. Brearley, F. Brenker, S. Brennan, J.C. Bridges, N.D. Browning, J.R. Brucato, E. Bullock, M.J. Burchell, H. Busemann, A. Butterworth, M. Chaussidon, A. Cheuvront, M. Chi, M.J. Cintala, B.C. Clark, S.J. Clemett, G. Cody, L. Colangeli, G. Cooper, P. Cordier, C. Daghlian, Z. Dai, L. D'Hendecourt, Z. Djouadi, G. Dominguez, T. Duxbury, J.P. Dworkin, D.S. Ebel, T.E. Economou, S. Fakra, S.A.J. Fairey, S. Fallon, G. Ferrini, T. Ferroir, H. Fleckenstein, C. Floss, G. Flynn, I.A. Franchi, M. Fries, Z. Gainsforth, J.P. Gallien, M. Genge, M.K. Gilles, P. Gillet, J. Gilmour, D.P. Glavin, M. Gounelle, M.M. Grady, G.A. Graham, P.G. Grant, S.F. Green, F. Grossemy, L. Grossman, J.N. Grossman, Y. Guan, K. Hagiya, R. Harvey, P. Heck, G.F. Herzog, P. Hoppe, F. Hörz, J. Huth, I.D. Hutcheon, K. Ignatyev, H. Ishii, M. Ito, D. Jacob, C. Jacobsen, S. Jacobsen, S. Jones, D. Joswiak, A. Jurewicz, A.T. Kearsley, L.P. Keller, H. Khodja, A.L.D. Kilcoyne, J. Kissel, A. Krot, F. Langenhorst, A. Lanzirotti, L. Le, L.A. Leshin, J. Leitner, L. Lemelle, H. Leroux, M.C. Liu, K. Luening, I. Lyon, G. MacPherson, M.A. Marcus, K. Marhas, B. Marty, G. Matrajt, K. McKeegan, A. Meibom, V. Mennella, K. Messenger, S. Messenger, T. Mikouchi, S. Mostefaoui, T. Nakamura, T. Nakano, M. Newville, L.R. Nittler, I. Ohnishi, K. Ohsumi, K. Okudaira, D.A. Papanastassiou, R. Palma, M.E. Palumbo, R.O. Pepin, D. Perkins, M. Perronnet, P. Pianetta, W. Rao, F.J.M. Rietmeijer, F. Robert, D. Rost, A. Rotundi, R. Ryan, S.A. Sandford, C.S. Schwandt, T.H. See, D. Schlutter, J. Sheffield-Parker, A. Simionovici, S. Simon, I. Sitnitsky, C.J. Snead, M.K. Spencer, F.J. Stadermann, A. Steele, T. Stephan, R. Stroud, J. Susini, S.R. Sutton, Y. Suzuki, M. Taheri, S. Taylor, N. Teslich, K. Tomeoka, N. Tomioka, A. Toppani, J.M. Trigo-Rodríguez, D. Troadec, A. Tsuchiyama, A.J. Tuzzolino, T. Tyliszczak, K. Uesugi, M. Velbel, J. Vellenga, E. Vicenzi, L. Vincze, J. Warren, I. Weber, M. Weisberg, A.J. Westphal, S. Wirick, D. Wooden, B. Wopenka, P. Wozniakiewicz, I. Wright, H. Yabuta, H. Yano, E.D. Young, R.N. Zare, T. Zega, K. Ziegler, L. Zimmerman, E. Zinner, M. Zolensky, Comet 81P/Wild 2 under a microscope. Science **314**, 1711 (2006). https://doi.org/10.1126/science.1135840

D.E. Brownlee, Cosmic dust—collection and research. Annu. Rev. Earth Planet. Sci. **13**, 147–173 (1985). https://doi.org/10.1146/annurev.ea.13.050185.001051

D.L. Buczkowski, O.S. Barnouin-Jha, L.M. Prockter, 433 Eros lineaments: global mapping and analysis. Icarus **193**, 39–52 (2008). https://doi.org/10.1016/j.icarus.2007.06.028

A. Buffington, M.M. Bisi, J.M. Clover, P.P. Hick, B.V. Jackson, T.A. Kuchar, S.D. Price, Measurements of the gegenschein brightness from the solar mass ejection imager (smei). Icarus **203**(1), 124–133 (2009)

A. Buffington, M.M. Bisi, J.M. Clover, P.P. Hick, B.V. Jackson, T.A. Kuchar, S.D. Price, Measurements and an empirical model of the zodiacal brightness as observed by the solar mass ejection imager (smei). Icarus **272**, 88–101 (2016)

J.A. Burns, P.L. Lamy, S. Soter, Radiation forces on small particles in the solar system. Icarus **40**, 1–48 (1979). https://doi.org/10.1016/0019-1035(79)90050-2

M.D. Campbell-Brown, High resolution radiant distribution and orbits of sporadic radar meteoroids. Icarus **196**, 144–163 (2008). https://doi.org/10.1016/j.icarus.2008.02.022

M.D. Campbell-Brown, D. Koschny, Model of the ablation of faint meteors. Astron. Astrophys. **418**, 751–758 (2004). https://doi.org/10.1051/0004-6361:20041001-1

M.D. Campbell-Brown, J. Kero, C. Szasz, A. Pellinen-Wannberg, R.J. Weryk, Photometric and ionization masses of meteors with simultaneous EISCAT UHF radar and intensified video observations. J. Geophys. Res. Space Phys. **117**, A09323 (2012). https://doi.org/10.1029/2012JA017800

M.D. Campbell-Brown, J. Borovička, P.G. Brown, E. Stokan, High-resolution modelling of meteoroid ablation. Astron. Astrophys. **557**, A41 (2013). https://doi.org/10.1051/0004-6361/201322005

M.D. Campbell-Brown, R. Blaauw, A. Kingery, Optical fluxes and meteor properties of the camelopardalid meteor shower. Icarus **277**, 141–153 (2016). https://doi.org/10.1016/j.icarus.2016.05.001

Z. Ceplecha, J. Borovička, W.G. Elford, D.O. Revelle, R.L. Hawkes, V. Porubčan, M. Šimek, Meteor phenomena and bodies. Space Sci. Rev. **84**, 327–471 (1998). https://doi.org/10.1023/A:1005069928850

E. Charon, C. Engrand, K. Benzerara, H. Leroux, S. Swaraj, R. Belkhou, J. Duprat, E. Dartois, M. Godard, L. Delauche, A C-, N-, O-XANES/STXM and TEM study of organic matter and minerals in ultracarbonaceous Antarctic micrometeorites (UCAMMs), in *Lunar and Planetary Science Conference*, vol. 48 (2017), p. 2085

A.A. Christou, R.M. Killen, M.H. Burger, The meteoroid stream of comet Encke at Mercury: implications for Mercury surface, space environment, geochemistry, and ranging observations of the exosphere. Geophys. Res. Lett. **42**, 7311–7318 (2015). https://doi.org/10.1002/2015GL065361

F.J. Ciesla, Outward transport of high-temperature materials around the midplane of the solar nebula. Science **318**, 613 (2007). https://doi.org/10.1126/science.1147273

F.J. Ciesla, S.A. Sandford, Organic synthesis via irradiation and warming of ice grains in the solar nebula. Science **336**, 452 (2012). https://doi.org/10.1126/science.1217291
B.C. Clark, S.F. Green, T.E. Economou, S.A. Sandford, M.E. Zolensky, N. McBride, D.E. Brownlee, Release and fragmentation of aggregates to produce heterogeneous, lumpy coma streams. J. Geophys. Res., Planets **109**(E18), E12S03 (2004). https://doi.org/10.1029/2004JE002319
S.J. Clemett, X.D.F. Chillier, S. Gillette, R.N. Zare, M. Maurette, C. Engrand, G. Kurat, Observation of indigenous polycyclic aromatic hydrocarbons in 'giant' carbonaceous Antarctic micrometeorites. Orig. Life Evol. Biosph. **28**, 425–448 (1998)
C. Cordier, L. Folco, C. Suavet, C. Sonzogni, P. Rochette, Major, trace element and oxygen isotope study of glass cosmic spherules of chondritic composition: the record of their source material and atmospheric entry heating. Geochim. Cosmochim. Acta **75**, 5203–5218 (2011). https://doi.org/10.1016/j.gca.2011.06.014
B.G. Cour-Palais, Meteoroid environment model-1969 [Near Earth to Lunar Surface]. NASA SP-8013, NASA (1969)
A. Czechowski, I. Mann, Formation and acceleration of nano dust in the inner heliosphere. Astrophys. J. **714**, 89 (2010). https://doi.org/10.1088/0004-637X/714/1/89
E. Dartois, C. Engrand, R. Brunetto, J. Duprat, T. Pino, E. Quirico, L. Remusat, N. Bardin, G. Briani, S. Mostefaoui, G. Morinaud, B. Crane, N. Szwec, L. Delauche, F. Jamme, C. Sandt, P. Dumas, Ultracarbonaceous Antarctic micrometeorites, probing the solar system beyond the nitrogen snow-line. Icarus **224**, 243–252 (2013). https://doi.org/10.1016/j.icarus.2013.03.002
E. Dartois, C. Engrand, J. Duprat, M. Godard, E. Charon, L. Delauche, C. Sandt, F. Borondics, Dome C ultracarbonaceous Antarctic micrometeorites. Infrared and Raman fingerprints. Astron. Astrophys. **609**, A65 (2018). https://doi.org/10.1051/0004-6361/201731322. arXiv:1711.00647
B.T. de Gregorio, R.M. Stroud, G.D. Cody, L.R. Nittler, A.L. David Kilcoyne, S. Wirick, Correlated microanalysis of cometary organic grains returned by stardust. Meteorit. Planet. Sci. **46**, 1376–1396 (2011). https://doi.org/10.1111/j.1945-5100.2011.01237.x
F.E. DeMeo, B. Carry, Solar system evolution from compositional mapping of the asteroid belt. Nature **505**, 629 (2014)
S. Dermott, P. Nicholson, J. Burns, J. Houck, Origin of the solar system dust bands discovered by iras. Nature **312**(5994), 505–509 (1984)
S.F. Dermott, K. Grogan, D.D. Durda, S. Jayaraman, T.J.J. Kehoe, S.J. Kortenkamp, M.C. Wyatt, *Orbital Evolution of Interplanetary Dust* (2001), p. 569
V. Dikarev, E. Grün, J. Baggaley, D. Galligan, M. Landgraf, R. Jehn, Modeling the sporadic meteoroid background cloud. Earth Moon Planets **95**, 109–122 (2004). https://doi.org/10.1007/s11038-005-9017-y
V. Dikarev, E. Grün, J. Baggaley, D. Galligan, M. Landgraf, R. Jehn, The new ESA meteoroid model. Adv. Space Res. **35**, 1282–1289 (2005). https://doi.org/10.1016/j.asr.2005.05.014
N. Divine, Five populations of interplanetary meteoroids. J. Geophys. Res. **98**(17), 029 (1993). https://doi.org/10.1029/93JE01203. 048
E. Dobrică, C. Engrand, J. Duprat, M. Gounelle, H. Leroux, E. Quirico, J.N. Rouzaud, Connection between micrometeorites and Wild 2 particles: from Antarctic snow to cometary ices. Meteorit. Planet. Sci. **44**, 1643–1661 (2009). https://doi.org/10.1111/j.1945-5100.2009.tb01196.x
E. Dobrică, C. Engrand, J. Duprat, M. Gounelle, A statistical overview of CONCORDIA Antarctic micrometeorites. Meteorit. Planet. Sci. Suppl. **73**, 5213 (2010)
E. Dobrică, C. Engrand, H. Leroux, J.N. Rouzaud, J. Duprat, Transmission electron microscopy of CONCORDIA ultracarbonaceous Antarctic micrometeorites (UCAMMs): mineralogical properties. Geochim. Cosmochim. Acta **76**, 68–82 (2012). https://doi.org/10.1016/j.gca.2011.10.025
E. Dobrică, C. Engrand, E. Quirico, G. Montagnac, J. Duprat, Raman characterization of carbonaceous matter in CONCORDIA Antarctic micrometeorites. Meteorit. Planet. Sci. **46**, 1363–1375 (2011). https://doi.org/10.1111/j.1945-5100.2011.01235.x
L. Dones, P.R. Weissman, H.F. Levison, M.J. Duncan, Oort cloud formation and dynamics, in *Comets II*, ed. by M.C. Festou, H.U. Keller, H.A. Weaver (University of Arizona Press, Tucson, 2004)
G. Drolshagen, V. Dikarev, M. Landgraf, H. Krag, W. Kuiper, Comparison of meteoroid flux models for near earth space. Earth Moon Planets **102**, 191–197 (2008). https://doi.org/10.1007/s11038-007-9199-6
J.D. Drummond, A test of comet and meteor shower associations. Icarus **45**, 545–553 (1981). https://doi.org/10.1016/0019-1035(81)90020-8
A. Dubietis, R. Arlt, Taurid resonant-swarm encounters from two decades of visual observations. Mon. Not. R. Astron. Soc. **376**, 890–894 (2007). https://doi.org/10.1111/j.1365-2966.2007.11488.x
R. Dumont, Phase function and polarization curve of interplanetary scatterers from zodiacal light photopolarimetry. Planet. Space Sci. **21**(12), 2149–2155 (1973)

R. Dumont, A.C. Levasseur-Regourd, Zodiacal light photopolarimetry, IV: annual variations of brightness and the symmetry plane of the zodiacal cloud: absence of solar-cycle variations. Astron. Astrophys. **64**, 9–16 (1978)
R. Dumont, A.L. Levasseur-Regourd, Zodiacal light gathered along the line of sight: retrieval of the local scattering coefficient from photometric surveys of the ecliptic plane. Planet. Space Sci. **33**(1), 1–9 (1985)
R. Dumont, F. Sanchez, Zodiacal light photopolarimetry, I: observations, reductions, disturbing phenomena, accuracy; II: gradients along the ecliptic and the phase functions of interplanetary matter. Astron. Astrophys. **38**, 397–403 (1975a)
R. Dumont, F. Sanchez, Zodiacal light photopolarimetry, II: gradients along the ecliptic and the phase functions of interplanetary matter. Astron. Astrophys. **38**, 405 (1975b)
J. Duprat, C. Engrand, M. Maurette, F. Naulin, G. Kurat, M. Gounelle, The micrometeorite mass flux as recorded in Dome C central Antarctic surface snow. Meteorit. Planet. Sci. Suppl. **41**, 5239 (2006)
J. Duprat, C. Engrand, M. Maurette, G. Kurat, M. Gounelle, C. Hammer, Micrometeorites from central Antarctic snow: the CONCORDIA collection. Adv. Space Res. **39**, 605–611 (2007). https://doi.org/10.1016/j.asr.2006.05.029
J. Duprat, E. Dobrică, C. Engrand, J. Aléon, Y. Marrocchi, S. Mostefaoui, A. Meibom, H. Leroux, J.N. Rouzaud, M. Gounelle, F. Robert, Extreme deuterium excesses in ultracarbonaceous micrometeorites from central Antarctic snow. Science **328**, 742 (2010). https://doi.org/10.1126/science.1184832
J. Duprat, N. Bardin, C. Engrand, D. Baklouti, R. Brunetto, E. Dartois, L. Delauche, M. Godard, J.L. Guerquin-Kern, G. Slodzian, T.D. Wu, Isotopic analysis of organic matter in ultra-carbonaceous antarctic micrometeorites, in *77th Annual Meeting of the Meteoritical Society*. LPI Contributions, vol. 1800 (2014), p. 5341
T.E. Economou, S.F. Green, D.E. Brownlee, B.C. Clark, Dust flux monitor instrument measurements during Stardust-NExT Flyby of Comet 9P/Tempel 1. Icarus **222**, 526–539 (2013). https://doi.org/10.1016/j.icarus.2012.09.019
C. Engrand, M. Maurette, Carbonaceous micrometeorites from Antarctica. Meteorit. Planet. Sci. **33**, 565–580 (1998). https://doi.org/10.1111/j.1945-5100.1998.tb01665.x
C. Engrand, E. Deloule, F. Robert, M. Maurette, G. Kurat, Extraterrestrial water in micrometeorites and cosmic spherules from Antarctica: an ion microprobe study. Meteorit. Planet. Sci. **34**, 773–786 (1999a). https://doi.org/10.1111/j.1945-5100.1999.tb01390.x
C. Engrand, K.D. McKeegan, L.A. Leshin, Oxygen isotopic compositions of individual minerals in Antarctic micrometeorites: further links to carbonaceous chondrites. Geochim. Cosmochim. Acta **63**, 2623–2636 (1999b). https://doi.org/10.1016/S0016-7037(99)00160-X
C. Engrand, K.D. McKeegan, L.A. Leshin, J.P. Bradley, D.E. Brownlee, Oxygen isotopic compositions of interplanetary dust particles: 16O-Excess in a GEMS-rich IDP, in *Lunar and Planetary Science Conference*, vol. 30 (1999c)
C. Engrand, K.D. McKeegan, L.A. Leshin, G.F. Herzog, C. Schnabel, L.E. Nyquist, D.E. Brownlee, Isotopic compositions of oxygen, iron, chromium, and nickel in cosmic spherules: toward a better comprehension of atmospheric entry heating effects. Geochim. Cosmochim. Acta **69**, 5365–5385 (2005). https://doi.org/10.1016/j.gca.2005.07.002
C. Engrand, J. Duprat, M. Maurette, M. Gounelle, Fe-Ni sulfides in Concordia Antarctic micrometeorites, in *Lunar and Planetary Science Conference*, vol. 38 (2007), p. 1668
C. Engrand, K. Benzerara, H. Leroux, J. Duprat, E. Dartois, N. Bardin, L. Delauche, Carbonaceous phases and mineralogy of ultracarbonaceous Antarctic micrometeorites identified by C- and N-XANES/STXM and TEM, in *Lunar and Planetary Science Conference*, vol. 46 (2015), p. 1902
E.M. Epifani, C. Snodgrass, D. Perna, M. Dall'Ora, P. Palumbo, V. Della Corte, A. Alvarez-Candal, M. Melita, A. Rotundi, Photometry of the Oort Cloud comet C/2009 P1 (Garradd): pre-perihelion observations at 5.7 and 2.5 AU. Planet. Space Sci. **132**, 23–31 (2016)
D. Fixsen, E. Dwek, The zodiacal emission spectrum as determined by cobe and its implications. Astrophys. J. **578**(2), 1009 (2002)
C. Floss, F.J. Stadermann, Isotopically primitive interplanetary dust particles of cometary origin: evidence from nitrogen isotopic compositions, in *Lunar and Planetary Science Conference*, ed. by S. Mackwell, E. Stansbery (2004), p. 1281
G.J. Flynn, D.D. Durda, Chemical and mineralogical size segregation in the impact disruption of inhomogeneous, anhydrous meteorites. Planet. Space Sci. **52**, 1129–1140 (2004). https://doi.org/10.1016/j.pss.2004.07.010
G.J. Flynn, S. Wirick, L.P. Keller, Organic grain coatings in primitive interplanetary dust particles: implications for grain sticking in the Solar Nebula. Earth Planets Space **65**, 1159–1166 (2013). https://doi.org/10.5047/eps.2013.05.007

G.J. Flynn, L.R. Nittler, C. Engrand, Composition of cosmic dust: sources and implications for the early solar system. Elements **12**(3), 177 (2016). https://doi.org/10.2113/gselements.12.3.177

S. Fornasier, M. Lazzarin, C. Barbieri, M.A. Barucci, Spectroscopic comparison of aqueous altered asteroids with CM2 carbonaceous chondrite meteorites. Astron. Astrophys. Suppl. Ser. **135**, 65–73 (1999). https://doi.org/10.1051/aas:1999161

N. Fray, A. Bardyn, H. Cottin, K. Altwegg, D. Baklouti, C. Briois, L. Colangeli, C. Engrand, H. Fischer, A. Glasmachers, E. Grün, G. Haerendel, H. Henkel, H. Höfner, K. Hornung, E.K. Jessberger, A. Koch, H. Krüger, Y. Langevin, H. Lehto, K. Lehto, L. Le Roy, S. Merouane, P. Modica, F.R. Orthous-Daunay, J. Paquette, F. Raulin, J. Rynö, R. Schulz, J. Silén, S. Siljeström, W. Steiger, O. Stenzel, T. Stephan, L. Thirkell, R. Thomas, K. Torkar, K. Varmuza, K.P. Wanczek, B. Zaprudin, J. Kissel, M. Hilchenbach, High-molecular-weight organic matter in the particles of comet 67P/Churyumov-Gerasimenko. Nature **538**, 72–74 (2016). https://doi.org/10.1038/nature19320

N. Fray, A. Bardyn, H. Cottin, D. Baklouti, C. Briois, C. Engrand, H. Fischer, K. Hornung, R. Isnard, Y. Langevin, H. Lehto, L. Le Roy, E.M. Mellado, S. Merouane, P. Modica, F.R. Orthous-Daunay, J. Paquette, J. Rynö, R. Schulz, J. Silén, S. Siljeström, O. Stenzel, L. Thirkell, K. Varmuza, B. Zaprudin, J. Kissel, M. Hilchenbach, Nitrogen-to-carbon atomic ratio measured by COSIMA in the particles of comet 67P/Churyumov-Gerasimenko. Mon. Not. R. Astron. Soc. **469**, S506–S516 (2017). https://doi.org/10.1093/mnras/stx2002

P.C. Frisch, J.M. Dorschner, J. Geiss, J.M. Greenberg, E. Grün, M. Landgraf, P. Hoppe, A.P. Jones, W. Krätschmer, T.J. Linde, G.E. Morfill, W. Reach, J.D. Slavin, J. Svestka, A.N. Witt, G.P. Zank, Dust in the local interstellar wind. Astrophys. J. **525**, 492–516 (1999)

A. Fujiwara, J. Kawaguchi, D.K. Yeomans, M. Abe, T. Mukai, T. Okada, J. Saito, H. Yano, M. Yoshikawa, D.J. Scheeres, O. Barnouin-Jha, A.F. Cheng, H. Demura, R.W. Gaskell, N. Hirata, H. Ikeda, T. Kominato, H. Miyamoto, A.M. Nakamura, R. Nakamura, S. Sasaki, K. Uesugi, The rubble-pile asteroid Itokawa as observed by Hayabusa. Science **312**, 1330–1334 (2006). https://doi.org/10.1126/science.1125841

M. Fulle, Dust from short-period comet P/Schwassmann-Wachmann 1 and replenishment of the interplanetary dust cloud. Nature **359**, 42–44 (1992)

M. Fulle, *Motion of Cometary Dust* (2004), pp. 565–575

M.J. Gaffey, T.B. McCord, Asteroid surface materials—mineralogical characterizations from reflectance spectra. Space Sci. Rev. **21**, 555–628 (1978). https://doi.org/10.1007/BF00240908

D.P. Galligan, W.J. Baggaley, Wavelet enhancement for detecting shower structure in radar meteoroid data, I: methodology, in *IAU Colloq. 181: Dust in the Solar System and Other Planetary Systems*, vol. 15, ed. by S.F. Green, I.P. Williams, J.A.M. McDonnell, N. McBride (2002), p. 42

D.P. Galligan, W.J. Baggaley, The orbital distribution of radar-detected meteoroids of the Solar system dust cloud. Mon. Not. R. Astron. Soc. **353**, 422–446 (2004). https://doi.org/10.1111/j.1365-2966.2004.08078.x

D.P. Galligan, W.J. Baggaley, The radiant distribution of AMOR radar meteors. Mon. Not. R. Astron. Soc. **359**, 551–560 (2005). https://doi.org/10.1111/j.1365-2966.2005.08918.x

M.J. Genge, Koronis asteroid dust within Antarctic ice. Geology **36**(9), 687–690 (2008). https://doi.org/10.1130/G24493A.1

M.J. Genge, M.M. Grady, R. Hutchison, The textures and compositions of fine-grained Antarctic micrometeorites—implications for comparisons with meteorites. Geochim. Cosmochim. Acta **61**, 5149 (1997). https://doi.org/10.1016/S0016-7037(97)00308-6

M.J. Genge, A. Gileski, M.M. Grady, Chondrules in Antarctic micrometeorites. Meteorit. Planet. Sci. **40**, 225 (2005). https://doi.org/10.1111/j.1945-5100.2005.tb00377.x

M.J. Genge, C. Engrand, M. Gounelle, S. Taylor, The classification of micrometeorites. Meteorit. Planet. Sci. **43**, 497–515 (2008). https://doi.org/10.1111/j.1945-5100.2008.tb00668.x

R. Giese, Light scattering by small particles and models of interplanetary matter derived from the zodiacal light. Space Sci. Rev. **1**(3), 589–611 (1963)

R. Giese, Optical properties of single-component zodiacal light models. Planet. Space Sci. **21**(3), 513–521 (1973)

R. Giese, K. Weiss, R. Zerull, T. Ono, Large fluffy particles-a possible explanation of the optical properties of interplanetary dust. Astron. Astrophys. **65**, 265–272 (1978)

J.C. Gómez Martín, D.L. Bones, J.D. Carrillo-Sánchez, A.D. James, J.M. Trigo-Rodríguez, B. Fegley Jr., J.M.C. Plane, Novel experimental simulations of the atmospheric injection of meteoric metals. Astrophys. J. **836**, 212 (2017). https://doi.org/10.3847/1538-4357/aa5c8f

M. Gounelle, M.E. Zolensky, J.C. Liou, P.A. Bland, O. Alard, Mineralogy of carbonaceous chondritic microclasts in howardites: identification of C2 fossil micrometeorites. Geochim. Cosmochim. Acta **67**, 507–527 (2003). https://doi.org/10.1016/S0016-7037(02)00985-7

M. Gounelle, C. Engrand, O. Alard, P.A. Bland, M.E. Zolensky, S.S. Russell, J. Duprat, Hydrogen isotopic composition of water from fossil micrometeorites in howardites. Geochim. Cosmochim. Acta **69**, 3431–3443 (2005a). https://doi.org/10.1016/j.gca.2004.12.021

M. Gounelle, C. Engrand, M. Maurette, G. Kurat, K.D. McKeegan, F. Brandsttter, Small Antarctic micrometeorites: a mineralogical and in situ oxygen isotope study. Meteorit. Planet. Sci. **40**, 917 (2005b). https://doi.org/10.1111/j.1945-5100.2005.tb00163.x

J. Gradie, E. Tedesco, Compositional structure of the asteroid belt. Science **216**, 1405–1407 (1982). https://doi.org/10.1126/science.216.4553.1405

M.M. Grady, C.T. Pillinger, Carbon isotope relationships in winonaites and forsterite chondrites. Geochim. Cosmochim. Acta **50**, 255–263 (1986). https://doi.org/10.1016/0016-7037(86)90174-2

A.L. Graps, E. Grün, H. Svedhem, H. Krüger, M. Horányi, A. Heck, S. Lammers, Io as a source of the jovian dust streams. Nature **405**, 48–50 (2000)

S.F. Green, J.A.M. McDonnell, N. McBride, M.T.S.H. Colwell, A.J. Tuzzolino, T.E. Economou, P. Tsou, B.C. Clark, D.E. Brownlee, The dust mass distribution of comet 81P/Wild 2. J. Geophys. Res., Planets **109**(E18), E12S04 (2004). https://doi.org/10.1029/2004JE002318

A. Grigorieva, P. Thébault, P. Artymowicz, A. Brandeker, Survival of icy grains in debris discs. The role of photosputtering. Astron. Astrophys. **475**, 755–764 (2007a). https://doi.org/10.1051/0004-6361:20077686. arXiv:0709.0811

A. Grigorieva, P. Thébault, P. Artymowicz, A. Brandeker, Survival of icy grains in debris disks: the role of photosputtering. Astron. Astrophys. **475**, 755–764 (2007b)

M. Gritsevich, D. Koschny, Constraining the luminous efficiency of meteors. Icarus **212**, 877–884 (2011). https://doi.org/10.1016/j.icarus.2011.01.033

E. Grün, M. Landgraf, Collisional consequences of big interstellar grains. J. Geophys. Res. **105**, 10,291–10,298 (2000)

E. Grün, N. Pailer, H. Fechtig, J. Kissel, Orbital and physical characteristics of micrometeoroids in the inner solar system as observed by HELIOS 1. Planet. Space Sci. **28**, 333–349 (1980). https://doi.org/10.1016/0032-0633(80)90022-7

E. Grün, H.A. Zook, H. Fechtig, R.H. Giese, Collisional balance of the meteoritic complex. Icarus **62**, 244–272 (1985). https://doi.org/10.1016/0019-1035(85)90121-6

E. Grün, H. Zook, M. Baguhl, A. Balogh, S. Bame, H. Fechtig, R. Forsyth, M. Hanner, M. Horanyi, J. Kissel, B.A. Lindblad, D. Linkert, G. Linkert, I. Mann, J. McDonnel, G. Morfill, J. Phillips, C. Polanskey, G. Schwehm, N. Siddique, P. Staubach, J. Svestka, A. Taylor, Discovery of Jovian dust streams and interstellar grains by the Ulysses spacecraft. Nature **362**, 428–430 (1993a)

E. Grün, H.A. Zook, M. Baguhl, A. Balogh, S. Bame, H. Fechtig, R. Forsyth, M. Manner, M. Horanyi, J. Kissel et al., Discovery of jovian dust streams and interstellar grains by the Ulysses spacecraft. Nature **362**(6419), 428–430 (1993b)

E. Grün, H.A. Zook, M. Baguhl, A. Balogh, S.J. Bame, H. Fechtig, R. Forsyth, M.S. Hanner, M. Horanyi, J. Kissel, B.A. Lindblad, D. Linkert, G. Linkert, I. Mann, J.A.M. McDonnell, G.E. Morfill, J.L. Phillips, C. Polanskey, G. Schwehm, N. Siddique, P. Staubach, J. Svestka, A. Taylor, Discovery of Jovian dust streams and interstellar grains by the ULYSSES spacecraft. Nature **362**, 428–430 (1993c). https://doi.org/10.1038/362428a0

E. Grün, B. Gustafson, I. Mann, M. Baguhl, G.E. Morfill, P. Staubach, A. Taylor, H.A. Zook, Interstellar dust in the heliosphere. Astron. Astrophys. **286**, 915–924 (1994)

E. Grün, M. Baguhl, D.P. Hamilton, R. Riemann, H.A. Zook, S. Dermott, H. Fechtig, B.A. Gustafson, M.S. Hanner, M. Horányi, K.K. Khurana, J. Kissel, M. Kivelson, B.A. Lindblad, D. Linkert, G. Linkert, I. Mann, J.A.M. McDonnell, G.E. Morfill, C. Polanskey, G. Schwehm, R. Srama, Constraints from Galileo observations on the origin of jovian dust streams. Nature **381**, 395–398 (1996). https://doi.org/10.1038/381395a0

E. Grün, P. Staubach, M. Baguhl, D.P. Hamilton, H.A. Zook, S. Dermott, B.A. Gustafson, H. Fechtig, J. Kissel, D. Linkert, G. Linkert, R. Srama, M.S. Hanner, C. Polanskey, M. Horányi, B.A. Lindblad, I. Mann, J.A.M. McDonnell, G.E. Morfill, G. Schwehm, South-north and radial traverses through the interplanetary dust cloud. Icarus **129**, 270–288 (1997). https://doi.org/10.1006/icar.1997.5789

E. Grün, M. Baguhl, H. Svedhem, H.A. Zook, *In situ Measurements of Cosmic Dust* (2001), p. 295

E. Grün, R. Srama, M. Horányi, H. Krüger, R. Soja, V. Sterken, Z. Sternovsky, P. Strub, Comparative analysis of the ESA and NASA interplanetary meteoroid enviroment models, in *6th European Conference on Space Debris*. ESA Special Publication, vol. 723 (2013), p. 36

P.S. Gural, Fully correcting for the spread in meteor radiant positions due to gravitational attraction. J. Int.l Meteor Org. **29**, 134–138 (2001)

D.A. Gurnett, E. Grun, D. Gallagher, W.S. Kurth, F.L. Scarf, Micron-sized particles detected near Saturn by the Voyager plasma wave instrument. Icarus **53**, 236–254 (1983). https://doi.org/10.1016/0019-1035(83)90145-8

D.A. Gurnett, T.F. Averkamp, F.L. Scarf, E. Grun, Dust particles detected near Giacobini-Zinner by the ICE plasma wave instrument. Geophys. Res. Lett. **13**, 291–294 (1986). https://doi.org/10.1029/GL013i003p00291
D.A. Gurnett, W.S. Kurth, K.L. Scarf, J.A. Burns, J.N. Cuzzi, Micron-sized particle impacts detected near Uranus by the Voyager 2 plasma wave instrument. J. Geophys. Res. Space Phys. **92**, 14,959–14,968 (1987). https://doi.org/10.1029/JA092iA13p14959
D.A. Gurnett, W.S. Kurth, L.J. Granroth, S.C. Allendorf, R.L. Poynter, Micron-sized particles detected near Neptune by the Voyager 2 plasma wave instrument. J. Geophys. Res. Space Phys. **96**, 19 (1991). https://doi.org/10.1029/91JA01270
D.A. Gurnett, J.A. Ansher, W.S. Kurth, L.J. Granroth, Micron-sized dust particles detected in the outer solar system by the Voyager 1 and 2 plasma wave instruments. Geophys. Res. Lett. **24**(24), 3125–3128 (1997)
D.A. Gurnett, W.S. Kurth, D.L. Kirchner, G.B. Hospodarsky, T.F. Averkamp, P. Zarka, A. Lecacheux, R. Manning, A. Roux, P. Canu, N. Cornilleau-Wehrlin, P. Galopeau, A. Meyer, R. Boström, G. Gustafsson, J.E. Wahlund, L. Åhlen, H.O. Rucker, H.P. Ladreiter, W. Macher, L.J.C. Woolliscroft, H. Alleyne, M.L. Kaiser, M.D. Desch, W.M. Farrell, C.C. Harvey, P. Louarn, P.J. Kellogg, K. Goetz, A. Pedersen, The Cassini radio and plasma wave investigation. Space Sci. Rev. **114**, 395–463 (2004). https://doi.org/10.1007/s11214-004-1434-0
B.A.S. Gustafson, Comet ejection and dynamics of nonspherical dust particles and meteoroids. Astrophys. J. **337**, 945–949 (1989). https://doi.org/10.1086/167164
B.A.S. Gustafson, Physics of zodiacal dust. Annu. Rev. Earth Planet. Sci. **22**, 553–595 (1994). https://doi.org/10.1146/annurev.ea.22.050194.003005
E. Hadamcik, A.C. Levasseur-Regourd, Imaging polarimetry of cometary dust: different comets and phase angles. J. Quant. Spectrosc. Radiat. Transf. **79**, 661–678 (2003)
M. Hajduková Jr, On the frequency of interstellar meteoroids. Astron. Astrophys. **288**, 330–334 (1994)
M. Hajduková, Meteors in the IAU meteor data center on hyperbolic orbits. Earth Moon Planets **102**, 67–71 (2008). https://doi.org/10.1007/s11038-007-9171-5
M. Hajduková Jr, Interstellar meteoroids in the Japanese tv catalogue. Publ. Astron. Soc. Jpn. **63**, 481–487 (2011). https://doi.org/10.1093/pasj/63.3.481
M. Hajduková Jr, The occurrence of interstellar particles in the vicinity of the Sun an overview—25 years of research, in *International Meteor Conference Egmond*, ed. by A. Roggemans, P. Roggemans, the Netherlands, 2–5 June 2016 (2016), pp. 105–110
M. Hajduková, L. Kornoš, J. Tóth, Frequency of hyperbolic and interstellar meteoroids. Meteorit. Planet. Sci. **49**, 63–68 (2014a). https://doi.org/10.1111/maps.12119
M. Hajduková Jr, L. Kornoš, J. Tóth, Hyperbolic orbits in the EDMOND. Meteoroids **2013**, 289–295 (2014b)
M. Hajduková, V.J. Sterken, P. Wiegert, *Interstellar Meteoroids* (2018)
I. Halliday, A.A. Griffin, A.T. Blackwell, Detailed data for 259 fireballs from the Canadian camera network and inferences concerning the influx of large meteoroids. Meteorit. Planet. Sci. **31**, 185–217 (1996). https://doi.org/10.1111/j.1945-5100.1996.tb02014.x
D.P. Hamilton, E. Grün, M. Baguhl, Electromagnetic escape of dust from the solar system. Int. Astron. Union Colloq. **150**, 31 (1996). https://doi.org/10.1017/S0252921100501225
D. Han, A.R. Poppe, M. Piquette, E. Grün, M. Horányi, Constraints on dust production in the Edgeworth-Kuiper Belt from Pioneer 10 and New Horizons measurement. Geophys. Res. Lett. **38**, L24102 (2011)
M. Hanner, R. Giese, K. Weiss, R. Zerull, On the definition of albedo and application to irregular particles. Astron. Astrophys. **104**, 42–46 (1981)
M.S. Hanner, M.E. Zolensky, The mineralogy of cometary dust, in *Lecture Notes in Physics*, vol. 815, ed. by T. Henning (Springer, Berlin, 2010), pp. 203–232. https://doi.org/10.1007/978-3-642-13259-9_4
V. Haudebourg, M. Cabane, A.C. Levasseur-Regourd, Theoretical polarimetric responses of fractal aggregates, in relation with experimental studies of dust in the solar system. Phys. Chem. Earth, Part C, Sol.-Terr. Planet. Sci. **24**(5), 603–608 (1999)
R.L. Hawkes, S.C. Woodworth, Optical detection of two meteoroids from interstellar space. J. R. Astron. Soc. Can. **91**, 218 (1997)
G.S. Hawkins, Variation in the occurrence rate of meteors. Astron. J. **61**, 386 (1956). https://doi.org/10.1086/107367
G.S. Hawkins, Symposium: small meteoric particles in the earth's neighborhood: radar determination of meteor orbits. Astron. J. **67**, 241 (1962). https://doi.org/10.1086/108702
G.S. Hawkins, The Harvard radio meteor project. Smithson. Contrib. Astrophys. **7**, 53 (1963)
G.S. Hawkins, E.K.L. Upton, The influx rate of meteors in the Earth's atmosphere. Astrophys. J. **128**, 727 (1958). https://doi.org/10.1086/146585
G.F.H. Herzog, S. Xue, G.S. Hall, L.E. Nyquist, C. Shih, H. Wiesmann, D.E. Brownlee, Isotopic and elemental composition of iron, nickel, and chromium in type I deep-sea spherules: implications for origin

and composition of the parent micrometeoroids. Geochim. Cosmochim. Acta **63**, 1443–1457 (1999). https://doi.org/10.1016/S0016-7037(99)00011-3
K.A. Hill, L.A. Rogers, R.L. Hawkes, High geocentric velocity meteor ablation. Astron. Astrophys. **444**, 615–624 (2005). https://doi.org/10.1051/0004-6361:20053053
J.K. Hillier, S.F. Green, N. McBride, N. Altobelli, F. Postberg, S. Kempf, J. Schwanethal, R. Srama, J.A.M. McDonnell, E. Grün, Interplanetary dust detected by the Cassini CDA Chemical Analyser. Icarus **190**, 643–654 (2007). https://doi.org/10.1016/j.icarus.2007.03.024
T. Hiroi, C.M. Pieters, M.E. Zolensky, M.E. Lipschutz, Evidence of thermal metamorphism on the C, G, B, and F asteroids. Science **261**, 1016–1018 (1993). https://doi.org/10.1126/science.261.5124.1016
H.J. Hoffmann, H. Fechtig, E. Grün, J. Kissel, First results of the micrometeoroid experiment S 215 on the HEOS 2 satellite. Planet. Space Sci. **23**, 215–224 (1975a). https://doi.org/10.1016/0032-0633(75)90080-X
H.J. Hoffmann, H. Fechtig, E. Grün, J. Kissel, Temporal fluctuations and anisotropy of the micrometeoroid flux in the earth-moon system measured by HEOS 2. Planet. Space Sci. **23**, 985–991 (1975b). https://doi.org/10.1016/0032-0633(75)90186-5
P. Hoppe, G. Kurat, J. Walter, M. Maurette, Trace elements and oxygen isotopes in a CAI-bearing micrometeorite from Antarctica, in *Lunar and Planetary Science Conference*, vol. 26 (1995)
P. Horálek, L.L. Christensen, D. Nesvornỳ, R. Davies, Light phenomena over the eso observatories, III: zodiacal light. Messenger **164**, 45–47 (2016)
M. Horányi et al., The student dust counter on the New Horizons mission. Space Sci. Rev. **140**, 387–402 (2008)
F. Horz, R.P. Bernhard, Compositional analysis and classification of projectile residues in LDEF impact craters. NASA STI/Recon technical report No. 93 (1992)
F. Hörz, E. Schneider, D.E. Gault, J.B. Hartung, D.E. Brownlee, Catastrophic rupture of lunar rocks—a Monte Carlo simulation. Moon **13**, 235–258 (1975). https://doi.org/10.1007/BF00567517
W. Huang, X. Chu, C.S. Gardner, J.D. Carrillo-Sánchez, W. Feng, J.M.C. Plane, D. Nesvorný, Measurements of the vertical fluxes of atomic Fe and Na at the mesopause: Implications for the velocity of cosmic dust entering the atmosphere. Geophys. Res. Lett. **42**, 169–175 (2015). https://doi.org/10.1002/2014GL062390
D.H. Humes, Results of Pioneer 10 and 11 meteoroid experiments: interplanetary and near-Saturn. J. Geophys. Res. **85**(A11), 5841–5852 (1980)
G.R. Huss, The survival of presolar grains in solar system bodies, in *American Institute of Physics Conference Series*, vol. 402, ed. by T.J. Bernatowicz, E. Zinner (1997), pp. 721–748. https://doi.org/10.1063/1.53338
G.R. Huss, A.P. Meshik, J.B. Smith, C.M. Hohenberg, Presolar diamond, silicon carbide, and graphite in carbonaceous chondrites: implications for thermal processing in the solar nebula. Geochim. Cosmochim. Acta **67**, 4823–4848 (2003). https://doi.org/10.1016/j.gca.2003.07.019
G.R. Huss, A.E. Rubin, J.N. Grossman, *Thermal Metamorphism in Chondrites* (2006), pp. 567–586
M. Ishiguro, R. Nakamura, Y. Fujii, K. Morishige, H. Yano, H. Yasuda, S. Yokogawa, T. Mukai, First detection of visible zodiacal dust bands from ground-based observations. Astrophys. J. **511**(1), 432 (1999)
M. Ishiguro, H. Yang, F. Usui, J. Pyo, M. Ueno, T. Ootsubo, S.M. Kwon, T. Mukai, High-resolution imaging of the gegenschein and the geometric albedo of interplanetary dust. Astrophys. J. **767**(1), 75 (2013)
H.A. Ishii, J.P. Bradley, Z.R. Dai, M. Chi, A.T. Kearsley, M.J. Burchell, N.D. Browning, F. Molster, Comparison of comet 81P/Wild 2 dust with interplanetary dust from comets. Science **319**, 447 (2008). https://doi.org/10.1126/science.1150683
I. Jakšová, V. Porubčan, J. Klačka, Structure and sources of the sporadic meteor background from video observations. Publ. Astron. Soc. Jpn. **67**, 99 (2015). https://doi.org/10.1093/pasj/psv068
D. James, M. Horányi, V. Hoxie, Polyvinylidene fluoride detector response to particle impacts. Rev. Sci. Instrum. **81**(3), 034501 (2010). https://doi.org/10.1063/1.3340880
D. Janches, S. Close, J.L. Hormaechea, N. Swarnalingam, A. Murphy, D. O'Connor, B. Vandepeer, B. Fuller, D.C. Fritts, C. Brunini, The Southern Argentina Agile MEteor Radar Orbital System (SAAMER-OS): an initial sporadic meteoroid orbital survey in the southern sky. Astrophys. J. **809**, 36 (2015). https://doi.org/10.1088/0004-637X/809/1/36
P. Jenniskens, Quantitative meteor spectroscopy: elemental abundances. Adv. Space Res. **39**, 491–512 (2007). https://doi.org/10.1016/j.asr.2007.03.040
P. Jenniskens, *Meteoroid Streams and the Zodiacal Cloud* (2015), pp. 281–295. https://doi.org/10.2458/azu_uapress_9780816532131-ch015
P. Jenniskens, Meteor showers in review. Planet. Space Sci. **143**, 116–124 (2017). https://doi.org/10.1016/j.pss.2017.01.008
P. Jenniskens, P. Gural, A. Berdeu, CAMSS: a spectroscopic survey of meteoroid elemental abundances. Meteoroids **2013**, 117–124 (2014)

P. Jenniskens, Q. Nénon, J. Albers, P.S. Gural, B. Haberman, D. Holman, R. Morales, B.J. Grigsby, D. Samuels, C. Johannink, The established meteor showers as observed by CAMS. Icarus **266**, 331–354 (2016a). https://doi.org/10.1016/j.icarus.2015.09.013
P. Jenniskens, Q. Nénon, P.S. Gural, J. Albers, B. Haberman, B. Johnson, D. Holman, R. Morales, B.J. Grigsby, D. Samuels, C. Johannink, CAMS confirmation of previously reported meteor showers. Icarus **266**, 355–370 (2016b). https://doi.org/10.1016/j.icarus.2015.08.014
P. Jenniskens, Q. Nénon, P.S. Gural, J. Albers, B. Haberman, B. Johnson, R. Morales, B.J. Grigsby, D. Samuels, C. Johannink, CAMS newly detected meteor showers and the sporadic background. Icarus **266**, 384–409 (2016c). https://doi.org/10.1016/j.icarus.2015.11.009
D. Jewitt, L. Chizmadia, R. Grimm, D. Prialnik, Water in the small bodies of the solar system, in *Protostars and Planets V* (2007), pp. 863–878
J. Jones, Meteoroid engineering model—final report. Tech. rep., NASA/MSFC internal report SEE/CR-2004-400 (2004)
J. Jones, P. Brown, Sporadic meteor radiant distributions - Orbital survey results. Mon. Not. R. Astron. Soc. **265**, 524 (1993). https://doi.org/10.1093/mnras/265.3.524
J. Jones, M. Campbell, S. Nikolova, Modelling of the sporadic meteoroid sources, in *Meteoroids 2001 Conference*, ed. by B. Warmbein. ESA Special Publication, vol. 495 (2001), pp. 575–580
T.J. Jopek, P.M. Jenniskens, The working group on meteor showers nomenclature: a history, current status and a call for contributions, in *Meteoroids: the Smallest Solar System Bodies*, ed. by W.J. Cooke, D.E. Moser, B.F. Hardin, D. Janches (2011), pp. 7–13
T.J. Jopek, Z. Kaňuchová, Current status of the IAU MDC Meteor Showers Database. Meteoroids **2013**, 353–364 (2014)
T.J. Jopek, R. Rudawska, P. Bartczak, Meteoroid stream searching: the use of the vectorial elements. Earth Moon Planets **102**, 73–78 (2008). https://doi.org/10.1007/s11038-007-9197-8
A. Juhász, M. Horányi, Dynamics and distribution of nano-dust particles in the inner solar system. Geophys. Res. Lett. **40**, 2500–2504 (2013). https://doi.org/10.1002/grl.50535
L.P. Keller, K.L. Thomas, D.S. McKay, An interplanetary dust particle with links to CI chondrites. Geochim. Cosmochim. Acta **56**, 1409–1412 (1992). https://doi.org/10.1016/0016-7037(92)90072-Q
L.P. Keller, K.L. Thomas, D.S. McKay, Carbon in primitive interplanetary dust particles, in *Analysis of Interplanetary Dust Particles*, ed. by E. Zolensky, T.L. Wilson, F.J.M. Rietmeijer, G.J. Flynn. American Institute of Physics Conference Series, vol. 310, (1994), p. 159. https://doi.org/10.1063/1.46531
L.P. Keller, S. Messenger, G.J. Flynn, S. Clemett, S. Wirick, C. Jacobsen, The nature of molecular cloud material in interplanetary dust. Geochim. Cosmochim. Acta **68**, 2577–2589 (2004). https://doi.org/10.1016/j.gca.2003.10.044
M.S. Kelley, C.E. Woodward, D.E. Harker, D.H. Wooden, R.D. Gehrz, H. Campins, M.S. Hanner, S.M. Lederer, D.J. Osip, J. Pittichová, E. Polomski, A Spitzer study of comets 2P/Encke, 67P/Churyumov-Gerasimenko, and C/2001 HT50 (LINEAR-NEAT). Astrophys. J. **651**, 1256–1271 (2006). https://doi.org/10.1086/507701. astro-ph/0607416
M.S. Kelley, Y.R. Fernández, J. Licandro, C.M. Lisse, W.T. Reach, M.F. A'Hearn, J. Bauer, H. Campins, A. Fitzsimmons, O. Groussin, P.L. Lamy, S.C. Lowry, K.J. Meech, J. Pittichová, C. Snodgrass, I. Toth, H.A. Weaver, The persistent activity of Jupiter-family comets at 3–7 AU. Icarus **225**, 475–494 (2013)
P.J. Kellogg, K. Goetz, S.J. Monson, Dust impact signals on the wind spacecraft. J. Geophys. Res. Space Phys. **121**, 966–991 (2016). https://doi.org/10.1002/2015JA021124
J.F. Kerridge, Carbon, hydrogen and nitrogen in carbonaceous chondrites abundances and isotopic compositions in bulk samples. Geochim. Cosmochim. Acta **49**, 1707–1714 (1985). https://doi.org/10.1016/0016-7037(85)90141-3
D.J. Kessler, Meteoroid environment model-1970 [Interplanetary and planetary]. NASA SP-8038, NASA (1970)
J.B. Kikwaya, M. Campbell-Brown, P.G. Brown, Bulk density of small meteoroids. Astron. Astrophys. **530**, A113 (2011). https://doi.org/10.1051/0004-6361/201116431
H. Kimura, Light-scattering properties of fractal aggregates: numerical calculations by a superposition technique and the discrete-dipole approximation. J. Quant. Spectrosc. Radiat. Transf. **70**(4), 581–594 (2001)
H. Kimura, I. Mann, Radiation pressure on porous micrometeoroids, in *Meteroids*, ed. by W.J. Baggaley, V. Porubcan (1999), p. 283. 1998
H. Kimura, I. Mann, D.A. Biesecker, E.K. Jessberger, Dust grains in the comae and tails of sungrazing comets: modeling of their mineralogical and morphological properties. Icarus **159**, 529–541 (2002a). https://doi.org/10.1006/icar.2002.6940
H. Kimura, H. Okamoto, T. Mukai, Radiation pressure and the Poynting-Robertson effect for fluffy dust particles. Icarus **157**, 349–361 (2002b). https://doi.org/10.1006/icar.2002.6849
H. Kimura, L. Kolokolova, I. Mann, Optical properties of cometary dust-constraints from numerical studies on light scattering by aggregate particles. Astron. Astrophys. **407**(1), L5–L8 (2003)

H. Kimura, L. Kolokolova, I. Mann, Light scattering by cometary dust numerically simulated with aggregate particles consisting of identical spheres. Astron. Astrophys. **449**(3), 1243–1254 (2006)
J. Kissel, F.R. Krueger, The organic component in dust from comet Halley as measured by the PUMA mass spectrometer on board Vega 1. Nature **326**, 755–760 (1987). https://doi.org/10.1038/326755a0
W. Klöck, F.J. Stadermann, Mineralogical and chemical relationships of interplanetary dust particles micrometeorites and meteorites, in *Analysis of Interplanetary Dust Particles*, ed. by E. Zolensky, T.L. Wilson, F.J.M. Rietmeijer, G.J. Flynn. American Institute of Physics Conference Series, vol. 310 (1994), p. 51. https://doi.org/10.1063/1.46523
H. Kobayashi, J. Kimura, S. Yamamoto, S. Watanabe, T. Yamamoto, Ice sublimation of dust particles and their detection in the outer solar system. Earth Planets Space **62**, 57–61 (2010)
H. Kobayashi, H. Kimura, S.Watanabe, T. Yamamoto, S. Müller, Sublimation temperature of circumstellar dust particles and its importance for dust ring formation. Earth Planets Space **63**, 1067 (2011)
L. Kolokolova, H. Kimura, Effects of electromagnetic interaction in the polarization of light scattered by cometary and other types of cosmic dust. Astron. Astrophys. **513**, A40 (2010)
L. Kolokolova, J. Hough, A.C. Levasseur-Regourd, *Polarimetry of stars and planetary systems* (Cambridge University Press, Cambridge, 2015)
D. Koschny, E. Drolshagen, S. Drolshagen, J. Kretschmer, T. Ott, G. Drolshagen, B. Poppe, Flux densities of meteoroids derived from optical double-station observations. Planet. Space Sci. **143**, 230–237 (2017). https://doi.org/10.1016/j.pss.2016.12.007
Y. Kozai, Secular perturbations of asteroids with high inclination and eccentricity. Astron. J. **67**, 591 (1962). https://doi.org/10.1086/108790
L. Kresak, Cometary dust trails and meteor storms. Astron. Astrophys. **279**, 646–660 (1993)
H. Krüger, E. Grün, D.P. Hamilton, M. Baguhl, S. Dermott, H. Fechtig, B.A. Gustafson, M.S. Hanner, M. Horányi, J. Kissel, B.A. Lindblad, D. Linkert, G. Linkert, I. Mann, J.A.M. McDonnell, G.E. Morfill, C. Polanskey, R. Riemann, G. Schwehm, R. Srama, H.A. Zook, Three years of Galileo dust data, II: 1993–1995. Planet. Space Sci. **47**, 85–106 (1998). https://doi.org/10.1016/S0032-0633(98)00097-X. astro-ph/9809318
H. Krüger, N. Altobelli, B. Anweiler, S.F. Dermott, V. Dikarev, A.L. Graps, E. Grün, B.A. Gustafson, D.P. Hamilton, M.S. Hanner, M. Horányi, J. Kissel, M. Landgraf, B.A. Lindblad, D. Linkert, G. Linkert, I. Mann, J.A.M. McDonnell, G.E. Morfill, C. Polanskey, G. Schwehm, R. Srama, H.A. Zook, Five years of Ulysses dust data: 2000. Planet. Space Sci. **54**, 932–956 (2006). https://doi.org/10.1016/j.pss.2006.04.015. 2004
H. Krüger, V. Dikarev, B. Anweiler, S.F. Dermott, A.L. Graps, E. Grün, B.A. Gustafson, D.P. Hamilton, M.S. Hanner, M. Horányi, J. Kissel, D. Linkert, G. Linkert, I. Mann, J.A.M. McDonnell, G.E. Morfill, C. Polanskey, G. Schwehm, R. Srama, Three years of Ulysses dust data: 2005. Planet. Space Sci. **58**, 951–964 (2010). https://doi.org/10.1016/j.pss.2009.11.002. to 2007. 0908.1279
M.J. Kuchner, C.C. Stark, Collisional grooming models of the Kuiper belt dust cloud. Astron. J. **140**, 1007–1019 (2010)
G. Kurat, C. Koeberl, T. Presper, F. Brandstätter, M. Maurette, Petrology and geochemistry of Antarctic micrometeorites. Geochim. Cosmochim. Acta **58**, 3879–3904 (1994). https://doi.org/10.1016/0016-7037(94)90369-7
G. Kurat, P. Hoppe, C. Engrand, A chondrule micrometeorite from antarctica with vapor-fractionated trace-element abundances. Meteorit. Planet. Sci. Suppl. **31**, A75–A76 (1996)
W.S. Kurth, T.F. Averkamp, D.A. Gurnett, Z. Wang, Cassini RPWS observations of dust in Saturn's E ring. Planet. Space Sci. **54**, 988–998 (2006). https://doi.org/10.1016/j.pss.2006.05.011
S. Kwon, S. Hong, J. Weinberg, An observational model of the zodiacal light brightness distribution. New Astron. **10**(2), 91–107 (2004)
H. Laakso, R. Grard, A. Pedersen, G. Schwehm, Impacts of large dust particles on the VEGA spacecraft. Adv. Space Res. **9**, 269–272 (1989). https://doi.org/10.1016/0273-1177(89)90273-1
H. Lai, C.T. Russell, H. Wei, T. Zhang, The evolution of co-orbiting material in the orbit of 2201 Oljato from 1980 to 2012 as deduced from Pioneer Venus Orbiter and Venus Express magnetic records. Meteorit. Planet. Sci. **49**, 28–35 (2014). https://doi.org/10.1111/maps.12102
M. Landgraf, Modellierung der dynamik und interpretation der in-situ-messung interstellaren staubs in der lokalen umgebung des sonnensystems. PhD thesis, Ruprecht-Karls-Universität Heidelberg (1998)
M. Landgraf, Modeling the motion and distribution of interstellar dust inside the heliosphere. J. Geophys. Res. **105**, 10,303–10,316 (2000)
M. Landgraf, J.C. Liou, H.A. Zook, E. Grün, Origins of solar system dust beyond Jupiter. Astron. J. **123**, 2857–2861 (2002)
J. Lasue, A.C. Levasseur-Regourd, N. Fray, H. Cottin, Inferring the interplanetary dust properties-from remote observations and simulations. Astron. Astrophys. **473**(2), 641–649 (2007)

J. Lasue, A. Levasseur-Regourd, A. Lazarian, Interplanetary dust, in *Polarimetry of Stars and Planetary Systems*, ed. by Kolokolova et al. (2015)
D.S. Lauretta (OSIRIS-Rex Team), An overview of the OSIRIS-REx asteroid sample return mission, in *Lunar and Planetary Science Conference*. Lunar and Planetary Inst. Technical Report, vol. 43 (2012), p. 2491
M.E. Lawler, D.E. Brownlee, CHON as a component of dust from comet Halley. Nature **359**, 810–812 (1992). https://doi.org/10.1038/359810a0
A. Lazarian, B. Andersson, T. Hoang, Grain alignment: role of radiative torques and paramagnetic relaxation, in *Polarimetry of Stars and Planetary Systems*, ed. by Kolokolova et al. (2015)
C. Leinert, Zodiacal light—a measure of the interplanetary environment. Space Sci. Rev. **18**(3), 281–339 (1975)
C. Leinert, E. Grün, Interplanetary dust, in *Physics of the Inner Heliosphere I*, ed. by R. Schwenn, E. Marsch (Springer, Berlin, 1990), pp. 207–275
C. Leinert, S. Roser, J. Buitrago, How to maintain the spatial distribution of interplanetary dust. Astron. Astrophys. **118**, 345–357 (1983a)
C. Leinert, S. Roser, J. Buitrago, How to maintain the spatial distribution of interplanetary dust. Astron. Astrophys. **118**, 345–357 (1983b)
C. Leinert, S. Bowyer, L. Haikala, M. Hanner, M. Hauser, A.C. Levasseur-Regourd, I. Mann, K. Mattila, W. Reach, W. Schlosser et al., The 1997 reference of diffuse night sky brightness. Astron. Astrophys. Suppl. Ser. **127**(1), 1–99 (1998)
A.C. Levasseur, J. Blamont, Satellite observations of intensity variations of the zodiacal light. Nature **246**(5427), 26–28 (1973)
A. Levasseur-Regourd, J. Renard, R. Dumont, Dust optical properties: a comparison between cometary and interplanetary grains. Adv. Space Res. **11**(12), 175–182 (1991)
A. Levasseur-Regourd, M. Cabane, J. Worms, V. Haudebourg, Physical properties of dust in the solar system: relevance of a computational approach and of measurements under microgravity conditions. Adv. Space Res. **20**(8), 1585–1594 (1997)
A.C. Levasseur-Regourd, Optical and thermal properties of zodiacal dust, in *IAU Colloq. 150: Physics, Chemistry, and Dynamics of Interplanetary Dust*, vol. 104, ed. by B.A.S. Gustafson, M.S. Hanner (Astron. Soc. of the Pacific Press, San Francisco, 1996a), p. 301
A.C. Levasseur-Regourd, Physical properties of dust grains deduced by optical probing techniques. Adv. Space Res. **17**(12), 117–122 (1996b)
A.C. Levasseur-Regourd, R. Dumont, Absolute photometry of zodiacal light. Astron. Astrophys. **84**, 277–279 (1980)
A.C. Levasseur-Regourd, E. Hadamcik, J. Renard, Evidence for two classes of comets from their polarimetric properties at large phase angles. Astron. Astrophys. **313**, 327–333 (1996)
A.C. Levasseur-Regourd, I. Mann, R. Dumont, M.S. Hanner, Optical and thermal properties of interplanetary dust, in *Interplanetary Dust*, ed. by E. Grün, B.A.S. Gustafson, S.F. Dermott, H. Fechtig (Springer, Berlin, 2001), pp. 57–94
A.C. Levasseur-Regourd, T. Mukai, J. Lasue, Y. Okada, Physical properties of cometary and interplanetary dust. Planet. Space Sci. **55**(9), 1010–1020 (2007)
A.C. Levasseur-Regourd, J. Agarwal, H. Cottin, C. Engrand, G. Flynn, M. Fulle, T. Gombosi, Y. Langevin, J. Lasue, T. Mannel, S. Merounane, O. Poch, N. Thomas, A. Westphal, Cometary dust. Space Sci. Rev. **214**, 64 (2018). https://doi.org/10.1007/s11214-018-0496-3
L.F. Lim, L.R. Nittler, Elemental composition of 433 eros: new calibration of the NEAR-Shoemaker XRS data. Icarus **200**, 129–146 (2009). https://doi.org/10.1016/j.icarus.2008.09.018
J.C. Liou, H.A. Zook, Evolution of interplanetary dust particles in mean motion resonances with planets. Icarus **128**(2), 354–367 (1997)
J.C. Liou, H.A. Zook, Signatures of the giant planets imprinted on the Edgeworth-Kuiper belt dust disk. Astron. J. **118**, 580–590 (1999)
J.C. Liou, H.A. Zook, S.F. Dermott, Kuiper belt dust grains as a source of interplanetary dust particles. Icarus **124**, 429–440 (1996a). https://doi.org/10.1006/icar.1996.0220
S.G. Love, D.E. Brownlee, A direct measurement of the terrestrial mass accretion rate of cosmic dust. Science **262**, 550–553 (1993). https://doi.org/10.1126/science.262.5133.550
K. Lumme, J. Rahola, J. Hovenier, Light scattering by dense clusters of spheres. Icarus **126**(2), 455–469 (1997)
D.M. Malaspina, L.B. Wilson, A database of interplanetary and interstellar dust detected by the Wind spacecraft. J. Geophys. Res. Space Phys. **121**, 9369–9377 (2016). https://doi.org/10.1002/2016JA023209
D.M. Malaspina, M. Horányi, A. Zaslavsky, K. Goetz, L.B. Wilson, K. Kersten, Interplanetary and interstellar dust observed by the Wind/WAVES electric field instrument. Geophys. Res. Lett. **41**, 266–272 (2014). https://doi.org/10.1002/2013GL058786

D.M. Malaspina, L.E. O'Brien, F. Thayer, Z. Sternovsky, A. Collette, Revisiting STEREO interplanetary and interstellar dust flux and mass estimates. J. Geophys. Res. Space Phys. **120**, 6085–6100 (2015). https://doi.org/10.1002/2015JA021352

I. Mann, Interstellar grains in the solar system: requirements for an analysis. Space Sci. Rev. **78**(1), 259–264 (1996)

I. Mann, H. Okamoto, T. Mukai, H. Kimura, Y. Kitada, Fractal aggregate analogues for near solar dust properties. Astron. Astrophys. **291**, 1011–1018 (1994)

I. Mann, H. Kimura, D.A. Biesecker, B.T. Tsurutani, E. Grün, R.B. McKibben, J.C. Liou, R.M. MacQueen, T. Mukai, M. Guhathakurta et al., Dust near the sun. Space Sci. Rev. **110**(3), 269–305 (2004)

G. Matrajt, S. Taylor, G. Flynn, D. Brownlee, D. Joswiak, A nuclear microprobe study of the distribution and concentration of carbon and nitrogen in Murchison and Tagish lake meteorites, Antarctic micrometeorites, and IDPs: implications for astrobiology. Meteorit. Planet. Sci. **38**, 1585–1600 (2003). https://doi.org/10.1111/j.1945-5100.2003.tb00003.x

G. Matrajt, S. Pizzarello, S. Taylor, D. Brownlee, Concentration and variability of the AIB amino acid in polar micrometeorites: implications for the exogenous delivery of amino acids to the primitive Earth. Meteorit. Planet. Sci. **39**, 1849–1858 (2004). https://doi.org/10.1111/j.1945-5100.2004.tb00080.x

M. Maurette, Cometary micrometeorites in planetology, exobiology, and early climatology, in *Comets and the Origin and Evolution of Life*, ed. by P.J. Thomas, R.D. Hicks, C.F. Chyba, C.P. McKay (2006), p. 69. https://doi.org/10.1007/3-540-33088-7_3

M. Maurette, C. Hammer, N. Reeh, D.E. Brownlee, H.H. Thomsen, Placers of cosmic dust in the blue ice lakes of Greenland. Science **233**, 869–872 (1986). https://doi.org/10.1126/science.233.4766.869

M. Maurette, C. Jehanno, E. Robin, C. Hammer, Characteristics and mass distribution of extraterrestrial dust from the Greenland ice CAP. Nature **328**, 699–702 (1987). https://doi.org/10.1038/328699a0

M. Maurette, C. Olinger, M.C. Michel-Levy, G. Kurat, M. Pourchet, F. Brandstatter, M. Bourot-Denise, A collection of diverse micrometeorites recovered from 100 tonnes of Antarctic blue ice. Nature **351**, 44–47 (1991). https://doi.org/10.1038/351044a0

M. Maurette, C. Engrand, A. Brack, G. Kurat, S. Leach, M. Perreau, Carbonaceous phases in Antarctic micrometeorites and their mineralogical environment. Their contribution to the possible role of micrometeorites as "chondritic chemical reactors" in atmospheres, waters and/or ices, in *Lunar and Planetary Science Conference*, vol. 26 (1995)

M. Maurette, J. Duprat, C. Engrand, M. Gounelle, G. Kurat, G. Matrajt, A. Toppani, Accretion of neon, organics, $CO_2$, nitrogen and water from large interplanetary dust particles on the early Earth. Planet. Space Sci. **48**, 1117–1137 (2000). https://doi.org/10.1016/S0032-0633(00)00086-6

N. McBride, S.F. Green, J.A.M. McDonnell, Meteoroids and small sized debris in low earth orbit and at 1 Au: results of recent modelling. Adv. Space Res. **23**, 73–82 (1999). https://doi.org/10.1016/S0273-1177(98)00232-4

K.D. McKeegan, Ion microprobe measurements of H, C, O, Mg, and SI isotopic abundances in individual interplanetary dust particles. PhD thesis, Washington Univ., Seattle (1987a)

K.D. McKeegan, Oxygen isotopes in refractory stratospheric dust particles—proof of extraterrestial origin. Science **237**, 1468–1471 (1987b). https://doi.org/10.1126/science.237.4821.1468

K.D. McKeegan, R.M. Walker, E. Zinner, Ion microprobe isotopic measurements of individual interplanetary dust particles. Geochim. Cosmochim. Acta **49**, 1971–1987 (1985). https://doi.org/10.1016/0016-7037(85)90091-2

H. McNamara, J. Jones, B. Kauffman, R. Suggs, W. Cooke, S. Smith, Meteoroid engineering model (MEM): a meteoroid model for the inner solar system. Earth Moon Planets **95**, 123–139 (2004). https://doi.org/10.1007/s11038-005-9044-8

A. Meibom, B.E. Clark, Invited review: evidence for the insignificance of ordinary chondritic material in the asteroid belt. Meteorit. Planet. Sci. **34**, 7–24 (1999)

D.D. Meisel, D. Janches, J.D. Mathews, Extrasolar micrometeors radiating from the vicinity of the local interstellar bubble. Astrophys. J. **567**, 323–341 (2002). https://doi.org/10.1086/322317

S. Messenger, Identification of molecular-cloud material in interplanetary dust particles. Nature **404**, 968–971 (2000). https://doi.org/10.1038/35010053

S. Messenger, L.P. Keller, F.J. Stadermann, R.M. Walker, E. Zinner, Samples of stars beyond the solar system: silicate grains in interplanetary dust. Science **300**, 105–108 (2003). https://doi.org/10.1126/science.1080576

N. Meyer-Vernet, P. Couturier, S. Hoang, C. Perche, J.L. Steinberg, J. Fainberg, C. Meetre, Plasma diagnosis from thermal noise and limits on dust flux or mass in comet Giacobini-Zinner. Science **232**, 370–374 (1986). https://doi.org/10.1126/science.232.4748.370

N. Meyer-Vernet, A. Lecacheux, M.L. Kaiser, D.A. Gurnett, Detecting nanoparticles at radio frequencies: jovian dust stream impacts on Cassini/RPWS. Geophys. Res. Lett. **36**, L03103 (2009a). https://doi.org/10.1029/2008GL036752

N. Meyer-Vernet, M. Maksimovic, A. Czechowski, I. Mann, I. Zouganelis, K. Goetz, M.L. Kaiser, O.C. St Cyr, J.L. Bougeret, S.D. Bale, Dust detection by the wave instrument on STEREO: nanoparticles picked up by the solar wind? Sol. Phys. **256**, 463–474 (2009b). https://doi.org/10.1007/s11207-009-9349-2. arXiv:0903.4141

M.I. Mishchenko, L.D. Travis, A.A. Lacis, *Scattering, Absorption, and Emission of Light by Small Particles* (Cambridge University Press, Cambridge, 2002)

A.V. Moorhead, Performance of D-criteria in isolating meteor showers from the sporadic background in an optical data set. Mon. Not. R. Astron. Soc. **455**, 4329–4338 (2016). https://doi.org/10.1093/mnras/stv2610

A.V. Moorhead, Deconvoluting measurement uncertainty from the meteor speed distribution. Meteorit. Planet. Sci. **1**, 1–7 (2018). https://doi.org/10.1111/maps.13066

A.V. Moorhead, H.M. Koehler, W.J. Cooke, NASA meteoroid engineering model release 2.0. NASA/TM-2015-218214 (2015)

A.V. Moorhead, R.C. Blaauw, D.E. Moser, M.D. Campbell-Brown, P.G. Brown, W.J. Cooke, A two-population sporadic meteoroid bulk density distribution and its implications for environment models. Mon. Not. R. Astron. Soc. **472**, 3833–3841 (2017a). https://doi.org/10.1093/mnras/stx2175

A.V. Moorhead, P.G. Brown, M.D. Campbell-Brown, D. Heynen, W.J. Cooke, Fully correcting the meteor speed distribution for radar observing biases. Planet. Space Sci. **143**, 209–217 (2017). https://doi.org/10.1016/j.pss.2017.02.002

A. Moro-Martín, R. Malhotra, A study of the dynamics of dust from the Kuiper belt: spatial distribution and spectral energy distribution. Astron. J. **124**, 2305–2321 (2002)

A. Moro-Martín, R. Malhotra, Dynamical models of Kuiper belt dust in the inner and outer solar system. Astrophys. J. **125**, 2255–2265 (2003)

D.A. Morrison, U.S. Clanton, Properties of microcraters and cosmic dust of less than 1000 A dimensions, in *Lunar and Planetary Science Conference Proceedings*, vol. 10, ed. by N.W. Hinners (1979), pp. 1649–1663

S. Mostefaoui, G.W. Lugmair, P. Hoppe, A. El Goresy, Evidence for live $^{60}$Fe in meteorites. New Astron. Rev. **48**, 155–159 (2004). https://doi.org/10.1016/j.newar.2003.11.022

C.E. Moyano-Cambero, E. Pellicer, J.M. Trigo-Rodríguez, I.P. Williams, J. Blum, P. Michel, M. Küppers, M. Martínez-Jiménez, I. Lloro, J. Sort, Nanoindenting the Chelyabinsk meteorite to learn about impact deflection effects in asteroids. Astrophys. J. **835**, 157 (2017). https://doi.org/10.3847/1538-4357/835/2/157. 1612.07131

T. Mukai, G. Schwehm, Interaction of grains with the solar energetic particles. Astron. Astrophys. **95**, 373–382 (1981)

T. Mukai, A.M. Nakamura, J. Blum, R.E. Johnson, O. Havnes, *Physical Processes on Interplanetary Dust* (2001), p. 445

R. Musci, R.J. Weryk, P. Brown, M.D. Campbell-Brown, P.A. Wiegert, An optical survey for millimeter-sized interstellar meteoroids. Astrophys. J. **745**, 161 (2012). https://doi.org/10.1088/0004-637X/745/2/161. 1110.5882

R. Nakamura, H. Okamoto, Optical properties of fluffy aggregates as analogue of interplanetary dust particles. Adv. Space Res. **23**(7), 1209–1212 (1999)

T. Nakamura, T. Noguchi, T. Yada, Y. Nakamuta, N. Takaoka, Bulk mineralogy of individual micrometeorites determined by X-ray diffraction analysis and transmission electron microscopy. Geochim. Cosmochim. Acta **65**, 4385–4397 (2001). https://doi.org/10.1016/S0016-7037(01)00722-0

T. Nakamura, T. Noguchi, Y. Ozono, T. Osawa, K. Nagao, Mineralogy of ultracarbonaceous large micrometeorites. Meteorit. Planet. Sci. Suppl. **40**, 5046 (2005)

T. Nakamura, T. Noguchi, A. Tsuchiyama, T. Ushikubo, N.T. Kita, J.W. Valley, M.E. Zolensky, Y. Kakazu, K. Sakamoto, E. Mashio, K. Uesugi, T. Nakano, Chondrulelike objects in short-period comet 81P/Wild 2. Science **321**, 1664 (2008). https://doi.org/10.1126/science.1160995

T. Nakamura, T. Noguchi, M. Tanaka, M.E. Zolensky, M. Kimura, A. Nakato, T. Ogami, H. Ishida, A. Tsuchiyama, T. Yada, K. Shirai, R. Okazaki, A. Fujimura, Y. Ishibashi, M. Abe, T. Okada, M. Ueno, T. Mukai, Mineralogy and major element abundance of the dust particles recovered from Muses-C Regio on the asteroid Itokawa, in *Lunar and Planetary Science Conference*, vol. 42 (2011a), p. 1766

T. Nakamura, T. Noguchi, M. Tanaka, M.E. Zolensky, M. Kimura, A. Tsuchiyama, A. Nakato, T. Ogami, H. Ishida, M. Uesugi, T. Yada, K. Shirai, A. Fujimura, R. Okazaki, S.A. Sandford, Y. Ishibashi, M. Abe, T. Okada, M. Ueno, T. Mukai, M. Yoshikawa, J. Kawaguchi, Itokawa dust particles: a direct link between S-type asteroids and ordinary chondrites. Science **333**, 1113 (2011b). https://doi.org/10.1126/science.1207758

K. Nakamura-Messenger, S. Messenger, L.P. Keller, S.J. Clemett, M.E. Zolensky, Organic globules in the Tagish lake meteorite: remnants of the protosolar disk. Science **314**, 1439–1442 (2006). https://doi.org/10.1126/science.1132175

R.J. Naumann, The near-earth meteoroid environment. NASA technical note NASA TN D-3717 (1966)
L. Neslušan, M. Hajduková, Separation and confirmation of showers. Astron. Astrophys. **598**, A40 (2017). https://doi.org/10.1051/0004-6361/201629659
D. Nesvorný, P. Jenniskens, H.F. Levison, W.F. Bottke, D. Vokrouhlický, M. Gounelle, Cometary origin of the zodiacal cloud and carbonaceous micrometeorites. Implications for hot debris disks. Astrophys. J. **713**, 816–836 (2010). https://doi.org/10.1088/0004-637X/713/2/816. arXiv:0909.4322
D. Nesvorný, D. Janches, D. Vokrouhlický, P. Pokorný, W.F. Bottke, P. Jenniskens, Dynamical model for the zodiacal cloud and sporadic meteors. Astrophys. J. **743**(2), 129 (2011a)
D. Nesvorný, D. Vokrouhlický, P. Pokorný, D. Janches, Dynamics of dust particles released from Oort cloud comets and their contribution to radar meteors. Astrophys. J. **743**, 37 (2011b). https://doi.org/10.1088/0004-637X/743/1/37. arXiv:1109.2981
F.M. Neubauer, K.H. Glassmeier, A.J. Coates, R. Goldstein, M.H. Acuna, Hypervelocity dust particle impacts observed by the Giotto magnetometer and plasma experiments. Geophys. Res. Lett. **17**, 1809–1812 (1990). https://doi.org/10.1029/GL017i011p01809
T. Noguchi, T. Nakamura, W. Nozaki, Mineralogy of phyllosilicate-rich micrometeorites and comparison with Tagish lake and Sayama meteorites. Earth Planet. Sci. Lett. **202**, 229–246 (2002). https://doi.org/10.1016/S0012-821X(02)00777-X
T. Noguchi, H. Yabuta, S. Itoh, N. Sakamoto, T. Mitsunari, A. Okubo, R. Okazaki, T. Nakamura, S. Tachibana, K. Terada, M. Ebihara, N. Imae, M. Kimura, H. Nagahara, Variation of mineralogy and organic material during the early stages of aqueous activity recorded in Antarctic micrometeorites. Geochim. Cosmochim. Acta **208**, 119–144 (2017). https://doi.org/10.1016/j.gca.2017.03.034
K.I. Öberg, H. Linnartz, R. Visser, E.F. van Dishoeck, Photodesorption of ices, II: $H_2O$ and $D_2O$. Astrophys. J. **693**, 1209–1218 (2009)
R.C. Ogliore, A.J. Westphal, Z. Gainsforth, A.L. Butterworth, S.C. Fakra, M.A. Marcus, Nebular mixing constrained by the stardust samples. Meteorit. Planet. Sci. **44**, 1675–1681 (2009). https://doi.org/10.1111/j.1945-5100.2009.tb01198.x
B.M. Pedersen, N. Meyer-Vernet, M.G. Aubier, P. Zarka, Dust distribution around Neptune—grain impacts near the ring plane measured by the Voyager planetary radio astronomy experiment. J. Geophys. Res. Space Phys. **96**, 19 (1991). https://doi.org/10.1029/91JA01601
S. Pizzarello, Y. Huang, L. Becker, R.J. Poreda, R.A. Nieman, G. Cooper, M. Williams, The organic content of the Tagish lake meteorite. Science **293**, 2236–2239 (2001). https://doi.org/10.1126/science.1062614
J.M.C. Plane, Cosmic dust in the earth's atmosphere. Chem. Soc. Rev. **41**, 6507–6518 (2012). https://doi.org/10.1039/c2cs35132c
J.M.C. Plane, W. Feng, E. Dawkins, M.P. Chipperfield, J. Höffner, D. Janches, D.R. Marsh, Resolving the strange behavior of extraterrestrial potassium in the upper atmosphere. Geophys. Res. Lett. **41**, 4753–4760 (2014). https://doi.org/10.1002/2014GL060334
J.M.C. Plane, G.J. Flynn, A. Maattanen, J.E. Moores, A.R. Poppe, J.D. Carrillo-Sanchez, C. Listowski, Impacts of cosmic dust on planetary atmospheres and surfaces. Space. Sci. Rev. **214**, 23 (2018)
P. Pokorný, P.G. Brown, A reproducible method to determine the meteoroid mass index. Astron. Astrophys. **592**, A150 (2016). https://doi.org/10.1051/0004-6361/201628134. arXiv:1605.04437
P. Pokorný, D. Vokrouhlický, D. Nesvorný, M. Campbell-Brown, P. Brown, Dynamical model for the toroidal sporadic meteors. Astrophys. J. **789**, 25 (2014). https://doi.org/10.1088/0004-637X/789/1/25
P. Pokorný, D. Janches, P.G. Brown, J.L. Hormaechea, An orbital meteoroid stream survey using the Southern Argentina Agile MEteor Radar (SAAMER) based on a wavelet approach. Icarus **290**, 162–182 (2017). https://doi.org/10.1016/j.icarus.2017.02.025
A.R. Poppe, Interplanetary dust influx to the Pluto-Charon system. Icarus **246**, 352–359 (2015)
A.R. Poppe, An improved model for interplanetary dust fluxes in the outer solar system. Icarus **264**, 369–386 (2016). https://doi.org/10.1016/j.icarus.2015.10.001
A. Poppe, B. Jacobsmeyer, D. James, M. Horányi, Simulation of polyvinylidene fluoride detector response to hypervelocity particle impact. Nucl. Instrum. Methods **622**(3), 583–587 (2010a)
A. Poppe, D. James, B. Jacobsmeyer, M. Horányi, First results from the Venetia Burney Student Dust Counter on the New Horizons mission. Geophys. Res. Lett. **37**, L11101 (2010b)
A. Poppe, D. James, M. Horányi, Measurements of the terrestrial dust influx variability by the cosmic dust experiment. Planet. Space Sci. **59**, 319–326 (2011)
W.T. Reach, P. Morris, F. Boulanger, K. Okumura, The mid-infrared spectrum of the zodiacal and exozodiacal light. Icarus **164**(2), 384–403 (2003)
W.T. Reach, M.S. Kelley, M.V. Sykes, A survey of debris trails from short-period comets. Icarus **191**(1), 298–322 (2007)
L. Remusat, Y. Guan, Y. Wang, J.M. Eiler, Accretion and preservation of D-rich organic particles in carbonaceous chondrites: evidence for important transport in the early solar system nebula. Astron. Astrophys. **713**, 1048–1058 (2010). https://doi.org/10.1088/0004-637X/713/2/1048

J. Renard, A. Levasseur-Regourd, R. Dumont, Properties of interplanetary dust from infrared and optical observations, II: brightness, polarization, temperature, albedo and their dependence on the elevation above the ecliptic. Astron. Astrophys. **304**, 602 (1995)
H.P. Robertson, Dynamical effects of radiation in the solar system. Mon. Not. R. Astron. Soc. **97**, 423 (1937). https://doi.org/10.1093/mnras/97.6.423
P. Rochette, L. Folco, C. Suavet, M. van Ginneken, J. Gattacceca, N. Perchiazzi, R. Braucher, R.P. Harvey, Micrometeorites from the transantarctic mountains. Proc. Natl. Acad. Sci. **105**, 18,206–18,211 (2008). https://doi.org/10.1073/pnas.0806049105
L. Rotelli, J.M. Trigo-Rodríguez, C.E. Moyano-Cambero, E. Carota, L. Botta, E. di Mauro, R. Saladino, The key role of meteorites in the formation of relevant prebiotic molecules in a formamide/water environment. Nat. Sci. Rep. **6**, 38888 (2016). https://doi.org/10.1038/srep38888
M. Rowan-Robinson, B. May, An improved model for the infrared emission from the zodiacal dust cloud: cometary, asteroidal and interstellar dust. Mon. Not. R. Astron. Soc. **429**, 2894 (2013)
A.E. Rubin, J.M. Trigo-Rodríguez, H. Huber, J.T. Wasson, Progressive aqueous alteration of CM carbonaceous chondrites. Geochim. Cosmochim. Acta **71**, 2361–2382 (2007). https://doi.org/10.1016/j.gca.2007.02.008
D.P. Rubincam, Asteroid orbit evolution due to thermal drag. J. Geophys. Res. **100**, 1585–1594 (1995). https://doi.org/10.1029/94JE02411
R. Rudawska, P. Matlovič, J. Tóth, L. Kornoš, Independent identification of meteor showers in EDMOND database. Planet. Space Sci. **118**, 38–47 (2015). https://doi.org/10.1016/j.pss.2015.07.011. arXiv:1406.6598
R. Rudawska, J. Tóth, D. Kalmančok, P. Zigo, P. Matlovič, Meteor spectra from AMOS video system. Planet. Space Sci. **123**, 25–32 (2016). https://doi.org/10.1016/j.pss.2015.11.018
S.S. Russell, G.R. Huss, A.J. Fahey, R.C. Greenwood, R. Hutchison, G.J. Wasserburg, An isotopic and petrologic study of calcium-aluminum-rich inclusions from CO3 meteorites. Geochim. Cosmochim. Acta **62**, 689–714 (1998). https://doi.org/10.1016/S0016-7037(97)00374-8
G.O. Ryabova, Modeling of meteoroid streams: the velocity of ejection of meteoroids from comets (a review). Sol. Syst. Res. **47**, 219–238 (2013). https://doi.org/10.1134/S0038094613030052
L.S. Schramm, D.E. Brownlee, M.M. Wheelock, Major element composition of stratospheric micrometeorites. Meteoritics **24**, 99–112 (1989)
E.R.D. Scott, R.H. Jones, Disentangling nebular and asteroidal features of CO3 carbonaceous chondrite meteorites. Geochim. Cosmochim. Acta **54**, 2485–2502 (1990). https://doi.org/10.1016/0016-7037(90)90235-D
E.R.D. Scott, A.N. Krot, Chondrites and their components. Treatise Geochem. **1**, 711 (2003). https://doi.org/10.1016/B0-08-043751-6/01145-2
Z. Sekanina, Activity of comet Hale-Bopp (1995 O1) beyond 6 AU from the Sun. Astron. Astrophys. **314**, 957–965 (1996)
A. Sekhar, D.J. Asher, Resonant behavior of comet Halley and the Orionid stream. Meteorit. Planet. Sci. **49**, 52–62 (2014). https://doi.org/10.1111/maps.12117. arXiv:1303.2928
A. Shu, S. Bugiel, E. Grün, J. Hillier, M. Horányi, T. Munsat, R. Srama, Cratering studies in polyvinylidene fluoride (PVDF) thin films. Planet. Space Sci. **89**, 29–35 (2013)
F.H. Shu, H. Shang, A.E. Glassgold, T. Lee, X-rays and fluctuating X-winds from protostars. Science **277**, 1475–1479 (1997). https://doi.org/10.1126/science.277.5331.1475
J.I. Simon, I.D. Hutcheon, S.B. Simon, J.E.P. Matzel, E.C. Ramon, P.K. Weber, L. Grossman, D.J. DePaolo, Oxygen isotope variations at the margin of a CAI records circulation within the solar nebula. Science **331**, 1175 (2011). https://doi.org/10.1126/science.1197970
J.A. Simpson, A.J. Tuzzolino, Polarized polymer films as electronic pulse detectors of cosmic dust particles. Nucl. Instrum. Methods Phys. Res., Sect. A **236**, 187–202 (1985)
J.A. Simpson, A.J. Tuzzolino, Cosmic dust investigations, II: instruments for measurement of particle trajectory, velocity and mass. Nucl. Instrum. Methods Phys. Res., Sect. A **279**, 625–639 (1989)
J.A. Simpson, D. Rabinowitz, A.J. Tuzzolino, Cosmic dust investigations, I: PVDF detector signal dependence on mass and velocity for penetrating particles. Nucl. Instrum. Methods Phys. Res., Sect. A **279**, 611–624 (1989)
R.B. Southworth, G.S. Hawkins, Statistics of meteor streams. Smithson. Contrib. Astrophys. **7**, 261 (1963)
R. Srama et al., The Cassini cosmic dust analyzer. Space Sci. Rev. **114**, 465–518 (2004)
O.C. St Cyr, M.L. Kaiser, N. Meyer-Vernet, R.A. Howard, R.A. Harrison, S.D. Bale, W.T. Thompson, K. Goetz, M. Maksimovic, J. Bougeret, D. Wang, S. Crothers, STEREO SECCHI and S/WAVES observations of spacecraft debris caused by micron-size interplanetary dust impacts. Sol. Phys. **256**, 475–488 (2009). https://doi.org/10.1007/s11207-009-9362-5
C.C. Stark, M.J. Kuchner, A new algorithm for self-consistent three-dimensional modeling of collisions in dust debris disks. Astrophys. J. **707**, 543–553 (2009)

P. Staubach, E. Grün, R. Jehn, The meteoroid environment near earth. Adv. Space Res. **19**, 301–308 (1997). https://doi.org/10.1016/S0273-1177(97)00017-3
J. Staude, T. Schmidt, Circular polarisation measurements of the zodiacal light. Astron. Astrophys. **20**, 163 (1972)
D.I. Steel, W.G. Elford, Collisions in the solar system, III: meteoroid survival times. Mon. Not. R. Astron. Soc. **218**, 185–199 (1986). https://doi.org/10.1093/mnras/218.2.185
S.A. Stern, Collisional time scales in the Kuiper disk and their implications. Astron. J. **110**, 2 (1995)
S.A. Stern, Signatures of collisions in the Kuiper disk. Astron. Astrophys. **310**, 999–1010 (1996)
S.A. Stern, The New Horizons Pluto Kuiper belt mission: an overview with historical context. Space Sci. Rev. **140**, 3–21 (2008)
E. Stokan, M.D. Campbell-Brown, A particle-based model for ablation and wake formation in faint meteors. Mon. Not. R. Astron. Soc. **447**, 1580–1597 (2015). https://doi.org/10.1093/mnras/stu2552
P. Strub, H. Krüger, V.J. Sterken, Sixteen years of Ulysses interstellar dust measurements in the solar system, II: fluctuations in the dust flow from the data. Astrophys. J. **812**, 140 (2015). https://doi.org/10.1088/0004-637X/812/2/140. arXiv:1508.03242
C. Suavet, A. Alexandre, I.A. Franchi, J. Gattacceca, C. Sonzogni, R.C. Greenwood, L. Folco, P. Rochette, Identification of the parent bodies of micrometeorites with high-precision oxygen isotope ratios. Earth Planet. Sci. Lett. **293**, 313–320 (2010). https://doi.org/10.1016/j.epsl.2010.02.046
D. Subasinghe, M.D. Campbell-Brown, E. Stokan, Physical characteristics of faint meteors by light curve and high-resolution observations, and the implications for parent bodies. Mon. Not. R. Astron. Soc. **457**, 1289–1298 (2016). https://doi.org/10.1093/mnras/stw019
R.M. Suggs, D.E. Moser, W.J. Cooke, R.J. Suggs, The flux of kilogram-sized meteoroids from lunar impact monitoring. Icarus **238**, 23 (2014)
J.R. Szalay, M. Horányi, Annual variation and synodic modulation of the sporadic meteoroid flux to the Moon. Geophys. Res. Lett. **42**, 10 (2015). https://doi.org/10.1002/2015GL066908
J.R. Szalay, M. Piquette, M. Horányi, The student dust counter: status report at 23 AU. Earth Planets Space **65**, 1145–1149 (2013)
A.D. Taylor, W.J. Baggaley, D.I. Steel, Discovery of interstellar dust entering the Earth's atmosphere. Nature **380**, 323–325 (1996). https://doi.org/10.1038/380323a0
S. Taylor, J.H. Lever, R.P. Harvey, Accretion rate of cosmic spherules measured at the South pole. Nature **392**, 899–903 (1998). https://doi.org/10.1038/31894
S. Taylor, J.H. Lever, R.P. Harvey, Numbers, types, and compositions of an unbiased collection of cosmic spherules. Meteorit. Planet. Sci. **35**, 651–666 (2000). https://doi.org/10.1111/j.1945-5100.2000.tb01450.x
E. Thomas, M. Horányi, D. Janches, T. Munsat, J. Simolka, Z. Sternovsky, Measurements of the ionization coefficient of simulated iron micrometeoroids. Geophys. Res. Lett. **43**, 3645–3652 (2016). https://doi.org/10.1002/2016GL068854
K.L. Thomas, G.E. Blanford, L.P. Keller, W. Klock, D.S. McKay, Carbon abundance and silicate mineralogy of anhydrous interplanetary dust particles. Geochim. Cosmochim. Acta **57**, 1551–1566 (1993). https://doi.org/10.1016/0016-7037(93)90012-L
J.I. Thorpe, C. Parvini, J.M. Trigo-Rodríguez, Detection and measurement of micrometeoroids with LISA Pathfinder. Astron. Astrophys. **586**, A107 (2016). https://doi.org/10.1051/0004-6361/201527658
F. Topputo, D.A. Dei Tos, A. Cipriano, Orbit design of LUMIO, a lunar meteoroid impact observer, in *42nd COSPAR Scientific Assembly, COSPAR Meeting*, vol. 42 (2018), pp. 1–28
M. Trieloff, E.K. Jessberger, I. Herrwerth, J. Hopp, C. Fiéni, M. Ghélis, M. Bourot-Denise, P. Pellas, Structure and thermal history of the H-chondrite parent asteroid revealed by thermochronometry. Nature **422**, 502–506 (2003). https://doi.org/10.1038/nature01499
J.M. Trigo-Rodríguez, Aqueous alteration in chondritic asteroids and comets from the study of carbonaceous chondrites, in *European Mineralogical Union Notes in Mineralogy*, vol. 15 (2015), pp. 67–87
J.M. Trigo-Rodríguez, J. Blum, The role of collisional compaction in primitive asteroids and comets, in *European Planetary Science Congress* (2008), p. 29
J.M. Trigo-Rodriguez, J. Blum, Tensile strength as an indicator of the degree of primitiveness of undifferentiated bodies. Planet. Space Sci. **57**, 243–249 (2009). https://doi.org/10.1016/j.pss.2008.02.011
J.M. Trigo-Rodriguez, J. Llorca, J. Borovicka, J. Fabregat, Chemical abundances determined from meteor spectra, I: ratios of the main chemical elements. Meteorit. Planet. Sci. **38**, 1283–1294 (2003). https://doi.org/10.1111/j.1945-5100.2003.tb00313.x
J.M. Trigo-Rodríguez, J. Llorca, J. Fabregat, Chemical abundances determined from meteor spectra, II: evidence for enlarged sodium abundances in meteoroids. Mon. Not. R. Astron. Soc. **348**, 802–810 (2004). https://doi.org/10.1111/j.1365-2966.2004.07389.x
J.M. Trigo-Rodríguez, C.E. Moyano-Cambero, J. Llorca, S. Fornasier, M.A. Barucci, I. Belskaya, Z. Martins, A.S. Rivkin, E. Dotto, J.M. Madiedo, A.A. Jacinto, UV to far-IR reflectance spectra of carbonaceous

chondrites, I: implications for remote characterization of dark primitive asteroids targeted by sample-return missions. Mon. Not. R. Astron. Soc. **437**, 227–240 (2014). https://doi.org/10.1093/mnras/stt1873. arXiv:1310.1742

J.M. Trigo-Rodríguez, R. Saladino, E. Di Mauro, L. Rotelli, C.E. Moyano-Cambero, E. Carota, L. Botta, The catalytic role of chondritic meteorites in the prebiotic enrichment of earth and other planetary-rich surfaces, under high meteoritic flux, in *Lunar and Planetary Science Conference*. Lunar and Planetary Inst. Technical Report, vol. 48 (2017), p. 1161

D. Tsintikidis, D.A. Gurnett, W.S. Kurth, L.J. Granroth, Micron-sized particles detected in the vicinity of Jupiter by the Voyager plasma wave instruments. Geophys. Res. Lett. **23**, 997–1000 (1996). https://doi.org/10.1029/96GL00961

Y. Tsuda, M. Yoshikawa, M. Abe, H. Minamino, S. Nakazawa, System design of the Hayabusa 2 asteroid sample return mission to 1999 JU3. Acta Astronaut. **91**, 356–362 (2013). https://doi.org/10.1016/j.actaastro.2013.06.028

B.T. Tsurutani, D.R. Clay, L.D. Zhang, B. Dasgupta, D. Brinza, M. Henry, A. Mendis, S. Moses, K.H. Glassmeier, G. Musmann, I. Richter, Dust impacts at comet P/Borrelly. Geophys. Res. Lett. **30**(22), 2134 (2003). https://doi.org/10.1029/2003GL017580

A.J. Tuzzolino, Two-dimensional position-sensing PVDF dust detectors for measurements of dust particle trajectory, velocity and mass. Nucl. Instrum. Methods Phys. Res., Sect. A **301** (1991)

A.J. Tuzzolino, PVDF copolymer dust detectors: particle response and penetration characteristics. Nucl. Instrum. Methods Phys. Res., Sect. A **316**, 223–237 (1992)

A.J. Tuzzolino, T.E. Economou, R.B. McKibben, J.A. Simpson, J.A.M. McDonnell, M.J. Burchell, B.A.M. Vaughan, P. Tsou, M.S. Hanner, B.C. Clark, D.E. Brownlee, Dust flux monitor instrument for the stardust mission to comet Wild 2. J. Geophys. Res. **108**, E10 (2003)

A.J. Tuzzolino, T.E. Economou, B.C. Clark, P. Tsou, D.E. Brownlee, S.F. Green, J.A.M. McDonnell, N. McBride, M.T.S.H. Colwell, Dust measurements in the coma of comet 81P/Wild 2 by the dust flux monitor instrument. Science **304**, 1776–1780 (2004). https://doi.org/10.1126/science.1098759

A.J. Tuzzolino et al., The Space Dust (SPADUS) instrument aboard the Earth-orbiting ARGOS spacecraft, I: instrument description. Planet. Space Sci. **49**, 689–703 (2001a)

A.J. Tuzzolino et al., The Space Dust (SPADUS) instrument aboard the Earth-orbiting ARGOS spacecraft, II: results form the first 16 months of flight. Planet. Space Sci. **49**, 705–729 (2001b)

A.J. Tuzzolino et al., Dust measurements in the coma of comet 81P/Wild 2 by the dust flux monitor instrument. Science **304**, 1776–1780 (2004)

G.B. Valsecchi, T.J. Jopek, C. Froeschle, Meteoroid stream identification: a new approach, I: theory. Mon. Not. R. Astron. Soc. **304**, 743–750 (1999). https://doi.org/10.1046/j.1365-8711.1999.02264.x

M. van Ginneken, J. Gattacceca, P. Rochette, C. Sonzogni, A. Alexandre, V. Vidal, M.J. Genge, The parent body controls on cosmic spherule texture: evidence from the oxygen isotopic compositions of large micrometeorites. Geochim. Cosmochim. Acta **212**, 196–210 (2017). https://doi.org/10.1016/j.gca.2017.05.008

J. Vaubaillon, F. Colas, Demonstration of gaps due to Jupiter in meteoroid streams. What happened with the 2003 Pi-Puppids? Astron. Astrophys. **431**, 1139–1144 (2005). https://doi.org/10.1051/0004-6361:20041391

J. Vaubaillon, F. Colas, L. Jorda, A new method to predict meteor showers, I: description of the model. Astron. Astrophys. **439**, 751–760 (2005). https://doi.org/10.1051/0004-6361:20041544

J. Vaubaillon, P. Lamy, L. Jorda, On the mechanisms leading to orphan meteoroid streams. Mon. Not. R. Astron. Soc. **370**, 1841–1848 (2006). https://doi.org/10.1111/j.1365-2966.2006.10606.x

P. Vernazza, M. Marsset, P. Beck, R.P. Binzel, M. Birlan, R. Brunetto, F.E. Demeo, Z. Djouadi, C. Dumas, S. Merouane, O. Mousis, B. Zanda, Interplanetary dust particles as samples of icy asteroids. Astrophys. J. **806**, 204 (2015). https://doi.org/10.1088/0004-637X/806/2/204

D. Vinković, Radiation-pressure mixing of large dust grains in protoplanetary disks. Nature **459**, 227 (2009)

C. Vitense, A.V. Krivov, H. Kobayashi, T. Löhne, An improved model of the Edgeworth-Kuiper debris disk. Astron. Astrophys. **540**, A30 (2012). https://doi.org/10.1051/0004-6361/201118551. arXiv:1202.2257

C. Vitense, A.V. Krivov, T. Löhne, Will New Horizons see dust clumps in the Edgeworth-Kuiper belt? Astron. J. **147** (2014)

V. Vojáček, J. Borovička, P. Koten, P. Spurný, R. Štork, Catalogue of representative meteor spectra. Astron. Astrophys. **580**, A67 (2015). https://doi.org/10.1051/0004-6361/201425047

D. Vokrouhlický, P. Farinella, Efficient delivery of meteorites to the Earth from a wide range of asteroid parent bodies. Nature **407**, 606–608 (2000). https://doi.org/10.1038/35036528

J. Walter, F. Brandstaetter, G. Kurat, C. Koeberl, M. Maurette, Cosmic spherules, micrometeorites, and chondrules, in *Lunar and Planetary Science Conference*, vol. 26 (1995)

A. Wehry, I. Mann, Identification of beta -meteoroids from measurements of the dust detector onboard the ULYSSES spacecraft. Astron. Astrophys. **341**, 296–303 (1999)

A. Wehry, H. Krüger, E. Grün, Analysis of Ulysses data: Radiation pressure effects on dust particles. Astron. Astrophys. **419**, 1169–1174 (2004). https://doi.org/10.1051/0004-6361:20035613
S.J. Weidenschilling, A.A. Jackson, Orbital resonances and Poynting-Robertson drag. Icarus **104**, 244–254 (1993). https://doi.org/10.1006/icar.1993.1099
J. Weinberg, J. Sparrow, *Zodiacal Light as an Indicator of Interplanetary Dust* (Wiley, Chichester, 1978), pp. 75–122
M.K. Weisberg, T.J. McCoy, A.N. Krot, *Systematics and Evaluation of Meteorite Classification* (2006), pp. 19–52
A.A. Weiss, J.W. Smith, A southern hemisphere survey of the radiants of sporadic meteors. Mon. Not. R. Astron. Soc. **121**, 5 (1960). https://doi.org/10.1093/mnras/121.1.5
R.J. Weryk, P. Brown, A search for interstellar meteoroids using the Canadian Meteor Orbit Radar (CMOR). Earth Moon Planets **95**, 221–227 (2004). https://doi.org/10.1007/s11038-005-9034-x
R.J. Weryk, P.G. Brown, Simultaneous radar and video meteors, II: photometry and ionisation. Planet. Space Sci. **81**, 32–47 (2013). https://doi.org/10.1016/j.pss.2013.03.012
M.S. Westley, R.A. Baragiola, R.E. Johnson, G.A. Baratta, Photodesorption from low-temperature water ice in interstellar and circumsolar grains. Nature **373**, 405–407 (1995)
A.J. Westphal, S.C. Fakra, Z. Gainsforth, M.A. Marcus, R.C. Ogliore, A.L. Butterworth, Mixing fraction of inner solar system material in comet 81P/Wild2. Astrophys. J. **694**, 18–28 (2009). https://doi.org/10.1088/0004-637X/694/1/18
A.J. Westphal, R.M. Stroud, H.A. Bechtel, F.E. Brenker, A.L. Butterworth, G.J. Flynn, D.R. Frank, Z. Gainsforth, J.K. Hillier, F. Postberg, A.S. Simionovici, V.J. Sterken, L.R. Nittler, C. Allen, D. Anderson, A. Ansari, S. Bajt, R.K. Bastien, N. Bassim, J. Bridges, D.E. Brownlee, M. Burchell, M. Burghammer, H. Changela, P. Cloetens, A.M. Davis, R. Doll, C. Floss, E. Grün, P.R. Heck, P. Hoppe, B. Hudson, J. Huth, A. Kearsley, A.J. King, B. Lai, J. Leitner, L. Lemelle, A. Leonard, H. Leroux, R. Lettieri, W. Marchant, R. Ogliore, W.J. Ong, M.C. Price, S.A. Sandford, J.A.S. Tresseras, S. Schmitz, T. Schoonjans, K. Schreiber, Evidence for interstellar origin of seven dust particles collected by the stardust spacecraft. Science **345**(6198), 786–791 (2014). https://doi.org/10.1126/science.1252496.
F.L. Whipple, The theory of micro-meteorites, part I: in an isothermal atmosphere. Proc. Natl. Acad. Sci. **36**, 687–695 (1950). https://doi.org/10.1073/pnas.36.12.687
F.L. Whipple, A comet model, III: the zodiacal light. Astrophys. J. **121**, 750 (1955)
F.L. Whipple, On maintaining the meteoritic complex. SAO Spec. Rep. **239**, 1 (1967)
P. Wiegert, J. Vaubaillon, M. Campbell-Brown, A dynamical model of the sporadic meteoroid complex. Icarus **201**, 295–310 (2009). https://doi.org/10.1016/j.icarus.2008.12.030
P.A. Wiegert, Hyperbolic meteors: interstellar or generated locally via the gravitational slingshot effect? Icarus **242**, 112–121 (2014). https://doi.org/10.1016/j.icarus.2014.06.031. 1404.2159
M.J. Willis, M.J. Burchell, T.J. Ahrens, H. Krüger, E. Grün, Decreased values of cosmic dust number density estimates in the solar system. Icarus **176**, 440–452 (2005). https://doi.org/10.1016/j.icarus.2005.02.018
R.D. Wolstencroft, J.C. Kemp, Circular polarization of the nightsky radiation. Astrophys. J. **177**, L137 (1972)
D.H. Wooden, H.M. Butner, D.E. Harker, C.E. Woodward, Mg-rich silicate crystals in comet Hale-Bopp: ISM relics or solar nebula condensates? Icarus **143**, 126–137 (2000). https://doi.org/10.1006/icar.1999.6240
P.J. Wozniakiewicz, Grain sorting in cometary dust from the outer solar nebula. Astrophys. J. Lett. **760**, L23 (2012). https://doi.org/10.1088/2041-8205/760/2/L23
M.C. Wyatt, The insignificance of P-R drag in detectable extrasolar planetesimal belts. Astron. Astrophys. **433**, 1007–1012 (2005). https://doi.org/10.1051/0004-6361:20042073. astro-ph/0501038
S.P. Wyatt, F.L. Whipple, The Poynting-Robertson effect on meteor orbits. Astrophys. J. **111**, 134–141 (1950). https://doi.org/10.1086/145244
E.M. Xilouris, A.Z. Bonanos, I. Bellas-Velidis, P. Boumis, A. Dapergolas, A. Maroussis, A. Liakos, I. Alikakos, V. Charmandaris, G. Dimou, A. Fytsilis, M. Kelley, D. Koschny, V. Navarro, K. Tsiganis, K. Tsinganos, NELIOTA: the wide-field, high-cadence, lunar monitoring system at the prime focus of the Kryoneri telescope. Astron. Astrophys. **619**, A141 (2018). https://doi.org/10.1051/0004-6361/201833499. arXiv:1809.00495
T. Yada, H. Kojima, The collection of micrometeorites in the Yamato meteorite ice field of Antarctica in 1998. Antarct. Meteor. Res. **13**, 9 (2000)
S. Yamamoto, T. Mukai, Dust production by impacts of interstellar dust on Edgeworth-Kuiper belt objects. Astron. Astrophys. **329**, 785–791 (1998)
H. Yang, M. Ishiguro, Origin of interplanetary dust through optical properties of zodiacal light. Astrophys. J. **813**(2), 87 (2015)
Q.Z. Ye, M.T. Hui, P.G. Brown, M.D. Campbell-Brown, P. Pokorný, P.A. Wiegert, X. Gao, When comets get old: a synthesis of comet and meteor observations of the low activity comet 209P/LINEAR. Icarus **264**, 48–61 (2016). https://doi.org/10.1016/j.icarus.2015.09.003. arXiv:1509.00560

A. Zaslavsky, N. Meyer-Vernet, I. Mann, A. Czechowski, K. Issautier, G. Le Chat, F. Pantellini, K. Goetz, M. Maksimovic, S.D. Bale, J.C. Kasper, Interplanetary dust detection by radio antennas: mass calibration and fluxes measured by STEREO/WAVES. J. Geophys. Res. Space Phys. **117**(A16), A05102 (2012). https://doi.org/10.1029/2011JA017480

K. Zhang, G.A. Blake, E.A. Bergin, Evidence of fast pebble growth near condensation fronts in the HL Tau protoplanetary disk. Astrophys. J. Lett. **806**, L7 (2015). https://doi.org/10.1088/2041-8205/806/1/L7. 1505.00882

E. Zinner, K.D. McKeegan, R.M. Walker, Laboratory measurements of D/H ratios in interplanetary dust. Nature **305**, 119–121 (1983). https://doi.org/10.1038/305119a0

E.K. Zinner, Presolar grains. Treatise Geochem. **1**, 711 (2003). https://doi.org/10.1016/B0-08-043751-6/01144-0

M.E. Zolensky, Refractory interplanetary dust particles. Science **237**, 1466–1468 (1987). https://doi.org/10.1126/science.237.4821.1466

M.E. Zolensky, T.J. Zega, H. Yano, S. Wirick, A.J. Westphal, M.K. Weisberg, I. Weber, J.L. Warren, M.A. Velbel, A. Tsuchiyama, P. Tsou, A. Toppani, N. Tomioka, K. Tomeoka, N. Teslich, M. Taheri, J. Susini, R. Stroud, T. Stephan, F.J. Stadermann, C.J. Snead, S.B. Simon, A. Simionovici, T.H. See, F. Robert, F.J.M. Rietmeijer, W. Rao, M.C. Perronnet, D.A. Papanastassiou, K. Okudaira, K. Ohsumi, I. Ohnishi, K. Nakamura-Messenger, T. Nakamura, S. Mostefaoui, T. Mikouchi, A. Meibom, G. Matrajt, M.A. Marcus, H. Leroux, L. Lemelle, L. Le, A. Lanzirotti, F. Langenhorst, A.N. Krot, L.P. Keller, A.T. Kearsley, D. Joswiak, D. Jacob, H. Ishii, R. Harvey, K. Hagiya, L. Grossman, J.N. Grossman, G.A. Graham, M. Gounelle, P. Gillet, M.J. Genge, G. Flynn, T. Ferroir, S. Fallon, D.S. Ebel, Z.R. Dai, P. Cordier, B. Clark, M. Chi, A.L. Butterworth, D.E. Brownlee, J.C. Bridges, S. Brennan, A. Brearley, J.P. Bradley, P. Bleuet, P.A. Bland, R. Bastien, Mineralogy and petrology of comet 81P/Wild 2 nucleus samples. Science **314**, 1735 (2006). https://doi.org/10.1126/science.1135842